

Mr BB Jacobsen 2535

ELECTRICAL COMMUNICATION

*Technical Journal of the
International Telephone and Telegraph Corporation
and Associate Companies*

MANUFACTURE OF A MAGNETRON

TEMPERATURE REGULATOR FOR PRODUCING GERMANIUM CRYSTALS

ELECTRONIC GENERATOR FOR OPERATING TELEPHONE RINGERS

TYPE-7 CROSSBAR SELECTOR

VALVE NOISE PRODUCED BY ELECTRODE MOVEMENT

WAVE PROPERTIES OF HELICAL CONDUCTORS

REFLECTION COEFFICIENTS AND LOSS OF A WAVEGUIDE JUNCTION

HIGH-FREQUENCY PROXIMITY-EFFECT FORMULA

UNITED STATES PATENTS ISSUED TO THE INTERNATIONAL SYSTEM



Volume 31

MARCH, 1954

Number 1



ELECTRICAL COMMUNICATION

*Technical Journal of the
International Telephone and Telegraph Corporation
and Associate Companies*

H. P. WESTMAN, Editor
J. E. SCHLAIKJER, Assistant Editor

EDITORIAL BOARD

H. Busignies H. H. Buttner G. Chevigny E. M. Deloraine W. Hatton B. C. Holding H. L. Hull
J. Kruithof W. P. Maginnis A. W. Montgomery E. D. Phinney G. Rabuteau N. H. Saunders
C. E. Scholz T. R. Scott C. E. Strong A. E. Thompson E. N. Wendell H. B. Wood

Published Quarterly by the
INTERNATIONAL TELEPHONE AND TELEGRAPH CORPORATION

67 BROAD STREET, NEW YORK 4, NEW YORK, U.S.A.

Sosthenes Behn, Chairman William H. Harrison, President
Geoffrey A. Ogilvie, Vice President and Secretary

Subscription, \$2.00 per year; single copies, 50 cents

Copyrighted 1954 by International Telephone and Telegraph Corporation

Volume 31

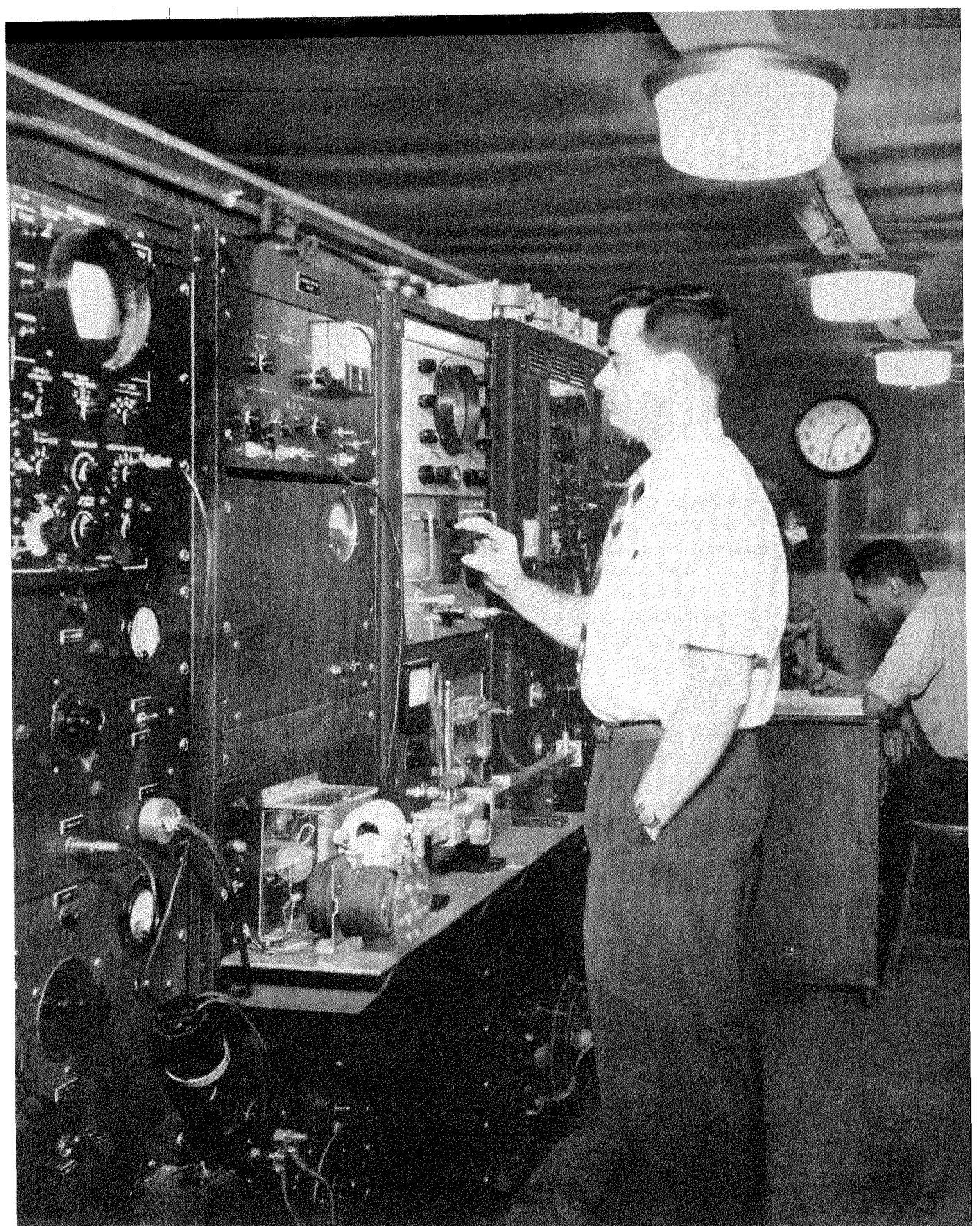
MARCH, 1954

Number 1

CONTENTS

MANUFACTURE OF A MAGNETRON	3
TEMPERATURE REGULATOR USED IN PRODUCING GERMANIUM CRYSTALS	19
<i>By G. J. Lehmann and C. A. Meuleau</i>	
ELECTRONIC GENERATOR FOR OPERATING TELEPHONE RINGERS	27
<i>By G. H. Brodie</i>	
TYPE-7 CROSSBAR SELECTOR	32
<i>By R. W. Hutton</i>	
VALVE NOISE PRODUCED BY ELECTRODE MOVEMENT	38
<i>By P. A. Handley and P. Welch</i>	
SOME WAVE PROPERTIES OF HELICAL CONDUCTORS	50
<i>By J. H. Bryant</i>	
DETERMINATION OF REFLECTION COEFFICIENTS AND INSERTION LOSS OF A WAVEGUIDE JUNCTION	57
<i>By G. A. Deschamps</i>	
NEW HIGH-FREQUENCY PROXIMITY-EFFECT FORMULA	63
<i>By A. C. Sim</i>	
UNITED STATES PATENTS ISSUED TO INTERNATIONAL TELEPHONE AND TELEGRAPH SYSTEM, AUGUST-OCTOBER, 1953	67
IN MEMORIAM—HENRY CONRAD ROEMER	70
WIDE-FREQUENCY-RANGE TUNED HELICAL ANTENNAS AND CIRCUITS (CORRECTION)	49
<i>By A. G. Kandoian and W. Sichak</i>	
CONTRIBUTORS TO THIS ISSUE	71

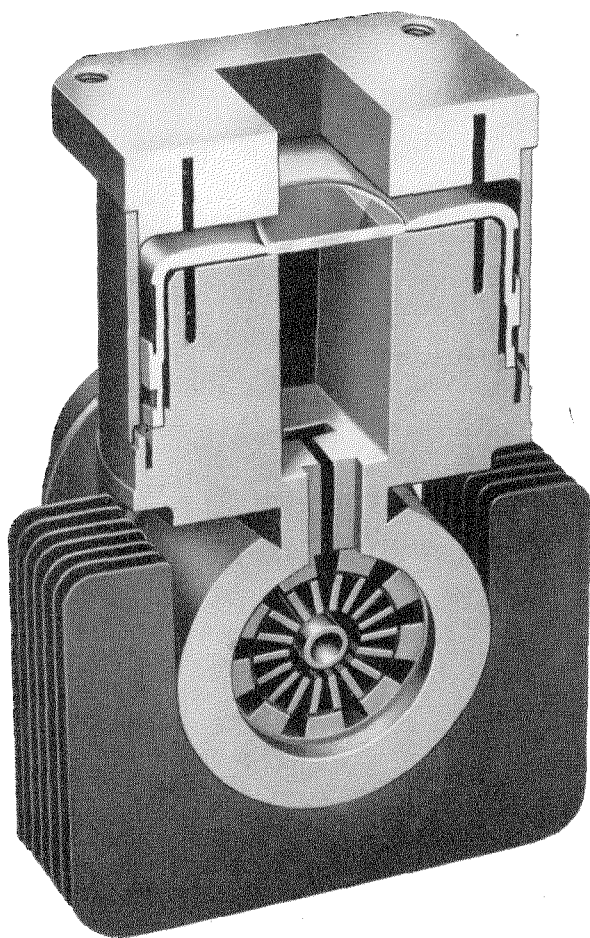
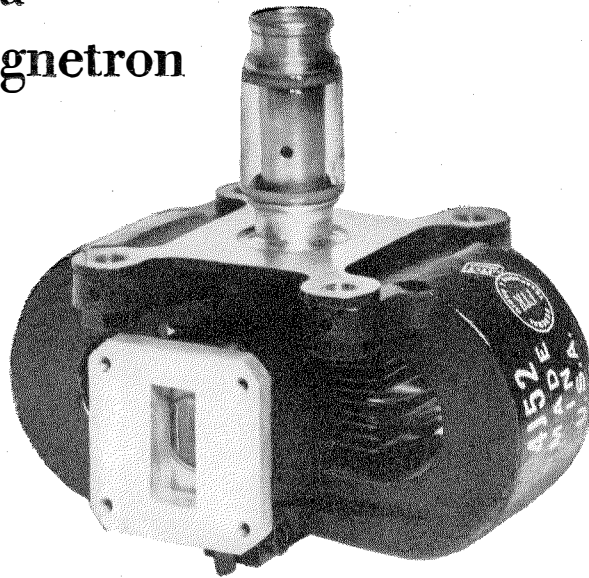




The magnetron testing cage is completely surrounded by metal screening that prevents external interference from affecting the measurements and also prevents the very-high-power output of the magnetron from interfering with opera-

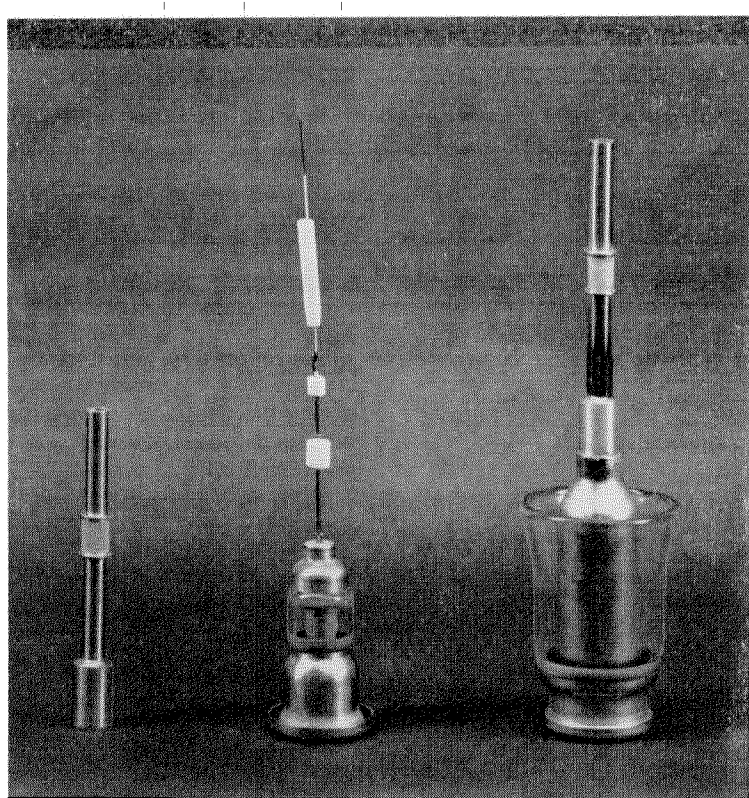
tions elsewhere in the factory. The magnetron with its cooling fan and waveguide connections is on the shelf in front of the engineer. Complete tests are made of all phases of operation of the finished tube before it is shipped to the customer.

Manufacture of a Magnetron



MAGNETRONS are vacuum tubes that generate the high-power short-time pulses of microwave energy on which radar works. The circular structure at the center of the 4J52 tube in the cutaway drawing at the left is a cylindrical cathode that emits electrons that would normally travel directly to the finned anode surrounding the cathode. A very strong field from a permanent magnet passes lengthwise through the space between the cathode and anode and turns the paths of the electrons so that they travel in spirals just in front of the ends of the anode fins. The fins and the open regions between them are of a size and shape that tunes them to the operating frequency of 9375 megacycles per second. The moving electrons induce voltages in these cavity resonators and the resulting electromagnetic fields pass into a waveguide, part of which is the large rectangular opening at the top.

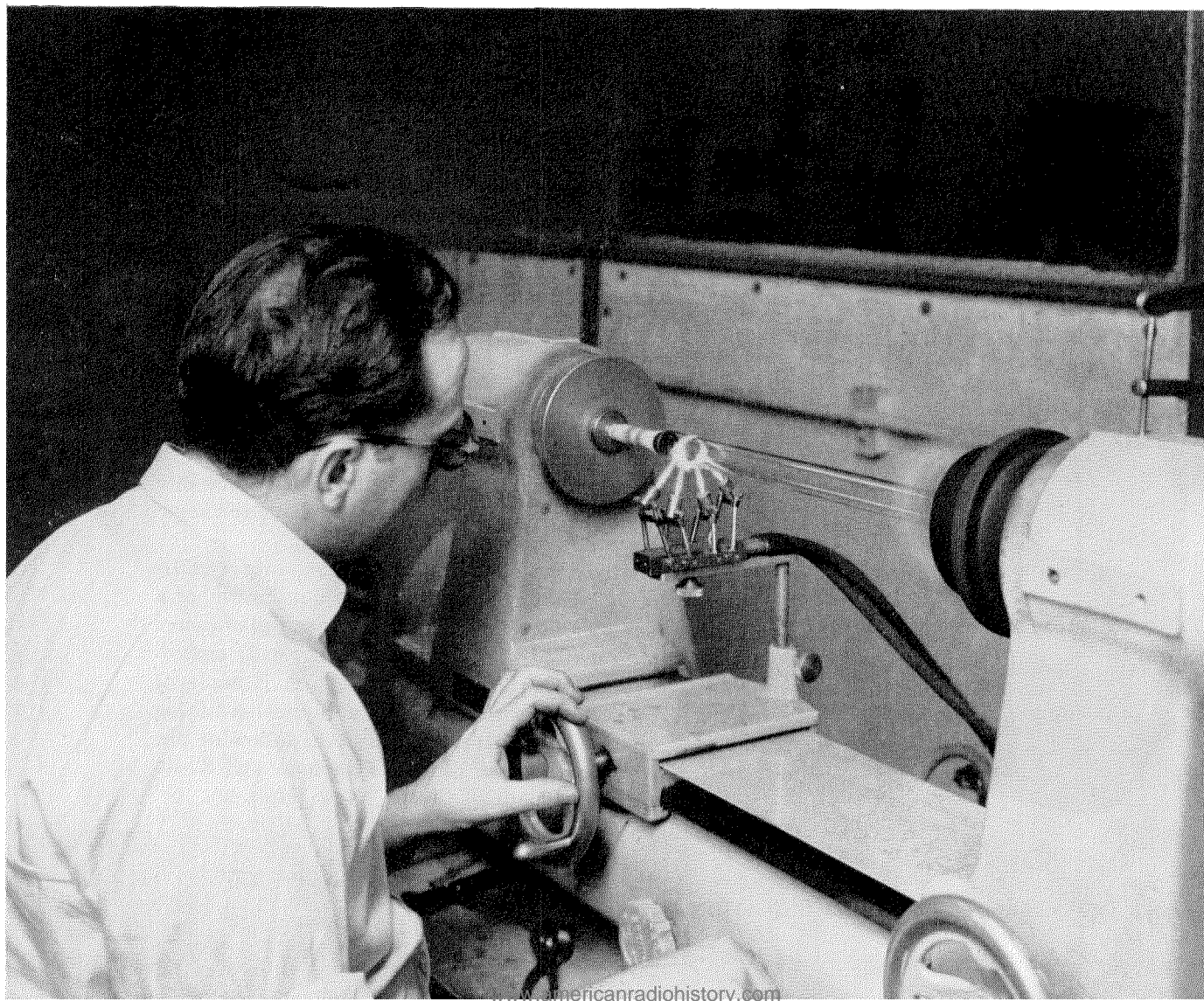
This type of tube produces an output pulse of 100 kilowatts lasting about a millionth of a second. In radar operation, these pulses of power are repeated several hundred times each second. The major part of the magnetron is made of copper and requires highly accurate machining operations, which are shown in the following pictures taken at the Federal Telephone and Radio Company plant in Clifton, New Jersey.



1. The molybdenum cathode sleeve at the left has a sintered nickel band around the central portion. This band will form the active region of the cathode. The long white cylindrical coil in the middle picture is the spiral heater, the two shorter cylinders below it being ceramic insulators. When assembled as at the right, the nickel cathode band is centered over the heater coil. The glass skirt will be fused to the anode assembly in the finished tube.

2. As will be evident from 1, the cathode assembly is composed of several metallic parts that are brazed together. The operator in the photograph at the bottom of this page is using a glass-working lathe to form the glass skirt on a kovar thimble.

3. On the facing page, the cathode sleeve is brazed to the heater assembly. Radio-frequency power flowing in the large rectangular metallic loop raises the cathode joint to white heat by induction, causing the gold brazing alloy to fill the joint. The glass bell jar is filled with inert gas to prevent oxidation of the heated parts.





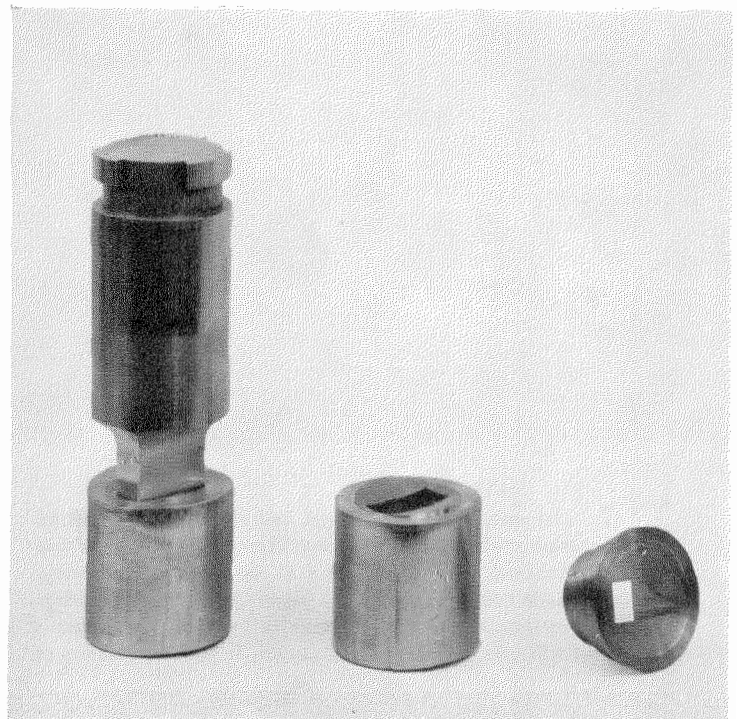
4. In a completely air-conditioned room, the barium-carbonate cathode-activating material is painted on the sintered-nickel band of the cathode. Moisture is baked out in an oven during exhaust. During a later operation in the exhaust station, the carbonate is converted to barium oxide, a compound that produces a prolific emission of electrons when heated.





5. The internal structures of both the waveguide section and the anode are formed by hobbing in a hydraulic press. Shown above is the operation in which a hob is driven into a solid copper cylinder in a 200-ton press to form the waveguide section. The units on the table have been hobbled.

6. At the left is a hob that has been driven into a solid copper cylinder about 2 inches (5 centimeters) in diameter. In the middle, the hob has been withdrawn. Machining operations are required to finish the outside of the piece and produce the waveguide section shown at the right.



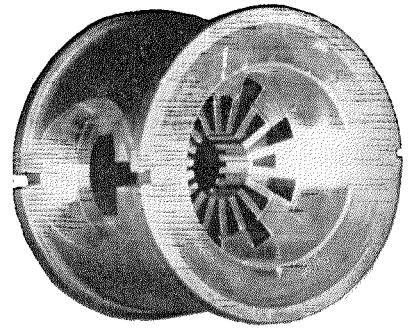


7. The anode also is hobbled and machined. It is then necessary to measure its resonant frequency to ensure that the finished tube will operate at the desired frequency. An anode has been placed in a jig on the measuring device. The operator is inserting dummy cathodes and pole-pieces that will give a close approximation to the dimensions of

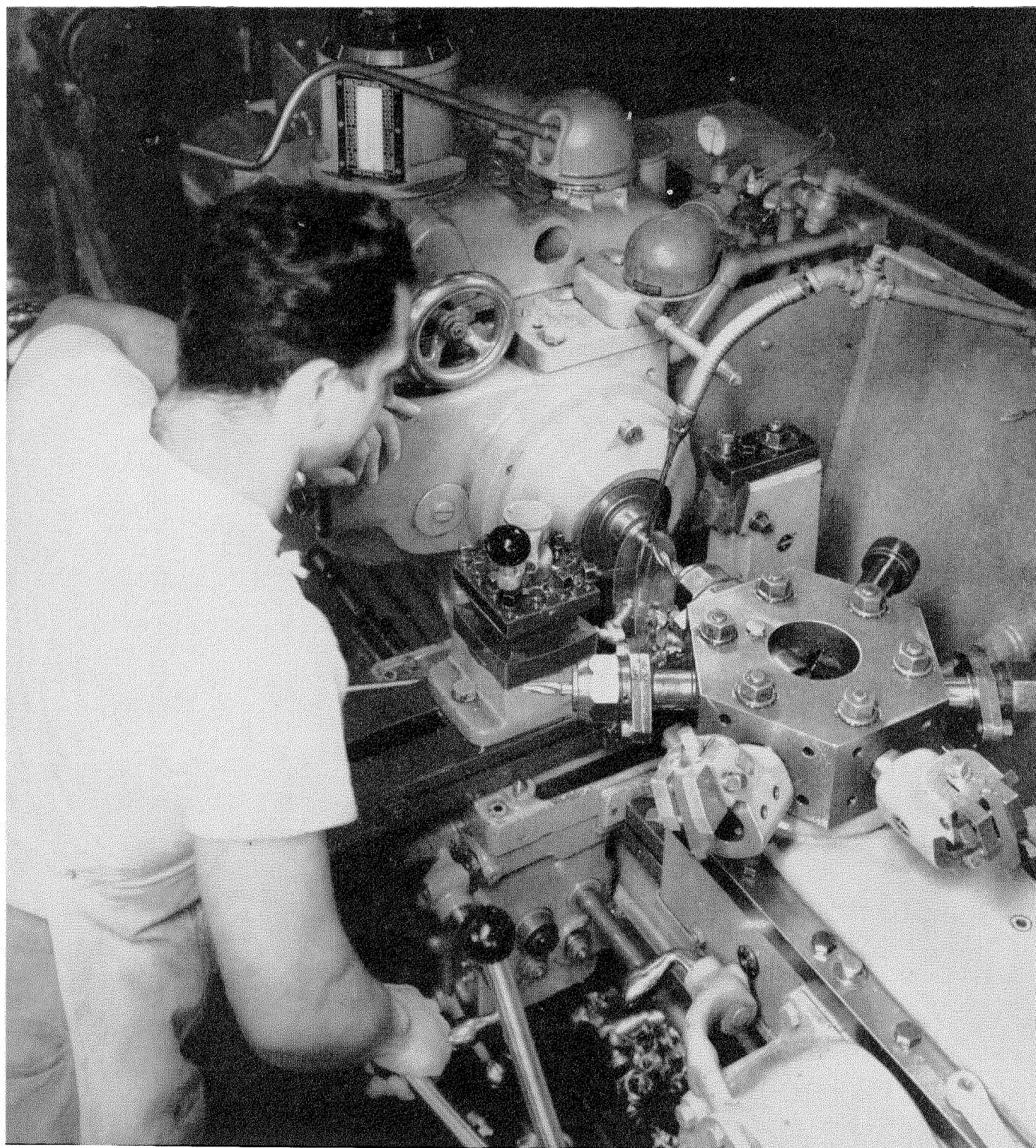
the finished tube. The wavemeter is the cylindrical cavity attached to the waveguide at the lower left corner of the spectrum analyzer. It will produce a slight dip in the curve on the oscilloscope screen, which, when superimposed on the larger dip caused by the anode, will enable accurate measurement of the anode frequency to be made.

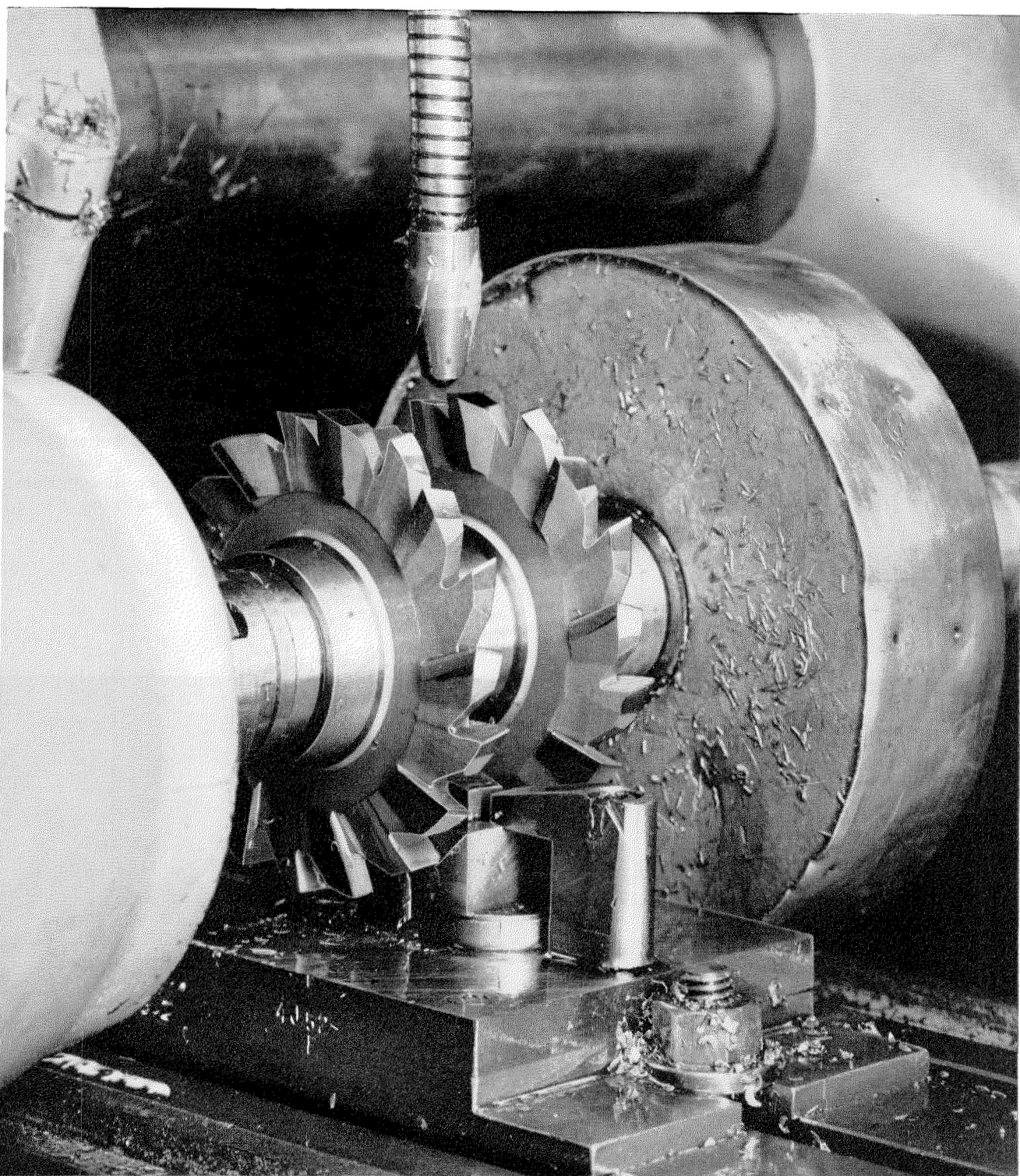
8. (Below) the resonant frequency of the anode is always made higher than that desired, and a slight groove is next cut near the base of the anode fins, thus lowering the frequency. Having determined from the preceding measurement just how much the frequency must be lowered, the depth of this groove can be made exactly right to bring the frequency to the proper value.

9. At the right, a finished anode. The slots in the outer circumference permit the anode to be keyed to the various parts that are brazed to it later, thus assuring proper alignment of the operating elements.

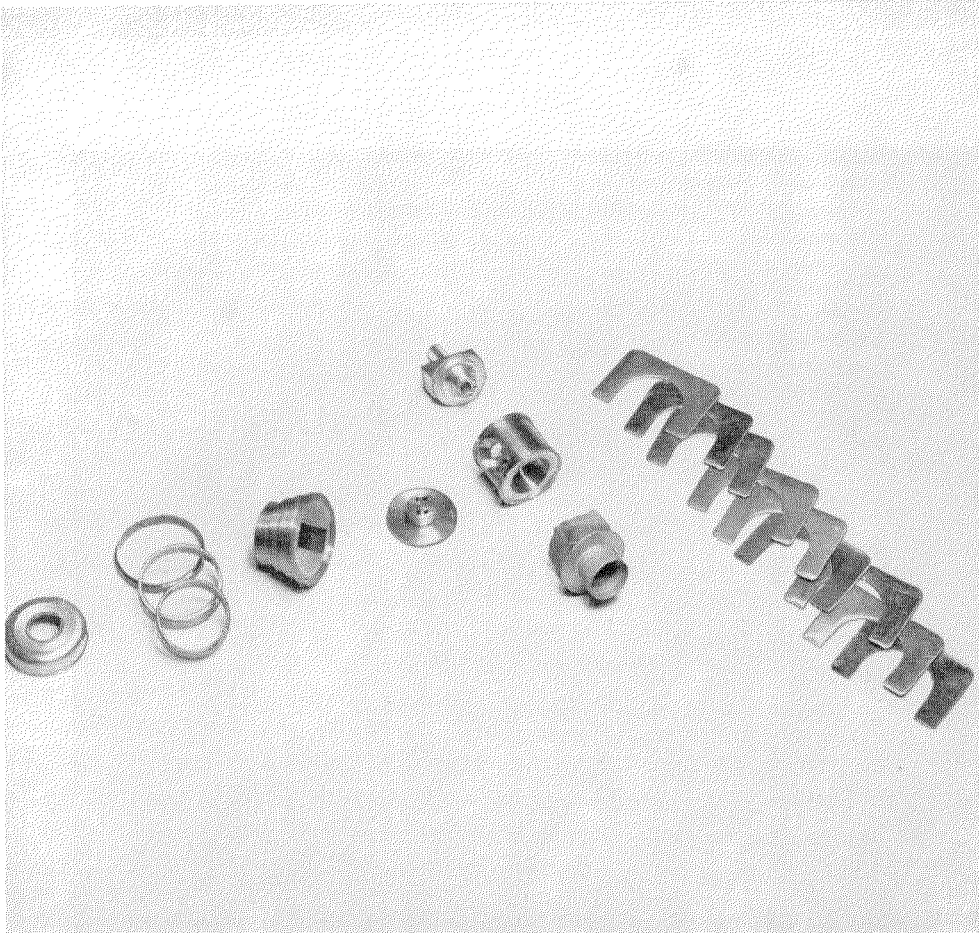


10. Soft-iron pole pieces fit into the ends of the anode to enclose the structure. Iron is used to assist in distributing the magnetic field uniformly within the anode. Shown below is an operation in which a pole piece is machined from an iron bar on a turret lathe.





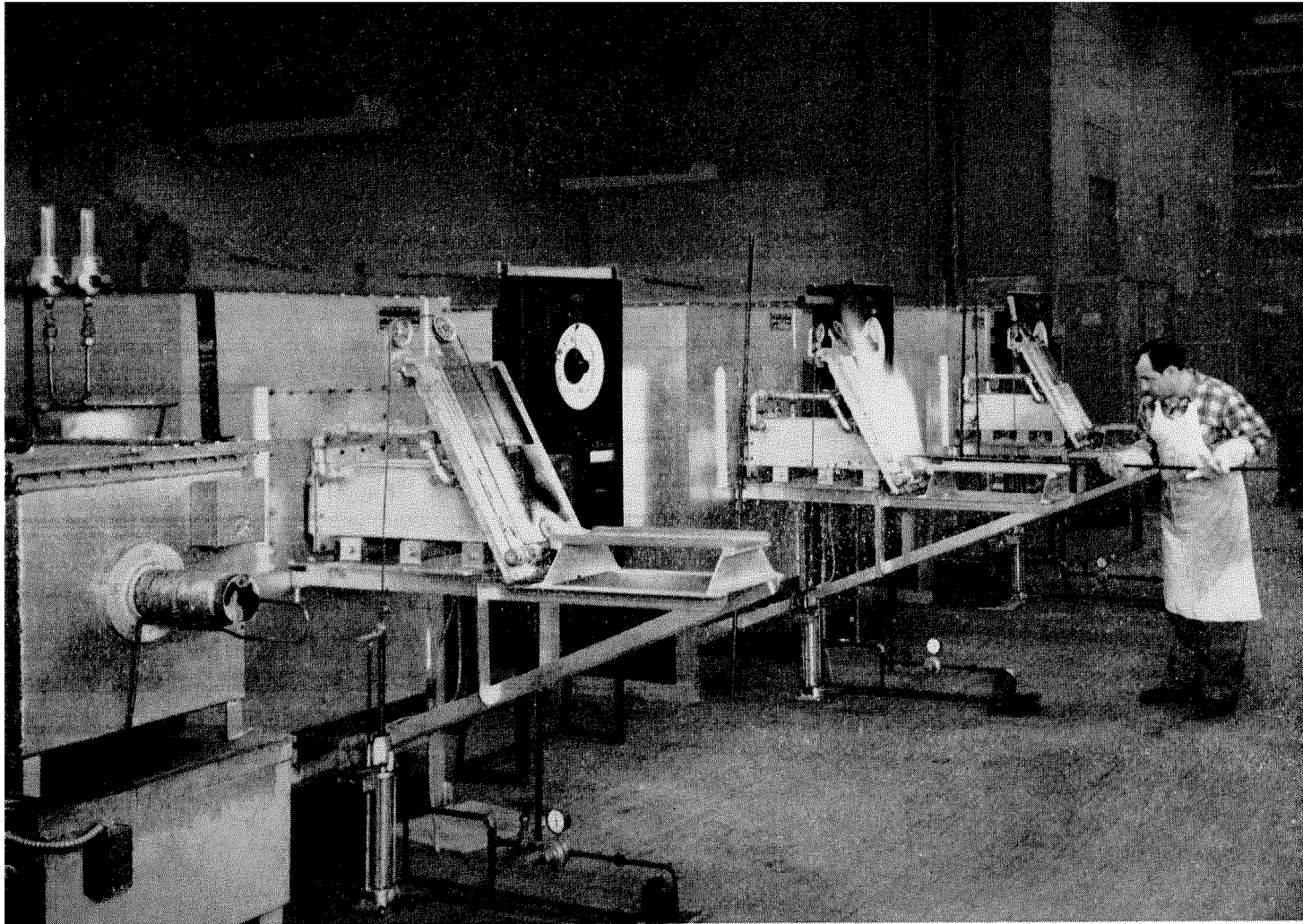
11. A milling operation squares up the rear faces of a pole piece. The magnet will fit against these faces.



12. At the left are various parts that will next be brazed together to make up the anode assembly. From left to right are the vacuum-tight window, rings comprising a waveguide-matching structure, waveguide section, H section that couples the anode cavities to the waveguide, anode and its pole pieces, and the cooling fins.

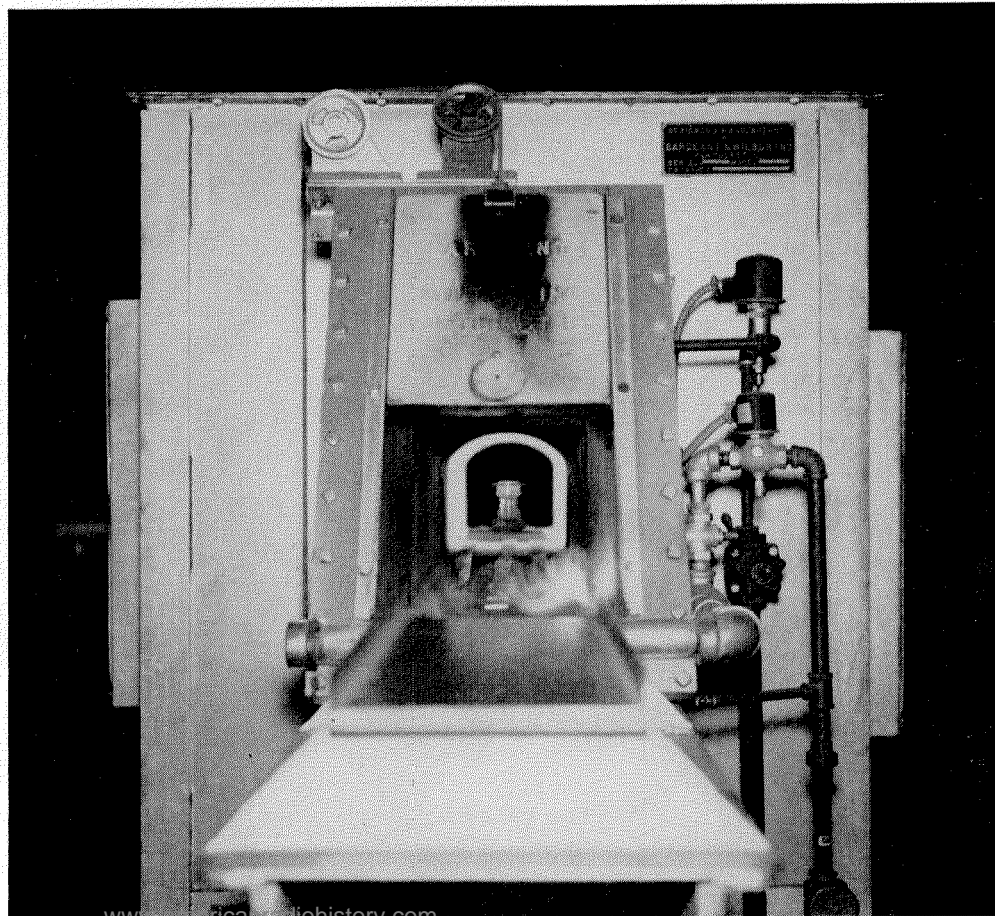
13. Below, operators assemble in jigs the parts for the anode structure. Gold-alloy brazing wire is placed so that it will flow to fill the joints when heated. The entire room is air conditioned as absolute cleanliness is a necessity.



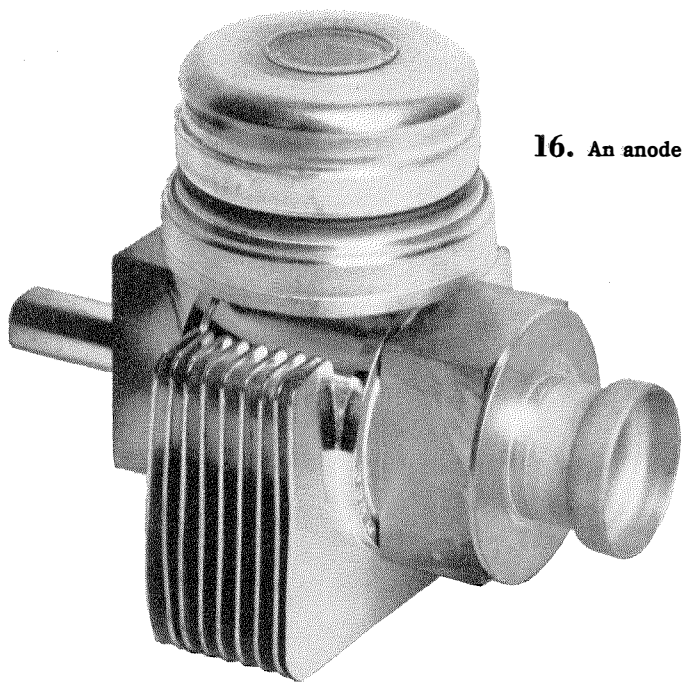


14. The brazing ovens are shown above. A sheet of flaming gas automatically fills the opening to exclude air when the door is raised. The oven is filled with hydrogen to clean the parts and to protect them from oxidation. The ovens are electrically heated.

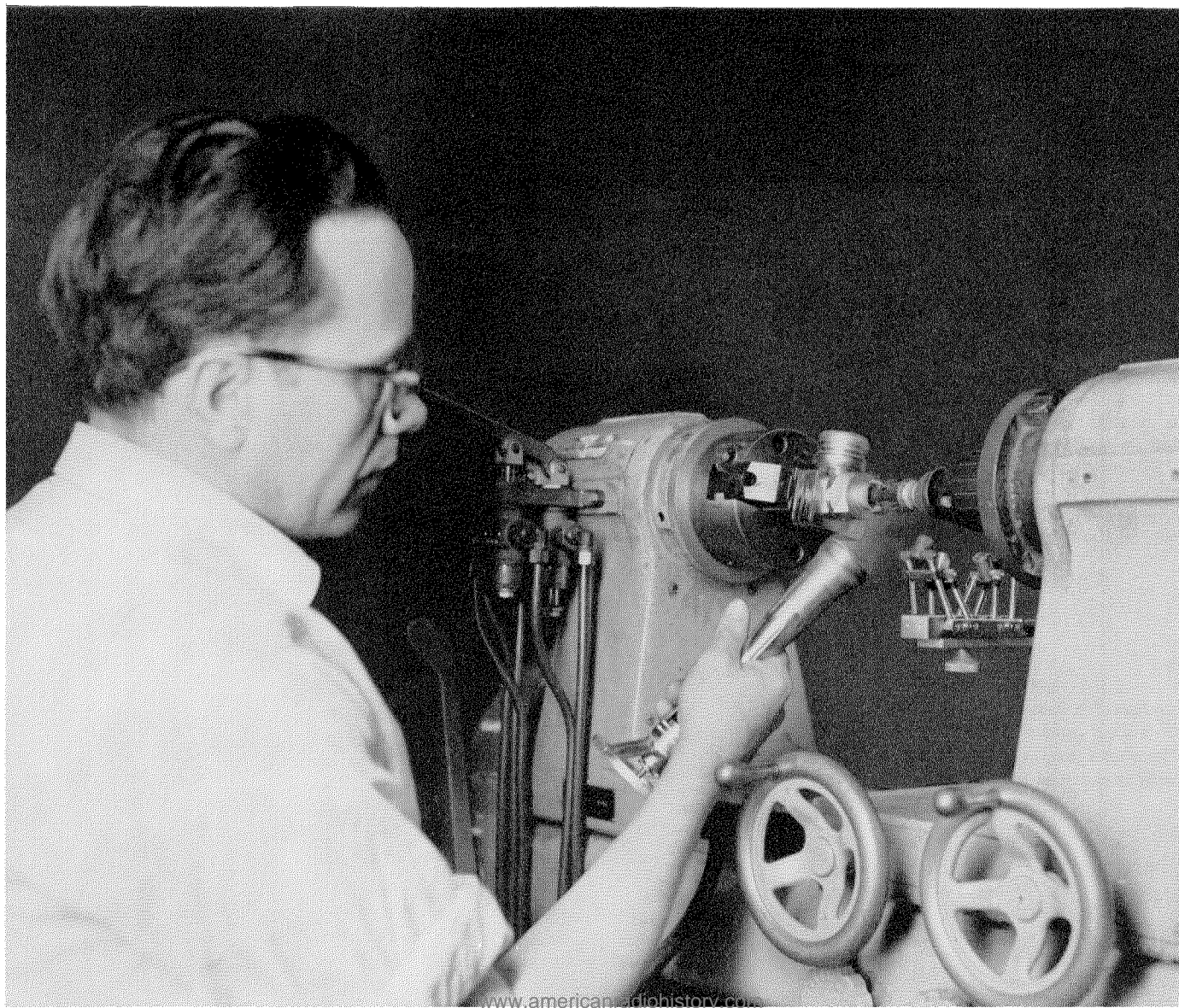
15. At the right, the white-hot interior of a brazing oven shows an anode assembly in process. The flame barrier was momentarily interrupted for this picture.

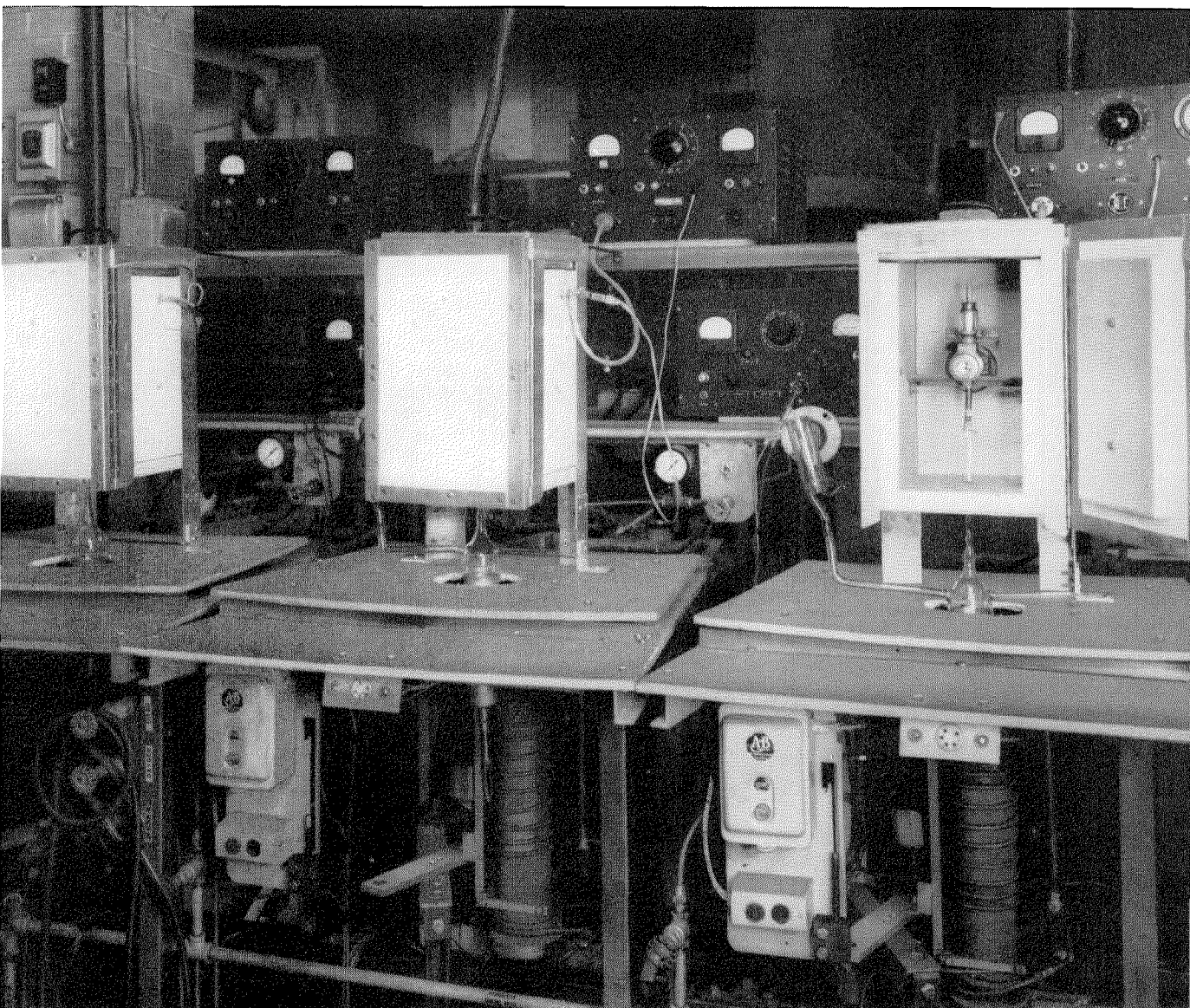


16. An anode assembly after all brazing operations have been completed.

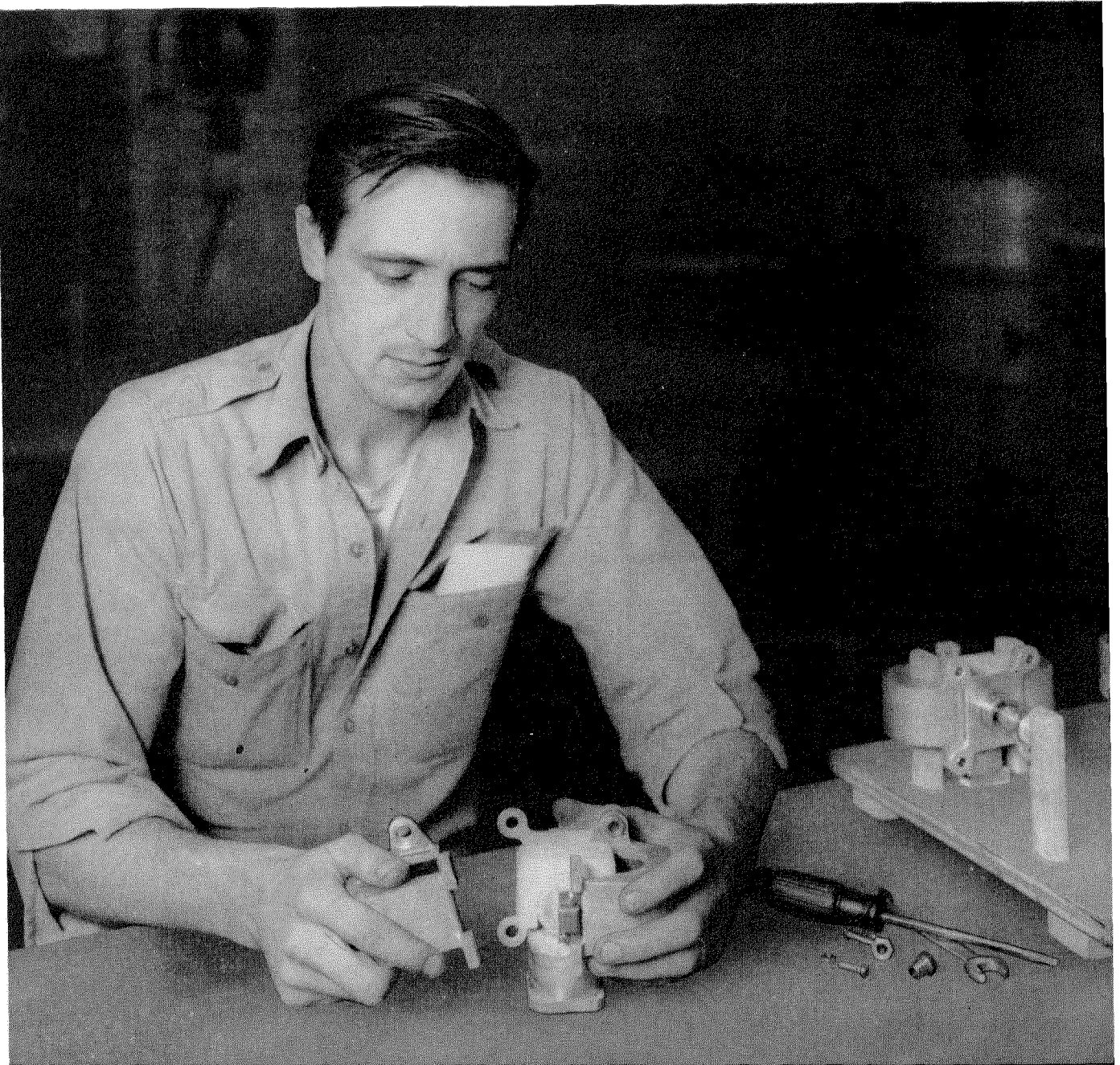


17. The photograph below shows a glass-lathe operator in the process of fusing together the completed anode and cathode assemblies. The operator is preheating the glass skirt on the cathode preparatory to making the seal.



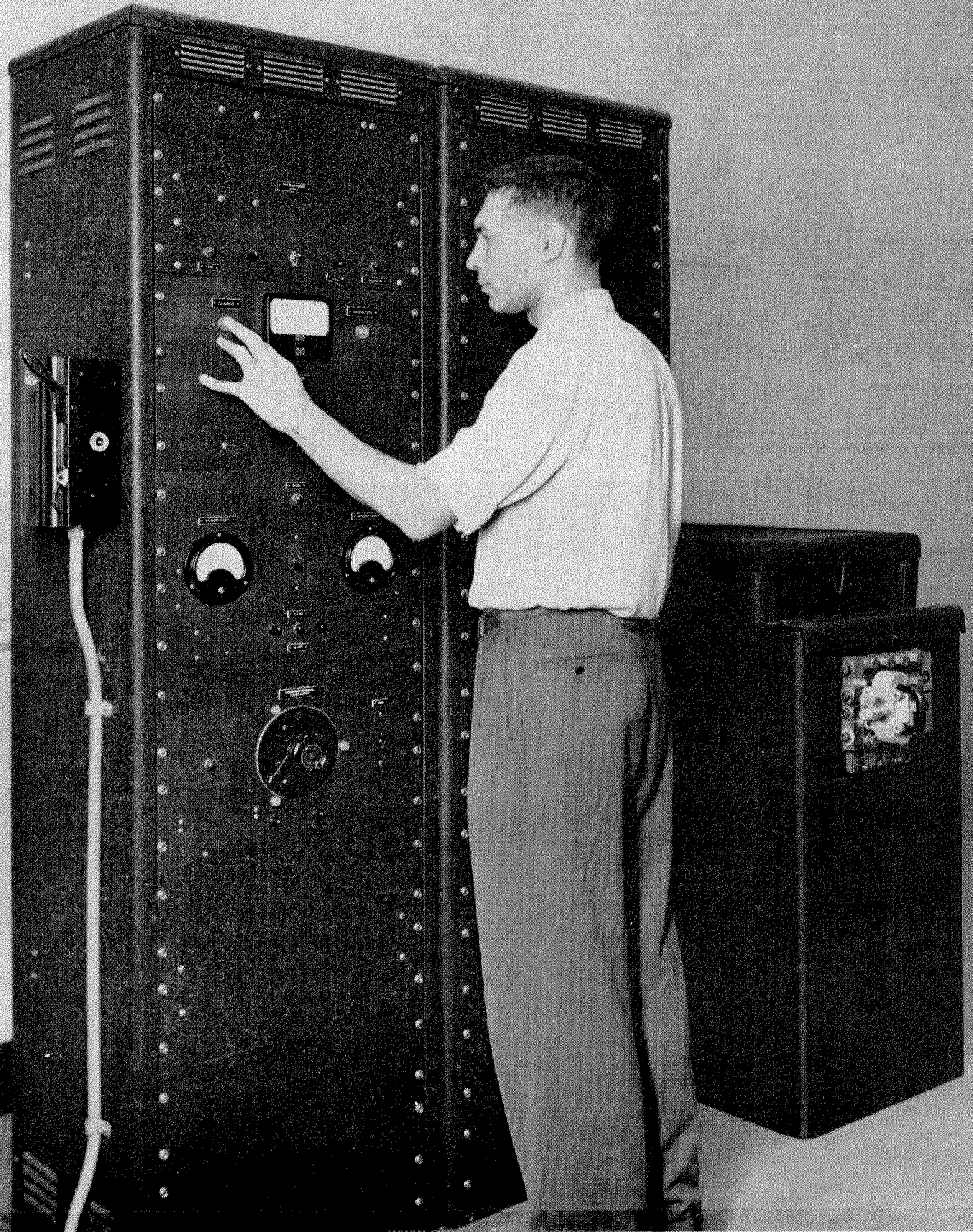


18. Three of the magnetron exhaust stations are shown here. After step 17, the tube is vacuum-tight, and the next operation is to evacuate the tube and activate the cathode. The oil-diffusion and mechanical backing pumps are mounted below the tables. A manometer gauge that electrically measures the degree of vacuum is also connected to the exhaust manifold. Indications of temperature and input power to the magnetron are displayed on the meters on the shelves to the rear.

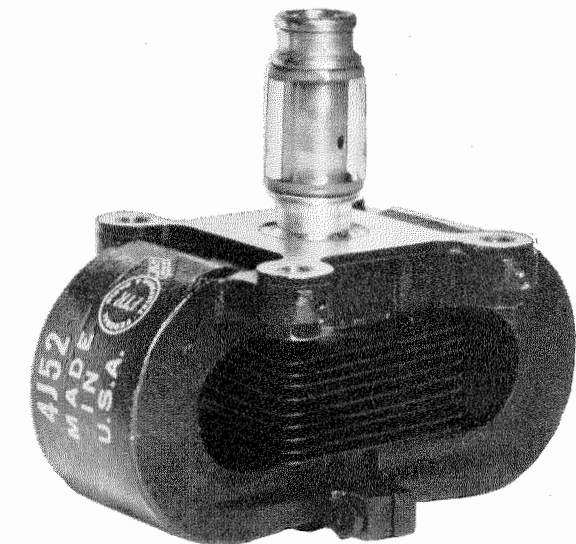
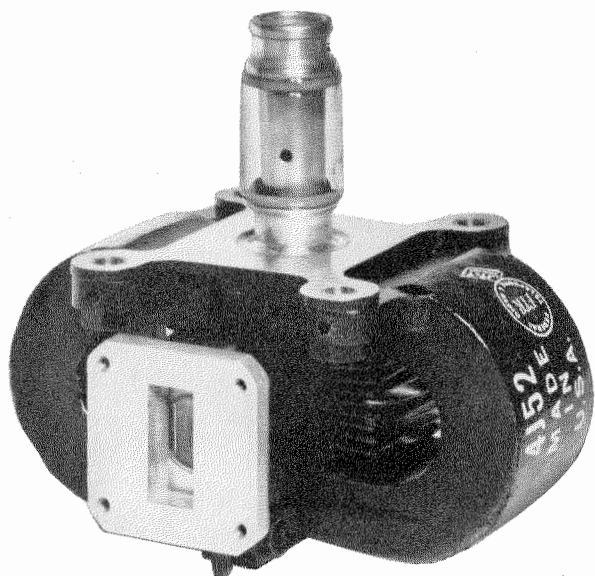


19. After exhaust, the next step is to assemble the magnets on the tube. An output section of waveguide is also soft-soldered over the waveguide glass window.

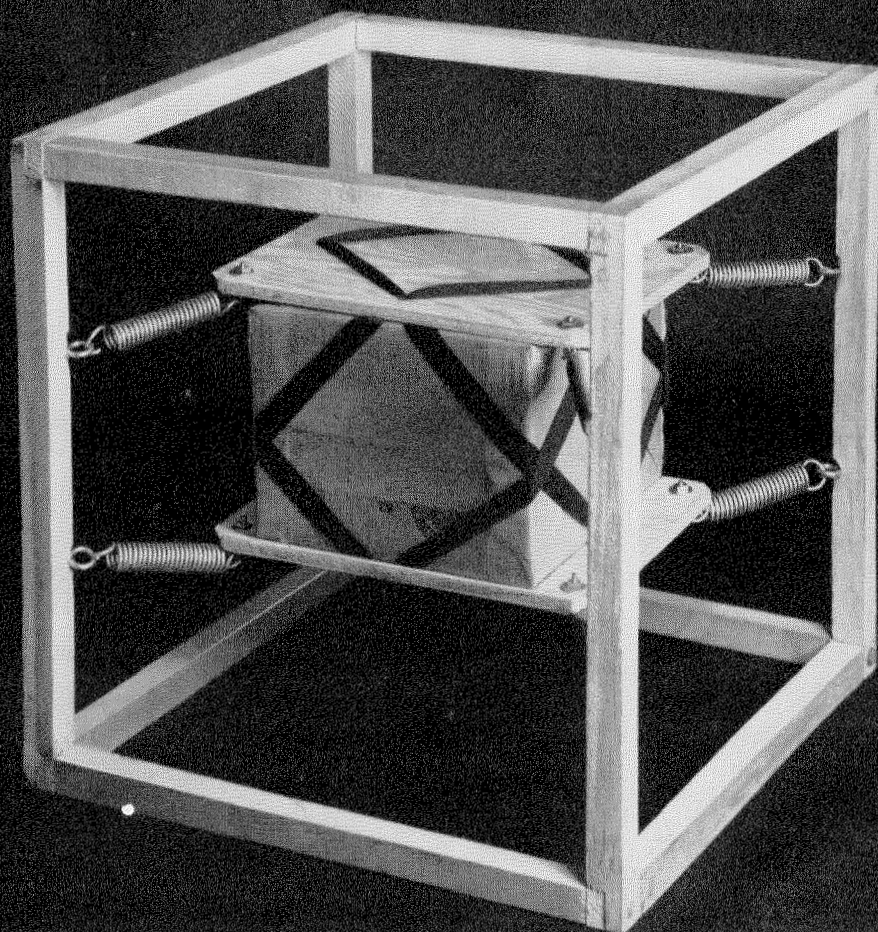
20. The alnico V magnets as obtained are not activated, and the charging operation on the facing page is performed after assembly. The magnetron is placed at the output terminals (right) of the charging device. A heavy copper bar is looped through the magnet. In the cabinets of the charging device a very large capacitor is charged to several thousand volts. When the capacitor is discharged through the copper loop, a current of thousands of amperes flows in a pulse that charges the magnet.



21. Two views of the finished *4J52* magnetron that has been completely tested (see frontispiece) and is now ready for shipment.



22. The tube is packaged in a cardboard carton that is suspended by springs in the center of a wooden framework. This prevents shocks from damaging the tube. A heavy cardboard carton (not shown) slips over the framework.



Temperature Regulator Used in Producing Germanium Crystals*

By G. J. LEHMANN

Laboratoire Central de Télécommunications and Société des Servomécanismes Electroniques; Paris, France

and C. A. MEULEAU

Laboratoire Central de Télécommunications; Paris, France

PREPARATION of large single crystals of germanium is an early stage in the manufacture of diodes and triodes.

After describing the construction of the high-frequency furnace and an electronic temperature regulator, a process for stabilizing the servo-mechanism and a method of adjusting the correction network are indicated.

Finally, the essential results are mentioned, particularly the stabilization of a temperature near 930 degrees centigrade to within ± 0.16 degree.

. . .

1. Problem

An early stage in the manufacture of germanium diodes and triodes is the preparation of a metallic ingot having predetermined characteristics; the resistivity, for instance, must be within certain narrow limits and is a function of the degree of purity of the metal.

Regardless of whether it is desired to produce point-contact or junction diodes or triodes, it is accepted that the ingot should be a single crystal. In addition, it is important that the crystal be as free as possible of lattice defects and that its characteristics be homogeneous from one point to another.

Various processes exist for obtaining single crystals. One of them, with which this article is particularly concerned, consists in melting the metal and placing a piece of a crystal in contact with the surface of the liquid to serve as a seed. When the temperature and speed with which the seed is withdrawn are suitable, a crystal develops between the seed and the liquid. This crystal has the crystallographic orientation of the initial seed.¹ Such an arrangement is shown in Figure 1.

* Reprinted from *L'Onde Electrique*, volume 33, pages 678-683; December, 1953.

¹ L. Roth and W. E. Taylor, "Preparation of Germanium Single Crystals," *Proceedings of the IRE*, volume 40, pages 1338-1341; November, 1952.

The properties required for useful crystals can be obtained only by a very strict control of the growth conditions, one essential element being the crucible temperature, close to 930 degrees centigrade. Temperature instability causes small-scale fluctuations of the properties of the metal that may make the crystal unsuitable for some of the desired uses.

Further, the making of good *np* junctions requires a very accurate control of temperature. We may recall that germanium is of the so-called *n* type when it contains a dominant impurity of the fifth group of the periodic chart of elements (such as arsenic or antimony, for instance) at a generally very low concentration of the order of one part in 10^8 . It is said to belong to the *p* type when the impurity is, for instance, boron, gallium, or indium, which belong to the third group.

An *np* junction may be obtained by introducing during the growth of the crystal a suitable impurity in the pool of molten metal. This operation is effected conveniently when the crystal is produced in accordance with the process described above.

Basic to the manufacture of junction-type transistors are the *npn* junctions, which are produced in the same manner. The intermediate layer has a very small thickness, expressed in hundredths of a millimeter. At the time when the junctions are effected, it is necessary to have a perfect control of the growth conditions for the crystal. These conditions depend essentially on temperature and are generally different at that moment when the *p* layer is formed than they are the rest of the time. In other words, it must be possible to control the temperature precisely in accordance with a predetermined schedule.

These two requirements, a high temperature stability and its precise variation according to

a predetermined schedule, are obtained in a furnace designed for this purpose.

The active portion of the furnace is represented in Figure 1 and comprises a graphite crucible that is heated by high-frequency currents, a temperature-sensitive resistor mounted in the wall of the crucible and connected in a

bridge circuit so that an unbalanced condition actuates the temperature-control system, and a thermocouple to indicate the temperature at any instant and also permit its continuous recording.

2. Apparatus Assembly

Figure 2 shows the general arrangement of the apparatus. To the left is the error detector, consisting of a thermosensitive resistor as one arm of a bridge. At the terminals of this bridge, supplied with 50-cycle-per-second alternating current at 4 volts, the error voltage appears as a carrierless amplitude-modulated signal. In normal operation, the amplitude of this signal is of the order of 10 microvolts.

The measuring bridge and thermosensitive element together with the stabilizing network of the servomechanism are the only components of the apparatus that had to be designed and built especially for the solution of the problem set forth here. All the other elements are production parts and were designed and manufactured in advance for use in various equipments.

The error signal is directed toward the demodulator and preamplifier, which consists of

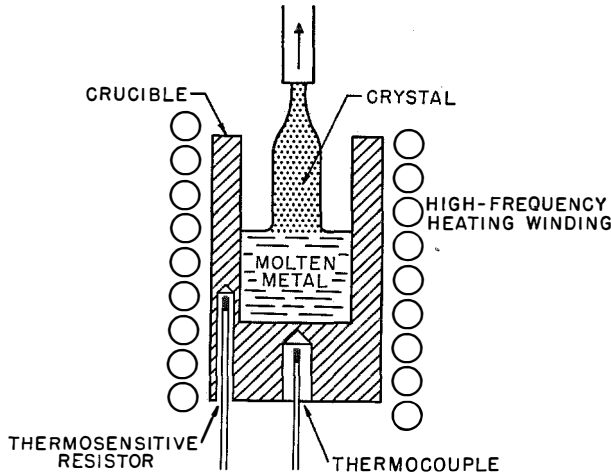


Figure 1—High-frequency furnace for melting germanium. Temperature is controlled by a bridge arrangement, the thermosensitive element being mounted in the wall of the crucible near the molten metal. The thermocouple permits continuous recording of temperature.

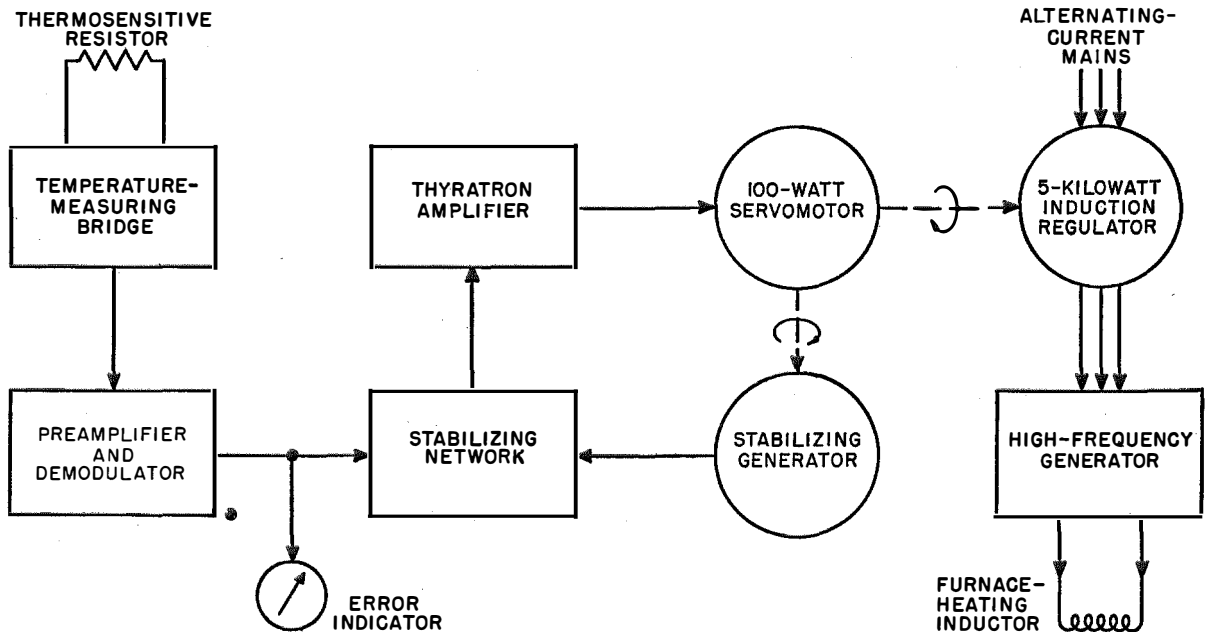


Figure 2—Arrangement for controlling the temperature of the high-frequency furnace. The thermosensitive resistor of the bridge is placed in the crucible in which the germanium is melted.

an alternating-current-signal amplifier with two electronic stages and a balanced demodulator using semiconductor-type rectifiers.

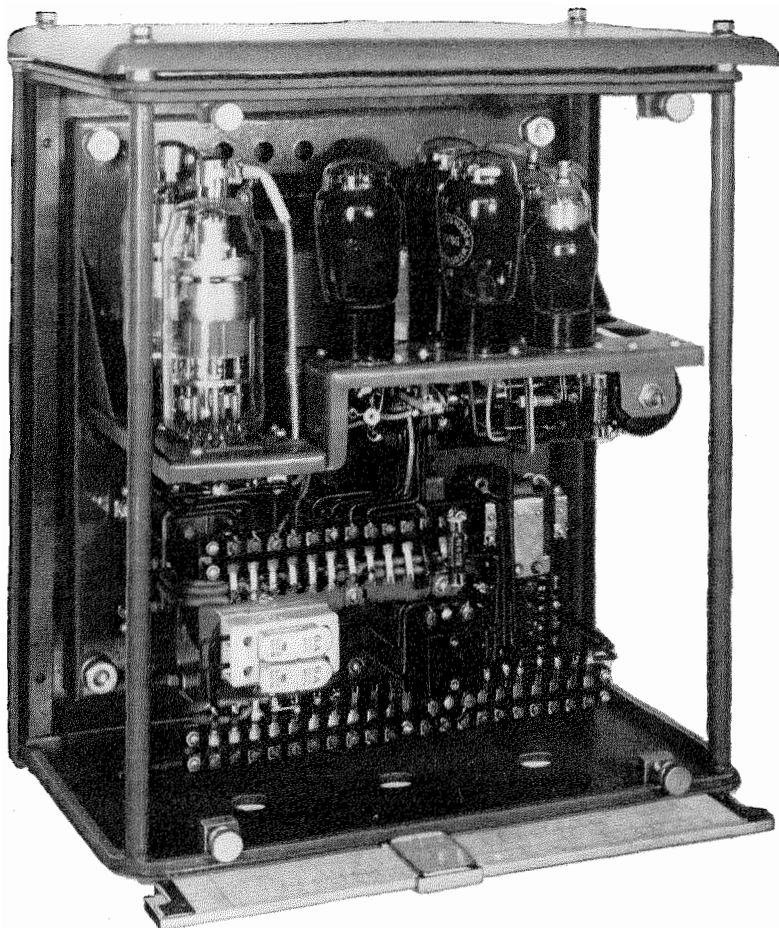


Figure 3—Main electronic amplifier capable of supplying 300 watts to the servomotor.

The error-signal output of this rectifier is a direct voltage of the order of magnitude of 1 volt across a 2000-ohm impedance.

Before being applied to the input of the main amplifier, the error signal goes through the correcting network where it is added to the signal from the stabilizing generator.

A secondary stabilizing loop is thus constituted.

The main electronic amplifier² consists of a

²G. Lehmann, "Rotary Amplifiers in Servomechanisms," *Electrical Communication*, volume 30, pages 12-25; March, 1953; also "Les Dynamos Amplificatrices leur emploi dans les Servomecanismes," *L'Onde Electrique*, volume 32, pages 78-88; March, 1952; and *Bulletin de la Société Française des Electriciens*, volume 2, pages 198-209; April, 1952.

direct-current stage followed by a reversible amplifier equipped with two 3868A thyatron tubes rated at 3 amperes. It is shown in Figure 3. The output signal, which may have a peak power of 300 watts, is applied to a 100-watt servomotor.

This servomotor drives the stabilizing generator by direct coupling and also drives through a reduction coupling the rotor of an induction regulator of 5-kilowatt rating.

The rotation of the latter controls the anode voltage of a 5-kilowatt radio-frequency vacuum-tube generator that supplies power to a high-frequency induction furnace in which the germanium is melted.

Thus the main loop of the servomechanism is closed.

3. Regulation Principle and Control Apparatus

3.1 THERMOSENSITIVE ELEMENT

The simplest method of controlling the temperature would be to obtain from the thermosensitive element an alternating error voltage capable of being directly amplified. A practical way of doing this is to have the thermosensitive resistor constitute one arm of a Wheatstone bridge supplied from a 50-cycle source.

The thermosensitive resistor itself had to be developed. Various pure and alloyed metals were tried, particularly platinum. The latter was obtained in various grades ranging from "commercially pure" to "pure, for thermocouples."

Unfortunately, these samples did not behave satisfactorily at temperature of about 1000 degrees centigrade. A rapid crystallization was observed, causing a resistance increase that could be noted every hour and generally terminated in breaking of the wire.

To save the time that would have been required to investigate other platinum samples

that might have been obtained, molybdenum was selected as it can be used in the inert atmosphere of the furnace. It is known, however, that a molybdenum wire heated to a high temperature contracts in length and a winding over a rigid refractory core would break under the operating conditions. In addition, even apart from this drawback, the electrical resistance would drift with time. A satisfactory solution was obtained by allowing a small strand of molybdenum wire to age for about 100 hours in one of the hydrogen furnaces at the laboratories. These furnaces operate at about 1100 degrees centigrade.

The resistor should have very small dimensions for this application. It was made of 30 centimeters (11.8 inches) of aged 0.05-millimeter (0.002-inch) molybdenum wire wound on a sintered alumina rod that was 2 millimeters (0.08 inch) in diameter. The turns do not touch but are very closely spaced, the length of the winding being about 6 millimeters (0.24 inch). The connecting wires are 0.4 millimeter (0.016 inch) in diameter and are of nickel. The ends of the molybdenum wire are electrically welded to two small nickel collars. The turns of the resistive wire are held in place by a very thin and slightly sintered alumina layer.

It will be noted in Figure 1 that this resistor is inserted in the wall of the crucible in such a position that it responds rapidly to the variations in the power induced in crucible by eddy currents. Otherwise the response would involve a time delay that would be detrimental to the accuracy of the regulator.

3.2 BRIDGE AND MANUAL CONTROLS

A desk within reach of the operator contains in addition to the control knobs for the equipment a Wheatstone bridge having several elements that may be adjusted by the operator. The circuit arrangement may be seen in Figure 4.

The thermosensitive resistor $R1$ has a value of 11.5 ohms at 20 degrees centigrade and about 60 ohms when hot. The resistances $R2$ and $R3$ being equal, $P1$ was made 500 ohms and $R4$ was made 82 ohms.

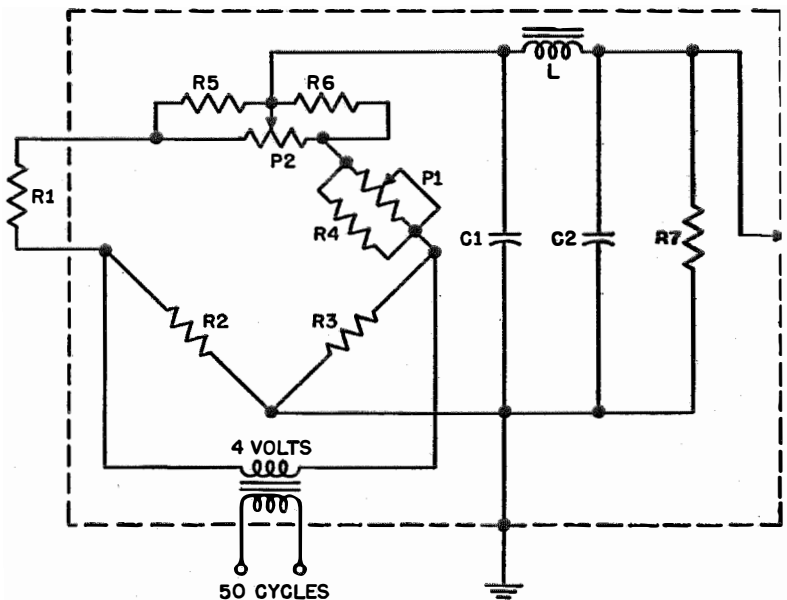


Figure 4—Diagram of temperature-measuring Wheatstone bridge.

The variable arm $P1$ is calibrated in terms of temperature by comparison with a thermocouple. The resistance $R4$ makes the variation extremely smooth between 900 and 1000 degrees centigrade with a possibility of evaluating 1 degree.

The 50-ohm variable resistor $P2$, also smoothed over half its track by two 5-ohm resistances, $R5$ and $R6$, allows a fine adjustment within 1 degree with a possibility of evaluating 0.1 degree over a range of ± 10 degrees.

The filter offers no special features; it passes a frequency of 50 cycles per second, cutting off the higher frequencies from the oscillator.

The line connecting the desk with the pre-amplifier is a few meters long and had to be carefully shielded to prevent the overloading of the amplifier by excessive high-frequency stray voltages.

The direct voltage obtained by amplification and demodulation of the error voltage is sent back to the desk to be read there on a zero-center instrument so as to check the temperature stability during operation and to allow the

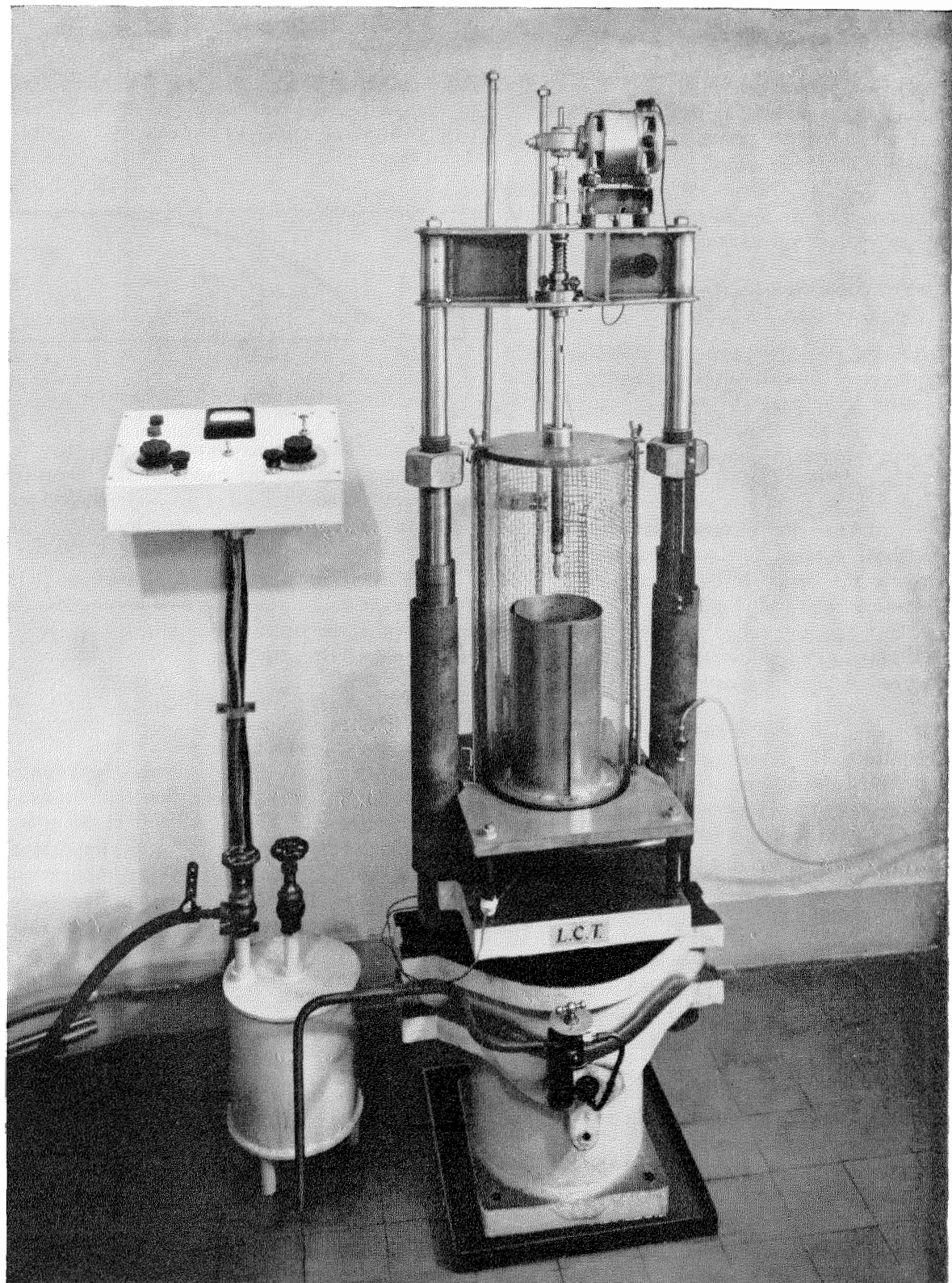


Figure 5—Furnace and control desk.

servomechanism to be put in operation when the error voltage is very small.

It should also be noted that the resistive elements of the bridge should have a very low temperature coefficient. It would be possible, if necessary, to provide means to control the temperature of the desk casing.

Figure 5 shows the assembly of the furnace used for producing single germanium crystals. The control desk is attached to the wall.

4. Stabilization, Adjustment of the Servomechanism

Study of the problem of stabilizing the regulator starts with an examination of the transmission ratio in the main loop, which is open as is the auxiliary loop.

As may be seen in Figure 2, this ratio is made up of the product of three terms.

A. The ratio of the electric elements, i.e. the ratio of the current flowing through the servomotor to the error voltage supplied by the temperature-measuring bridge.

In the frequency range involved (from 0 to approximately 2 cycles), this ratio may be considered as being a constant real number.

B. The ratio of the angle of rotation of the servomotor to the current flowing through it.

For use in the approximate theoretical study that precedes the experimental development of an equipment, this ratio may be taken as being equal to K/p^2 , where K is a constant and p is the complex variable.

For the conditions under which a series-excited servomotor operates, the electromagnetic torque is substantially proportional to the current; in the frequency range involved in the stabilizing action the stresses due to the inertia of the rotor predominate; hence the $1/p^2$ law.

C. The ratio of the error voltage from the temperature-measuring bridge to the angle of the induction regulator or servomotor.

This ratio is entirely controlled by the thermal phenomena taking place inside the furnace.

An inspection of Figure 1 shows that there are two main phenomena: a propagation inside the crucible wall of the temperature variations

originating at its outer surface and the effects of the thermal inertia of the germanium mass.

The temperature variations originate on the outer surface of the crucible wall due to changes in the high-frequency heating currents. These variations are propagated through the crucible

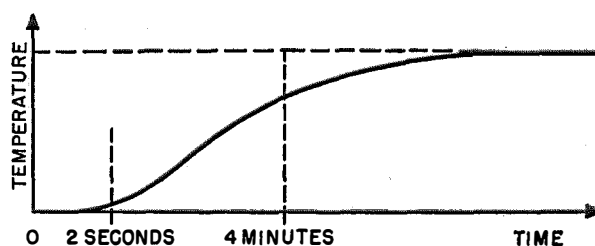


Figure 6—Transient response of the furnace alone.

wall to the thermosensitive resistor and then to the mass of molten germanium. The analytic aspect of the phenomenon of propagation of temperature variations has been known since Fourier's work.³

Without going into a detailed analysis, it is known⁴ that the presence of a heat propagation is translated in the transmission ratio by the presence of a factor of the form

$$\exp [-(T_1 p)^{1/2}],$$

T_1 being the propagation time constant.

Due to the actual construction of the furnace and to the location chosen for the thermosensitive resistor, T_1 has a low value of the order of magnitude of 10 seconds. It is most important to decrease the effects of such propagation phenomena as they introduce insurmountable limitations in the precision of the servomechanisms.⁵

The presence in the crucible of an important mass of liquid germanium introduces in the thermal transmission ratio a term of the form

$$\frac{1}{1 + T_2 p},$$

³ "Généralités Tome 1," Techniques de l'Ingénieur, Paris, France; 1952; page A-575-12—Transmission de la chaleur, régime variable.

⁴ Y. Chu, "Feedback Control Systems with Dead Time Lag or Distributed Lag by Root-Locus Method," *Transactions of the American Institute of Electrical Engineers*, Part 2, volume 71, pages 291-296; November, 1952.

⁵ G. Lehmann, "Note sur la Précision Maximum des Servomécanismes Parfaitement Stables," *L'Onde Electrique*, volume 30, pages 267-270; June, 1950.

T_2 being the main time constant of the system while T_1 concerns only the propagation in the solid wall of the crucible. The value of T_2 is of the order of 4 minutes.

The thermal transmission ratio should thus be of the form

$$\rho_{th} = K[1/(1 + T_2p) \exp[-(T_1p)^{1/2}]].$$

The complexity of the crucible makes a detailed theoretical analysis of the thermal transmission ratio useless, and after the above brief analysis an actual experiment was carried out to get closer to actual facts.

It consisted in suddenly modifying (step function) the heating current through the furnace and recording the transient response of voltage output of the temperature-measuring bridge. Figure 6 shows the shape of the recordings thus obtained, which cannot be reproduced easily to scale. They lead to giving the propagation time T_1 a value of the order of 10 seconds and to the time constant T_2 for the whole furnace a value of 4 minutes.

From this approximate analysis, the transmission ratio for the main loop may be put in the form

$$\rho = \frac{K \exp[-(T_1p)^{1/2}]}{p^2 (1 + T_2p)}$$

The adjusting method used by the Société des Servomécanismes Electroniques then consists in starting from the above expression to establish the principle diagram of the corrective network, which is set up in a provisional form by making

certain resistors variable to permit final adjustments to be made experimentally and thus obtain the desired result.

Figure 7 shows the stabilizing network inserted in the return circuit of the auxiliary loop; it comprises a total of 8 elements.

Provisional values of bridge elements are derived from preliminary runs made with open loops, and the final values are adjusted experimentally by observing the behavior of the regulator under actual operating conditions.

The efficiency of this method may be measured by the fact that the adjustment of the servomechanism effected in this manner did not require more than three days of work, thus adding only in a minor way to the over-all cost of the installation.

After this adjustment had been carried out, the temperature variations measured with the temperature-measuring bridge did not exceed $\pm \frac{1}{8}$ of 1 degree centigrade with variations of 10 percent in the mains voltage being frequently noted in the laboratory due to switching of heavy equipments that often share the same power-supply lines.

Actually, the exact temperature variations of the liquid germanium are certainly still lower due to the arrangement of the crucible. The response time for the entire servomechanism is 10 seconds with a good damping of the transient response.

These results meet the conditions required for the production of germanium crystals.

5. Results and Conclusions

As regards temperature regulation, the results were exactly those expected.

In the first place, what may be termed the short-period stability is better than $\pm \frac{1}{8}$ of 1 degree centigrade. This means that fluctuations in the mains voltage, in particular, which occur several times a minute do not cause a temperature variation higher than this value. Such a variation is visible on the voltmeter of the control desk.

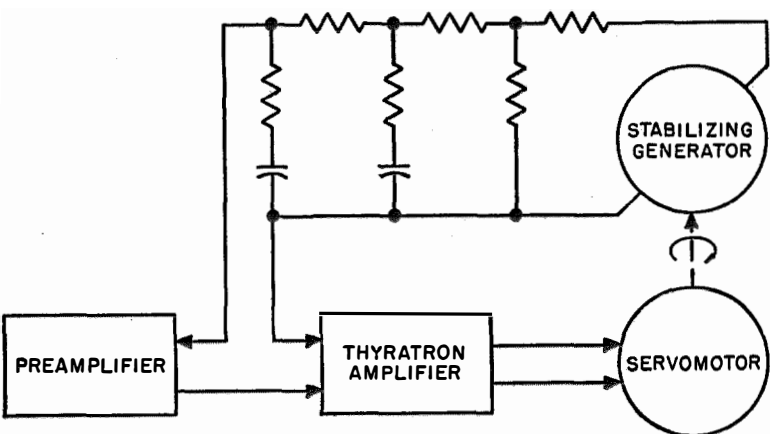


Figure 7—Stabilizing network in auxiliary feedback loop.

Practically, variations are lower than this limit and are still further attenuated in being transmitted to the molten metal due to thermal inertia.

As regards long-term stability, i.e. the slow drifting of temperature, it is dependent on the care taken in the construction of the measuring bridge and of the temperature-sensitive resistor. The nature of the work carried out may tolerate at the worst a variation of 1 degree centigrade during several hours of operation, and this stability was obtained without any special precautions. The thermocouple, which indicates temperature variations of 1 degree centigrade, does not detect any drifting of this order during the growth of a crystal, except during the very last moments. This variation, however, cannot be attributed to the regulating system. It should be noted that the thermocouple measures the temperature at some distance from the thermosensitive resistor. The latter keeps fulfilling its function but, when the crucible is almost empty and the crystalized germanium represents a large percentage of the initial material the heat losses due to radiation and conduction are modified and the difference between the respective indications of the thermosensitive resistor and the thermocouple is also slightly modified. This does not cause any trouble in producing crystals.

The process requires a temperature-variation program involving changes of the order of +5, -15 degrees, etc., which is determined by the two potentiometers.

The thermocouple begins to respond to these orders after about 10 seconds and stabilizes at the new value within a time of the order of 1 minute. These temperature changes are effected without any tentative adjustments, a char-

acteristic that makes the apparatus extremely practical.

It would be quite feasible to add a mechanical system to adjust the bridge elements automatically and thus institute a predetermined temperature schedule.

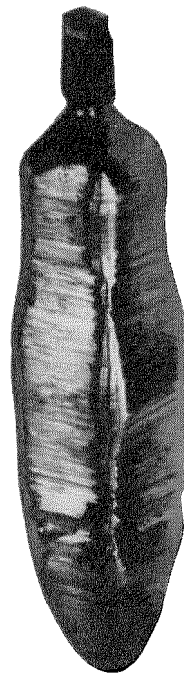


Figure 8—A single crystal of germanium produced in the furnace.

By way of example, there is shown in Figure 8 one of the single crystals of germanium that developed in a very satisfactory manner along the quaternary axis of the cube (1.0.0 axis). Its section is substantially square.

The striations are elements of parallel facets, as may be seen by reflecting light under a suitable angle. Physical measurements carried out on such crystals also demonstrate their high quality.

Electronic Generator for Operating Telephone Ringers

By G. H. BRODIE

Kellogg Switchboard and Supply Company, a division of International Telephone and Telegraph Corporation; Chicago, Illinois

TO MAKE the telephone effective as a means of voice communication, some method of signalling a distant station must be employed. This is accomplished in most cases by the sounding of the ringer bells associated with the distant telephone instrument. This ringer is operated by alternating or pulsating current of suitable voltage and frequency, which usually is placed on the line at the central office.

Where only a single telephone is used on each line, signalling is a rather simple matter; but if one line serves several stations, it becomes more involved. To avoid annoyance to other subscribers, only the ringer associated with the selected telephone instrument must be operated. Of the several methods or combinations of methods permitting single ringing on multiple-party lines, one of the more common arrangements makes use of mechanically tuned ringers, each of which will respond only to an electrical current of a specific frequency. With such ringers, it is customary to use a group of five frequencies within the range of 16 to $66\frac{2}{3}$ cycles per second, although any lesser number may be used as desired. These frequencies, which may be harmonically related within the same group, must be held within close tolerances. In this manner, maximum response from the desired ringer is obtained, and at the same time any tendency to cross ring on fundamental frequencies is reduced to a minimum.

Rotary generators supplying five predetermined and suitably controlled ringing frequencies are available and used to some extent, but chiefly because of high cost they have never been very generally accepted in the telephone field.

A static ringing-frequency converter that can supply the power-line frequency and four sub-multiples for a total of five ringing frequencies is also available. While this is a thoroughly practical device for certain applications, it lacks the frequency flexibility desirable for a general-purpose unit, and it is necessarily somewhat

heavy and expensive for use in exchanges of small to medium size.

More frequently, where tuned ringers are employed, ringing power is presently supplied by vibrating mechanical pole-changers or converters operated from the central-office battery. The simplified schematic of such a device is shown in Figure 1.

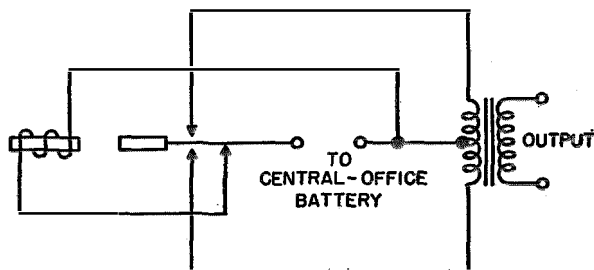


Figure 1—Schematic of a pole-changer source of ringing power.

These mechanical pole-changers, which have served the industry well for many years, offer the advantage of comparatively small initial investment. If properly adjusted, well maintained, and not overloaded, they give satisfactory service. On the other hand, the present demand for higher ringing voltages, along with greater power to handle the increased traffic and more heavily loaded lines, does tend to produce rapid erosion of the vibrator contacts and necessitates frequent adjustment and replacement. In addition, overloads may cause serious damage to the contacts with interruption of service. For these reasons, modern operating conditions call for an improved source of ringing power, although pole-changers still may serve satisfactorily as emergency equipment.

The development of an electronic ringing generator to produce up to five frequencies was undertaken to provide operating companies with a reliable source of multifrequency ringing power free from the maintenance problems and other disadvantages of the pole-changer, at little or no increase in cost.

1. Objectives

During the early stages of this development, the following objectives were set up for the proposed electronic ringing generator.

- A. Freedom from moving parts and from difficult adjustments.
- B. Reliability in operation with minimum maintenance over long periods.
- C. Ease of adjustment to the desired frequency.
- D. Frequency stability within $\frac{1}{3}$ cycle of the desired value under normal operating conditions.
- E. Delivery of full power* at each ringing frequency, regardless of simultaneous loads on other frequencies.
- F. Satisfactory regulation of output voltage with changes in load or in line voltage.
- G. Output waveform free from high-voltage transients and suitable for operating telephone ringers in an efficient manner.
- H. Construction and mounting compatible with other central-office equipment.
- I. Cost competitive with other sources of ringing power.

2. General Considerations

The idea of generating telephone ringing frequencies electronically is not new and it is known that work along these lines has been done in the past and is presently continuing in other laboratories. Nevertheless, we are unaware of any practical multifrequency electronic ringing system that previously was generally known or commercially available.

The reasons for previous lack of success probably lie in the high cost, inefficiency of power conversion, and in the complexity that results when one attempts to accomplish the desired objectives through use of conventional circuits and older types of power tubes.

As previously noted, any device that supplies power for

* Later determined to be approximately 20 watts with standard connections.

frequency-selective ringers must maintain its frequency very close to the assigned value under all operating conditions. Experience over many years has shown that average maximum deviations of $\pm \frac{1}{3}$ cycle do no appreciable harm, whereas deviations beyond this amount tend to cause operating difficulties that become more serious as the deviation increases.

While electronic frequency generators can be made extremely stable if desired, the order of stability required for ringing generators can be realized through good design in a simple and rugged circuit. To provide a degree of stability greater than is needed for this application would entail undesirable added cost and complexity.

Since considerable power is required, it is desirable for reasons of operating economy to obtain the highest possible over-all efficiency of power conversion. This suggests class-C amplification in the power output stage. However, to realize the benefits of good regulation and moderate plate voltage, the output tube should have the lowest possible plate impedance. Low impedance in this case goes hand in hand with low amplification, and such a tube would require excessive driving power to operate efficiently as a class-C amplifier. Thus, the over-all efficiency would be lower and the circuitry would be more involved.

It was felt that if a pair of very-low-impedance triodes of suitable power-handling capabilities could be utilized in a push-pull circuit in such a manner that the plate current could be turned on and off at the desired frequency without grid current being drawn, the basis for a practical and highly efficient ringing generator would be realized.

Fortunately, in the 6AS7 vacuum tube (or in one of its electrical equivalents), such a pair of triodes is available in a single envelope. This

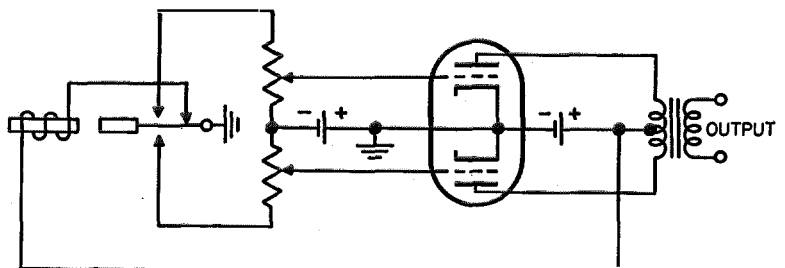


Figure 2—Schematic of a mechanical driving device.

tube is rather unique in that the plate resistance is very low (280 ohms for each triode section as compared with a more common value of several thousands) and the current carrying capacity is high (125 milliamperes per section).

The transconductance is high (7000 micro-mhos) and the amplification factor of 2 is low. By working this tube in an unconventional manner into a power output transformer having a high-inductance primary, it should be possible to realize a high order of efficiency when the plate-current flow in each section is periodically turned on and off by a negative potential on the grid. Since the grid would always be at least slightly negative with respect to the cathode, no grid current would flow and negligible driving power would be required.

It appeared further that a frequency-determining unit to place the desired cyclic negative potential on the grids of the 6AS7 or other suitable tube could be either mechanical or electronic.

3. Procedure

The schematic of a mechanical frequency-determining unit is shown in Figure 2. Experimental operation of a circuit of this type indicated that the output tube and its associated output transformer would perform as predicted. However, the idea of a mechanical driver was not developed further, since it was felt that the same results could be obtained more advantageously by electronic means.

An electronic driver unit was then developed and is shown together with the amplifier and output system in schematic form in Figure 3. This unit, which makes use of a 6SN7 (or its electrical equivalent) as a multivibrator, contains several unusual circuit variations to adapt it successfully to this particular application. It has the following features.

- A. Inherent frequency stability.
- B. Plug-in resistance-capacitance frequency-determining networks.
- C. Direct coupling to the power-tube grids.
- D. High-voltage push-pull output from a small twin triode.
- E. Low power consumption.

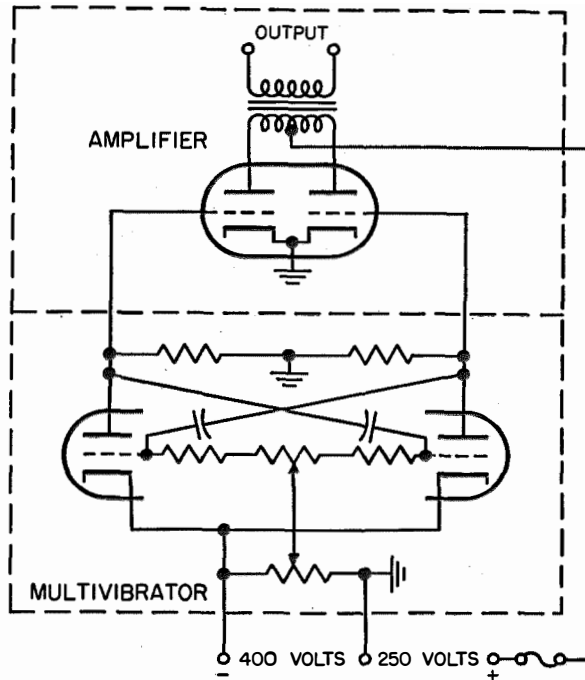


Figure 3—Multivibrator driver and amplifier comprising one frequency source for the ringing generator.

Thus, the basic electronic generator for each frequency consists essentially of two tubes, a source of power, the temperature-stabilized resistance-capacitance network, and the output transformer. Any one of these generators may be used by itself or as part of a group of two to five. A single power pack of moderate size can furnish plate and filament voltages for up to five frequency generators.

4. Results Obtained

In the electronic ringing generator, inherent frequency stability in the oscillator is attained through the use of stable resistive and capacitive components having the most favorable temperature coefficients available and used in a multivibrator circuit stabilized by a positive bias. The manner in which this positive bias increases stability is shown qualitatively in Figure 4. In the plot of capacitor-discharge voltage against time, curve *A* represents the "no-bias" condition. V_c is the point on the voltage discharge curve where the triode section, which has been cut off by the negative charge on the grid, begins to conduct. Because the discharge curve is approaching the horizontal at this point, even a

slight variation in V_c will have a considerable effect on the duration of the half cycle and hence on the frequency. With positive bias, as shown by curve *B*, V_c is reached before the curve

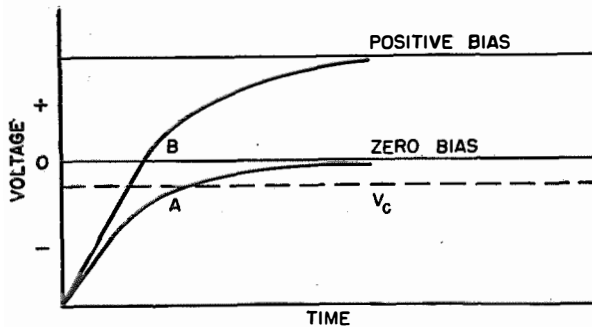
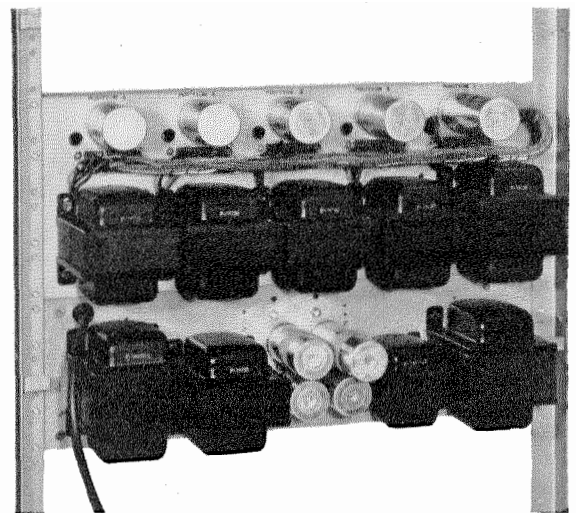
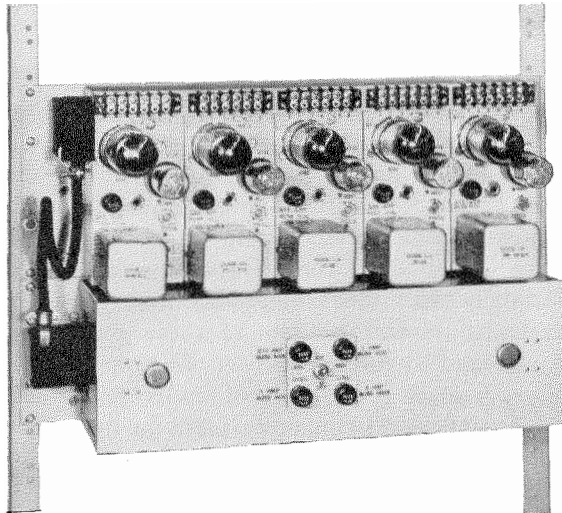


Figure 4—Capacitor-discharge curves for zero bias on the multivibrator grids (curve *A*) and for positive bias (curve *B*). V_c is the voltage at which the triode amplifier begins to conduct.



Figures 5 and 6—Front and rear views of 100 type electronic ringing generator.

begins to flatten to any marked extent. Consequently, small variations in V_c have only a very slight effect on the frequency and better stability results.

With the circuit arrangement described, satisfactory frequency stability is secured for applications subject to neither extreme temperature variations nor abnormal variations in the line voltage. Effective low-cost thermostatic controls are furnished where needed to provide good stability over a wider range of ambient temperature, and voltage regulation is available for installations subject to unusually wide variations in power-line voltage.

Following current practice, the power output transformers are designed to deliver approximately 105 volts on the lowest frequency in the series, gradually increasing with frequency to about 160 volts on the highest. These values, which are for moderate loads, may be varied considerably by selecting the most suitable tap on the secondary of each transformer.

While additional mounting arrangements may be used, the model now in production, which is known as the 100 type, is designed to mount compactly on a standard 19-inch (48-centimeter) relay rack as shown in Figures 5, 6, and 7.

5. Summary and Conclusions

Two years of laboratory and field testing of this equipment have shown that the objectives listed in section 1 have been reached and in some

respects surpassed. Along with freedom from vibrators, commutators, or other moving parts, the following additional advantages are offered.

- A. Operation is completely silent.
- B. Any individual frequency, as well as any number of frequencies up to five, may be used.
- C. Operation does not depend on close regulation of power-line frequency.
- D. Individual frequencies may be changed readily, if desired, and each one can be easily adjusted independently of the others.

E. Plug-in components and subassemblies facilitate rapid and easy maintenance.

F. Only 12½ inches (31 centimeters) of mounting space on a 19-inch (48-centimeter) rack is required for five frequency generators and their common power supply.

6. Acknowledgments

The author is indebted to Messrs. A. J. Radcliffe, W. C. Howe, E. N. Marsh, and other Kellogg engineers who made valuable contributions to the design and development of this equipment.

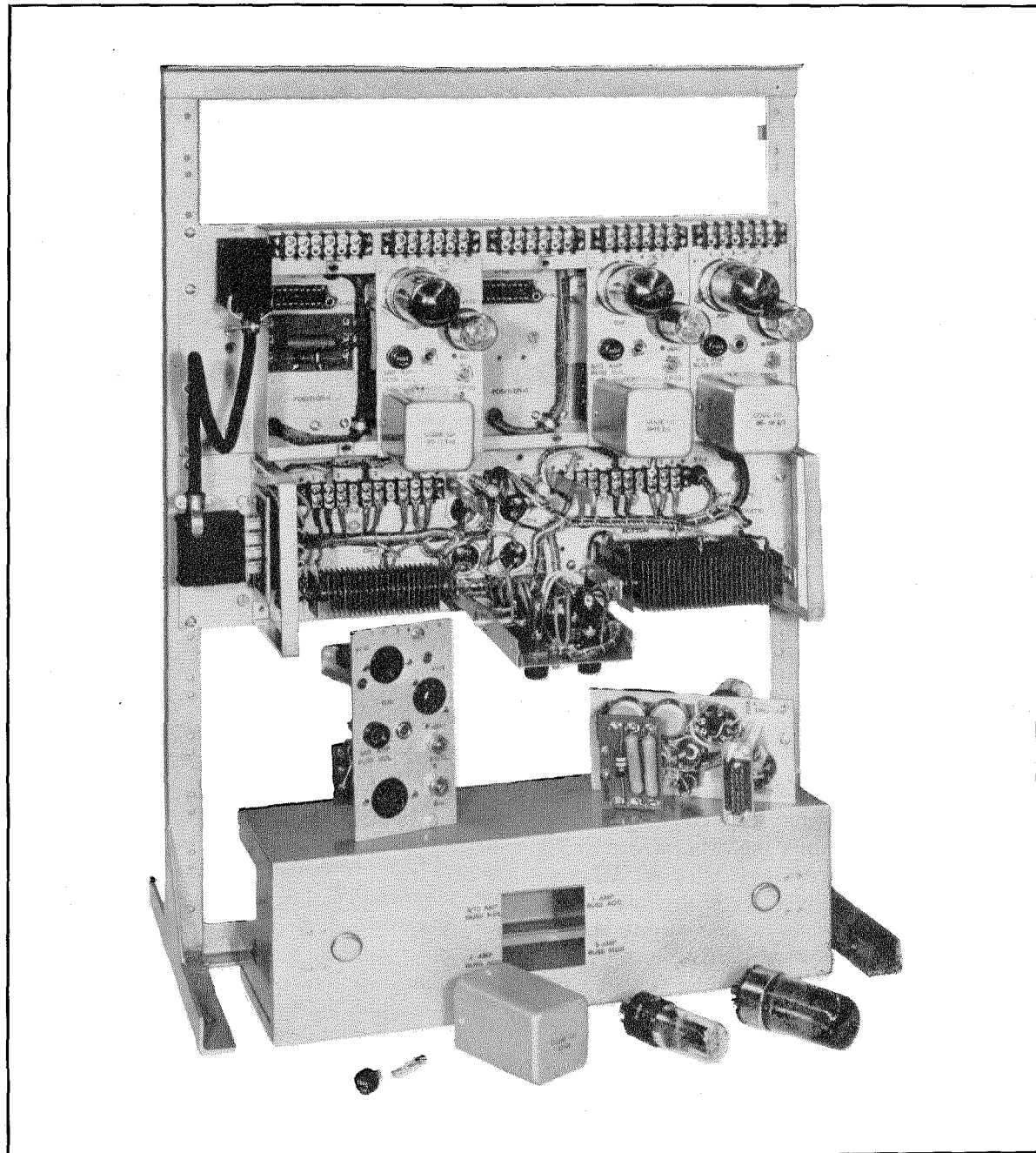


Figure 7—Front view with a number of plug-in assemblies removed.

Type-7 Crossbar Selector*

By R. W. HUTTON

*Kellogg Switchboard and Supply Company,
a division of International Telephone and Telegraph Corporation; Chicago, Illinois*

THE TYPE-7 crossbar selector is a mechanism for selecting one of several trunk groups in a dial telephone switching system. Each of these trunk groups may lead to a subsequent rank of group selectors, to connectors (final selectors), to outgoing trunks, or to one of several special services. Switching in this case is based on a system of decimal numbering; consequently the selector, in response to a single pull or digit of a telephone dial calling device, provides a choice of 1 trunk group out of 10. The selector consists of a group of relays, a magnetic impulse counter to register the digit, and certain permanently associated portions of several crossbar switches. Generally, each selector has access to 100 outlets, which are arranged in 10 groups of 10 paths each.

In modern telephone practice, it is widely recognized that even in small initial installations, such as a community dial office, group selectors are desirable and often a necessity to provide trunking flexibility. The ease of equipment growth thus gained is self-evident. With the advent of nationwide toll dialling and customer toll dialling, the area and exchange numbering plans frequently demand the use of so-called 2-5 numbering in the exchange, that is, 2 letters followed by 5 numerals. It is generally more practical and economical to accomplish this by the use of group selectors at the outset, and at the same time provide for an orderly growth beyond an initial equipment of say 60 or 80 line terminals. The fundamental operation of the type-7 selector and the division of available outlets into groups of 10 are based on well-known practices. However, the use of crossbar switches for estab-

lishing the selected path on a direct-access basis involves several details of operation that differ somewhat from those generally used in decimal systems. The following descriptions and illustrations are presented for the engineer and technician who are interested in the circuits,

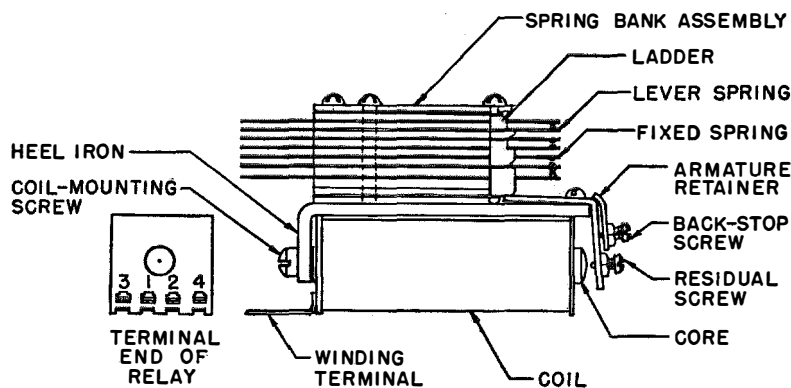


Figure 1—4000-type relay.

apparatus, and equipment arrangements employed.

1. Elements of Selector Equipment

The type-7 selector uses the 4000-type relay, which consists of a spring bank assembly, heel iron, relay coil, and armature assembly as shown in Figure 1. The spring bank assembly consists of contact springs, insulators, lifting cards (or ladders), and clamping plates. The contact springs have conventional terminals for soldered wire connections. The complete spring bank for a relay is clamped between 2 metallic plates and held by 3 screws. The spring bank is fastened to the heel iron by 2 assembly screws.

The winding of the relay coil is made up of layers of enamelled magnet wire with a sheet of cellulose acetate between adjacent layers. When the winding operation is completed, the protruding ends of the interleaved cellulose-acetate sheets are coalesced to seal the coil against entry of moisture.

* Reprinted from *Communication and Electronics*, number 10, pages 830-833; January, 1954.

The relay coil and spring bank are assembled to a conventional L-shaped heel iron, to which the armature assembly is also attached.

board, which is shown in Figure 2, has been in use for more than half a century. It should be noted that with a considerable number of lines, it is possible to connect any two of them together by connecting both to a commonly accessible link. For example; as shown in Figure 2, L-3 is connected to L-12.

The crossbar switch differs somewhat from other types of telephone switches, insofar as direct electric paths are established through precious-metal contacts with only 2 rapid relay-like operations. Associated apparatus that assists in making the connection is subsequently released for further calls. The crossbar switch, Figure 3, is composed of a formed metallic frame on which is mounted a multiple bank comprising a number of horizontal and vertical paths, the crosspoint selecting and establishing mechanisms, and magnets.

Located at the ends of the switch are 5 or 6 pairs of select magnets, each pair controlling the rotation of a select rod. The select rods span the distance between the switch-frame ends on the underside and carry a number of finger springs corresponding to the number of vertical-path elements the switch contains. Figure 4 shows how these finger springs actuate select levers, which are mounted on the armature assembly of each vertical element. When the switch is in an unoperated condition, each select lever rests between 2 adjacent ladders. When a select magnet is energized, the select rod rotates a few degrees, causing the finger springs to move each of the select levers under one of its adjacent ladders. The direction in which the select lever moves depends on which of its 2 controlling magnets is energized. When the select-rod action has taken place, Figure 4, the hold magnet of the appropriate vertical path is energized, operating its armature and causing the select lever to lift

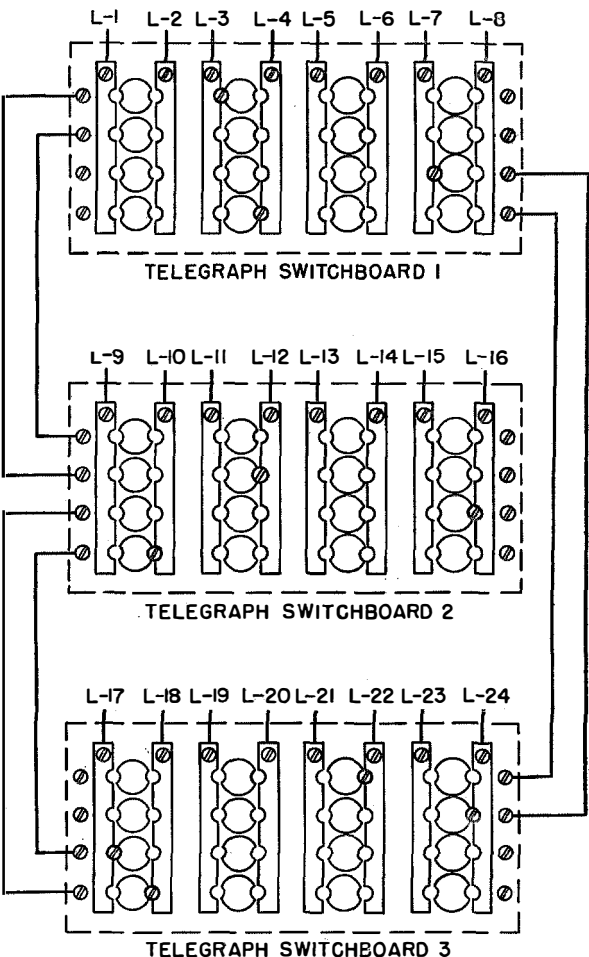
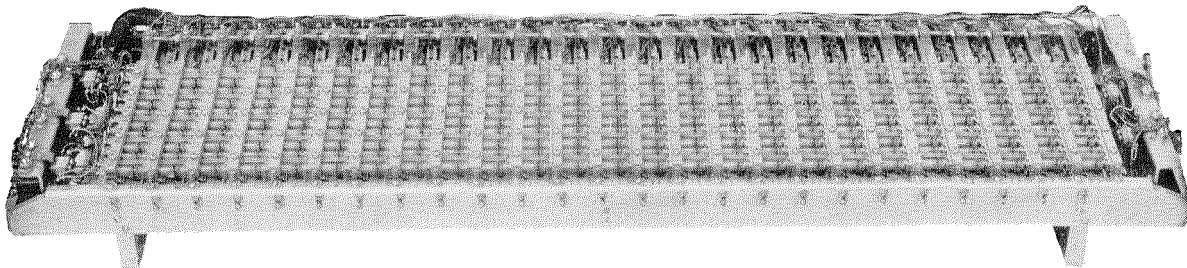


Figure 2—Peg-type telegraph switchboard. The lines are connected to vertical conducting strips and the circular conducting islands are connected in horizontal rows. Metallic pegs make contact between the crossbars.

Communication people have long understood the possibility of completing an electric path by connecting two crossed bars where they intersect. For example, the peg-type telegraph switch-

Figure 3—Below, a crossbar switch,



the ladder, closing the contacts of the selected vertical and horizontal paths. The select magnet is then released, restoring the select rod and all other finger springs to their normal positions, the switch is then available for another selection.

The hold-magnet armature remains operated until the subscriber releases the circuit.

The magnetic impulse counter pictured in Figure 5 is fundamentally a 2-step relay. However, instead of the usual single armature it has

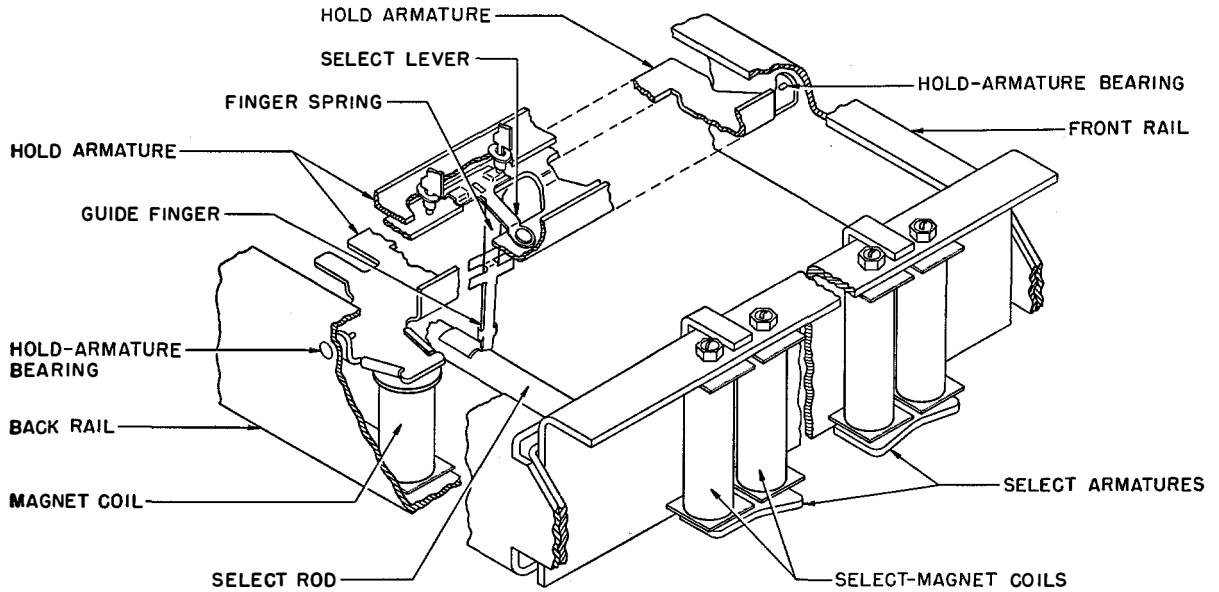


Figure 4—Select- and hold-magnet mechanism.

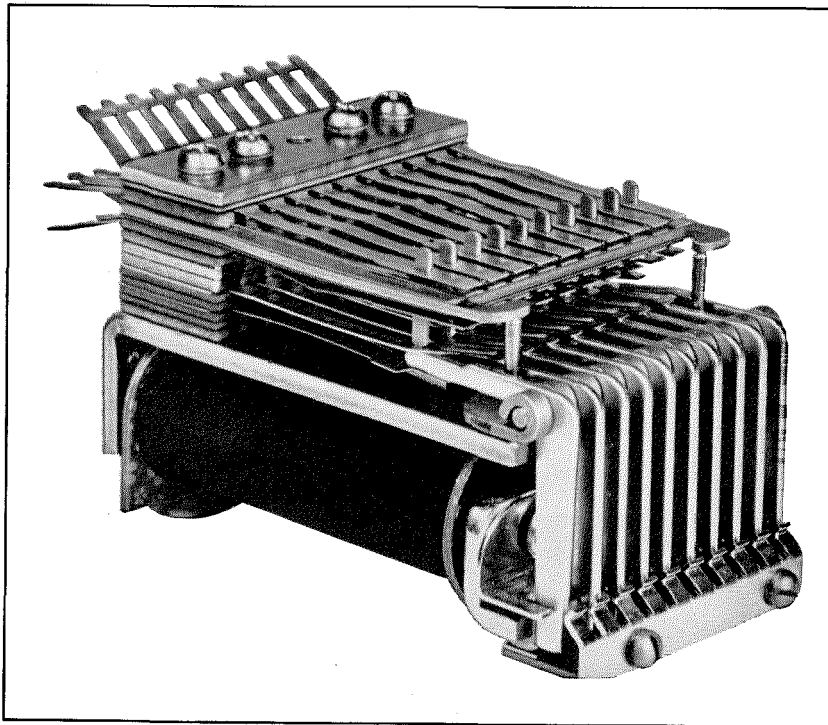


Figure 5—Magnetic impulse counter.

10 armatures. The armatures operate in sequence, each one responding to its respective pulse of current in the driving coil. Once operated, the armatures are held by the residual magnetism in the core. The counter is shown schematically in Figure 6.

The counter coil has in addition to its driving or pulsing winding, a second winding that is used to bring about the release of any operated armatures. Release is effected by passing direct current through the release winding in the proper direction to induce into the core a magnetic flux of opposite polarity to that induced by the

operating pulses. The release flux is of sufficient intensity to neutralize the residual flux left by the operating pulses, and the tension of the spring stacks is then sufficient to cause the armatures to restore to their normal positions.

Each armature acts on its own set, or stack, of contact springs, which are similar to the type of springs used in many conventional relays. The counter used in the type-7 group selector is equipped with 1 pair of normally closed contacts and 1 pair of normally open contacts in each of its 10 spring stacks.

2. Equipment Arrangement

The equipment used in the group-selecting stage of a type-7 office, shown diagrammatically in Figure 7, consists of the selector relay units, crossbar switches, and the common test circuits. Each selector relay unit has a group of relays and a magnetic impulse counter that perform the usual functions of digit registration, holding, etc. Also, each selector relay unit is permanently wired to a horizontal path of one or more crossbar switches, depending on the number of outlets required.

A test relay circuit is provided to serve each 12 selector relay units. It is capable of testing all paths in the selected group of outlets simultaneously, choosing the lowest numbered idle path, and directing the crossbar switch to

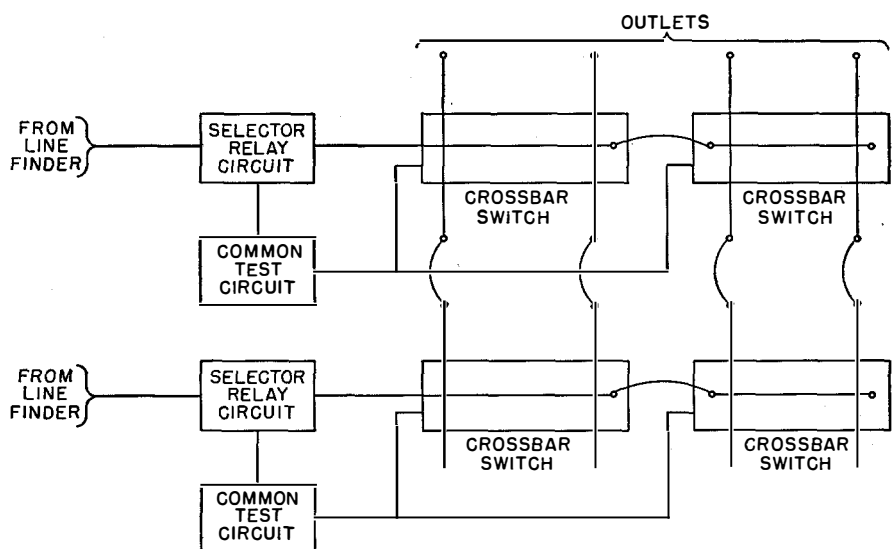


Figure 7—Block diagram of type-7 selector.

establish a connection to the chosen outlet. Such operation permits the trunks individually accessible to selectors of a group to be taken into use whenever available, reserving those commonly accessible to a greater number of selector groups for use when the individuals are all engaged.

3. Operation of Selector

Operation of the typical type-7 selector circuit is illustrated by Figure 8. The calling party lifting the telephone handset causes a selector to become associated with his line by way of a line finder. The selector relay unit returns dial tone to the calling party, indicating that it is prepared to receive signals from the telephone dial. The calling party dials the first digit of the number and the cut-through action of the selector is accomplished in the following manner.

The series relay, which operates on the first pulse, will release after the last pulse of the digit is received, extending ground through the off-normal contacts of the magnetic impulse counter to operate the chain relay of the selector.

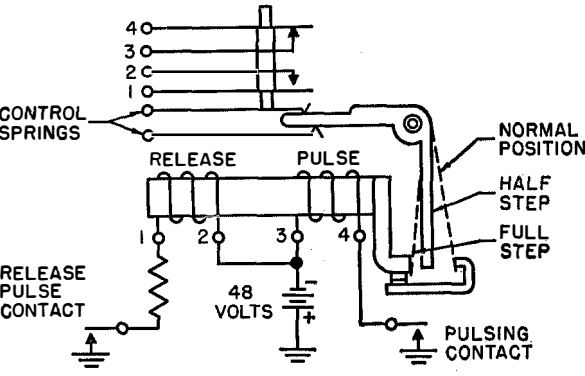


Figure 6—Operation of magnetic counter.

The chain relays (one in each selector) are interconnected so that only one can be operated at a given time. The operation of the chain relay connects ground through the selected path of the magnetic impulse counter to operate the call-in relays of the trunk group, corresponding to the digit dialed. These relays connect the sleeve leads of the selected trunk group to the common test relays, and prepare the select-magnet and hold-magnet operate paths to the associated crossbar switch. The chain relay also closes ground through contacts of the select-magnet operate relay to energize a select magnet of the crossbar switch. Since the selector relay circuit involved in the call being considered is permanently associated with a specific horizontal path in the crossbar switch, it is necessarily associated with a particular select magnet of the switch.

The trunk sleeve conductors, which have been "called in," are connected to the test relay circuit. There usually are 10 test relays, so arranged that only 1 of them can be fully operated at a time. They are adjusted so that they will operate in series with 250 ohms to negative battery (indicating an idle path condition); however, 2 relays testing the same sleeve wire cannot operate because of the current-limiting effect of the 250-ohm resistor. This prevents double selection of trunks on simultaneous testing by 2 selector groups. Operation of any common test relay chooses the path to the next stage. The select magnet operating closes off-normal ground through contacts of the operated

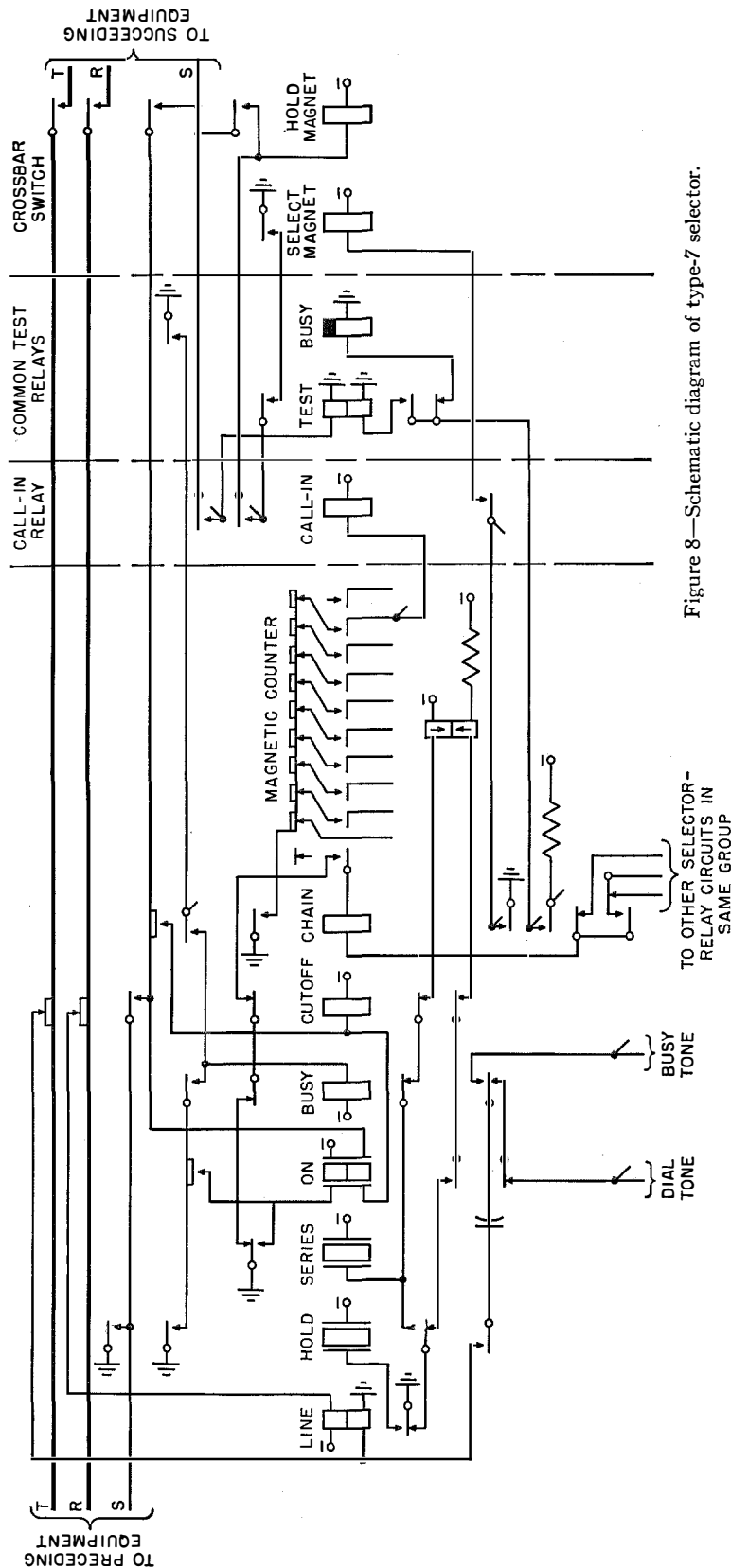


Figure 8—Schematic diagram of type-7 selector.

test relay to energize the corresponding hold magnet of the crossbar switch.

Operation of the hold magnet of the crossbar switch closes the selected crosspoint, and in turn grounds the sleeve to operate the cutoff relay in the selector relay unit. The cutoff relay releases the chain relay, which in turn releases the common test relay circuit. The hold magnet locks to ground on the sleeve and the loop of the calling line is extended through the operated crosspoints of the crossbar switch to the selected circuit in the next stage. Operation of the selector cutoff relay releases the line and hold relays of the selector, but the next-stage circuit returns ground on the sleeve conductor to maintain the established path. The magnetic impulse counter remains operated until the selector cutoff relay restores on release of the connection.

While at a given instant, only 1 call in a group of 12 selector circuits may be in the process of actual switching, the operation is so rapid that a single test circuit is well able to perform the tasks for the group. Only after the selecting digit has been recorded on its counter, is the selector permitted to demand the test circuit. The test circuit acts in a fraction of a second and having completed the switching operation for that call, becomes available for the next demand, which may come from any other selector circuit in the same group.

If the common test relay circuit finds that all trunks are busy, the busy relay of the selector relay unit will be operated. Associated common equipment will be released and busy tone returned to the calling party.

It should be pointed out that the selector just described is the basic one, and that there are variations to meet special requirements. One of these variations is the digit-absorbing selector. The necessity for such a switching device frequently arises because of the technical requirements of nationwide operator toll dialling, and nationwide customer toll dialling. Normally, the directory numbers in an exchange include only the digits necessary for the local switching and selecting functions. However, the introduction of long-distance dialling, with the nationwide

numbering plan, necessitates in some exchanges the prefixing of certain digits to the normal directory number. Since these prefix digits are not needed for locally originated calls, they must be absorbed.

The absorption of unneeded prefix digits is accomplished in the type-7 selector by registering them on the magnetic counter in the usual manner and, if the digit is to be absorbed, the counter is released so it will be prepared to receive the next digit. On receipt of a significant digit, the selector action proceeds as in the basic selector already described.

It should be mentioned that the connector (or final selector) of the type-7 crossbar system utilizes the same type of crossbar switches, relays, and magnetic counters used in the group selector. However, the connector normally permits selection of a particular line terminal in a group of 100 rather than choosing an idle path in a selected group of trunks.

4. Conclusion

While a crossbar switch associated with a selector group may have several of its transmission paths closed at a given time, only one path may be in the process of closing at a given instant. To minimize the time required in testing available paths and in closing the desired crosspoints, the type-7 selector has been arranged to test all available outlets of the selected group simultaneously rather than in sequence. By this method, the testing and connecting time is no greater for the last-choice path than for the first-choice path. These factors made possible the design of a direct-access decimal-type crossbar group selector that readily cooperates with decimal systems of other types.

5. Acknowledgment

The author acknowledges the contributions of other engineers in the development of the type-7 crossbar selector, particularly Mr. C. A. Adams, who did much of the basic work, Mr. A. T. Sigo and Mr. K. L. Liston, whose consultation and encouragement contributed greatly to the project.

Valve Noise Produced by Electrode Movement*

By PAMELA A. HANDLEY and PETER WELCH

Standard Telephones and Cables Limited; Footscray, Kentshire, England

CAUSES of valve noise are analysed and the distinction is made between "rattle" noise and that produced by resonances.

The contribution of various electrodes to the total noise produced is discussed and it is shown that the resonant frequencies of these electrodes may be calculated. Data are given proving the validity of these empirical equations.

Methods of measuring noise are outlined, and finally, the implications of the findings are applied to valve design improvements.

. . .

The major requirement for valves that are to be used in aircraft or guided missiles is that the noise output when the valves are subjected to high accelerations or continuous vibration shall be of a small order compared with the signal. In addition to this special requirement, there is a growing industrial demand for valves that will operate satisfactorily in equipment used with mechanical and electromechanical systems.

The special design of reliable valves to fulfil these exacting requirements has necessitated a closer study of the factors that cause noise in the valve.

1. Causes of Valve Noise

The most serious source of trouble to the circuit engineer is microphony. Normal receiving valves have a satisfactory level of microphony for the particular use for which they have been designed, but in practically all cases the noise level is too high when the valve is subjected to severe shock or continuous vibration. Apart from troubles caused by small pieces of fluff or hairs, which become carbonised during the valve processing and give rise to leakage noise, the main source of microphony can be traced to the movement of individual valve electrodes. This may be due either to inadequate positioning, in which case it is termed electrode "rattle," or it may be caused by an electrode vibrating at its own fundamental frequency.

* Reprinted from *Proceedings of the IRE*, volume 42, pages 565-573; March, 1954.

Besides these mechanical sources of noise there are noises due to hum and hiss. The former is caused by alternating-current heating of the cathode while the latter is fundamental to the nature of electron emission. Usually neither is of great importance compared with microphony.

The amount of noise produced by the movement of an electrode will depend on its position in the electron stream as well as on its rigidity and the method of fastening. Most normal valve structures are made in such a way that they may be considered as if they were two identical halves joined across the line of the grid-support members.

The anode current in either half-section of a planar system comprising cathode, grid, and anode is given by an expression¹ of the type:—

$$i = \frac{2.34 \times 10^{-6} (V_g + DV_a)^{3/2}}{(l_g^{4/3} + Dl_a^{4/3})^{3/2}}, \quad (1)$$

amperes per unit area, where V_g is corrected for contact potential, l_g and l_a are distances of grid and anode from the cathode, and $D = 1/\mu$.

It is a simple matter to differentiate this expression with respect to the appropriate distance l_g or l_a and arrive at a relation between change in distance and change in anode current. By a simple extension of the triode case, tetrode and pentode half-structures may be investigated.

The application of such an analysis, however, involves consideration of both halves at the same time. A movement in one half due to simple vibration is accompanied by an opposite movement in the other, and the changes in anode current produced in each section tend to cancel out by an amount that is proportional to the difference between the two currents. Despite this fact, the analysis shows that changes of anode current will be greatest for movement of the cathode and least for that of the anode, and this order of sensitivity may be inferred for the double-sided structure.

¹ J. H. Fremlin, "Calculation of Triode Constants," *Electrical Communication*, volume 18, pages 33-49; July, 1939.

Noise produced by the vibration of the individual lateral wires can be investigated by using one of the standard expressions for the calculation of amplification factor. Here again, however, the results are very inconclusive because in general each grid turn will have its individual resonant frequency and therefore the noise produced will vary with the frequency of excitation.

From the foregoing it has been realised that the exact amount of noise produced can not be calculated by a simple method. It is possible to generalise the results in the following way. Firstly, the rattle noise must be reduced by engineering design and, secondly, the resonant frequency of the electrodes must be as high as possible as the movement at resonance for a given excitation is smaller at the higher frequencies. Up to the present it has been the practice to design the valve and to test for resonant frequencies afterwards. It can be appreciated that valuable time could be saved if a method of evaluating the resonant frequencies existed in the design stage.

2. Resonant Frequencies—General

All valves undergo certain heating treatments during the process of manufacture. These may produce changes in the structure of the materials used and hence changes in the modulus of elasticity. Since the resonant frequency will depend on the physical dimensions, the method of mounting, and the modulus of elasticity, then a knowledge of the variations brought about during these heating cycles must be gained before any attempt is made to arrive at an empirical relation between these parameters and the resonant frequency.

TABLE 1
CHANGES IN YOUNG'S MODULUS

Material	Mean Value of Young's Modulus in Dynes per Square Centimetre $\times 10^{-11}$	
	Before Baking	After Baking
Nickel	19.90	19.90
Copper	10.69	14.09
5-Per-Cent Chrome-Copper	10.70	14.18
Mild Steel	21.20	21.20
Copper-Flashed Steel	14.40	14.40
Manganese-Nickel	22.3	22.3
Tungsten	34.15	34.15
Molybdenum	34.15	34.15

The most important of these processes from the point of view of the softening effect on the material is the high-temperature baking in hydrogen that is done to ensure that the part is free of grease and high-vapour-pressure impurities, and also the heating cycles associated with eddy-current heating of the valve components during the exhaust process.

Experiments have been conducted to evaluate the changes in Young's modulus with the normal heating cycles. Re-treatment showed little extra variation after the initial change. The following results have been obtained and are shown in Table 1.

The particular relation between the parameters established and the time of periodic motion or frequency at resonance will now depend only on the special way in which the electrode is mounted. Grid supports, the cathode, and other components are held at each end in a relatively thin insulator whilst the grid laterals on the other hand are usually clamped tightly in slots cut in the support members.

2.1 GRID RESONANCE

2.1.1 Grid Support

It was expected that the resonant frequency of the support wire would be of the form

$$\frac{1}{f} = T = 2\pi \left(\frac{kw l^4}{YI} \right)^{1/2} \quad (2)$$

or, since the wire is of circular cross section,

$$\frac{1}{f} = T = 2\pi l^2 \left(\frac{4k\rho}{Yr^2} \right)^{1/2}, \quad (3)$$

where

k = constant to be determined

w = weight per unit length

l = length

Y = Young's modulus

I = moment of inertia of cross section

r = radius of wire

ρ = density of material.

Wires of various materials and diameters were inserted into two insulators that were held at right angles to the wire by being a push fit into a glass tube of the same size as that used for miniature valves. The assembly was then mounted on the coil of a moving-coil vibrator, that was excited by a variable-frequency

oscillator, and the point of resonance found. Each wire was arranged so that the overhang beyond the insulator at each end was 0.10 inch (2.5 millimetres) and the length between the insulators was measured by means of a travelling microscope.

To check that the vibration was of the form given in (3), l^2 was plotted against T for each type of wire (Figure 1). Thence a relation between Y/w and l^4/T^2r^4 was deduced as in Figure 2. From the slope of this line the constant k was evaluated giving

$$\frac{1}{f} = T = 2\pi \left(\frac{wl^4}{90.4 YI} \right)^{1/2}, \quad (4)$$

i.e. for the round wire,

$$\frac{1}{f} = T = 2\pi l^2 \left(\frac{\rho}{22.6 Yr^2} \right)^{1/2}. \quad (5)$$

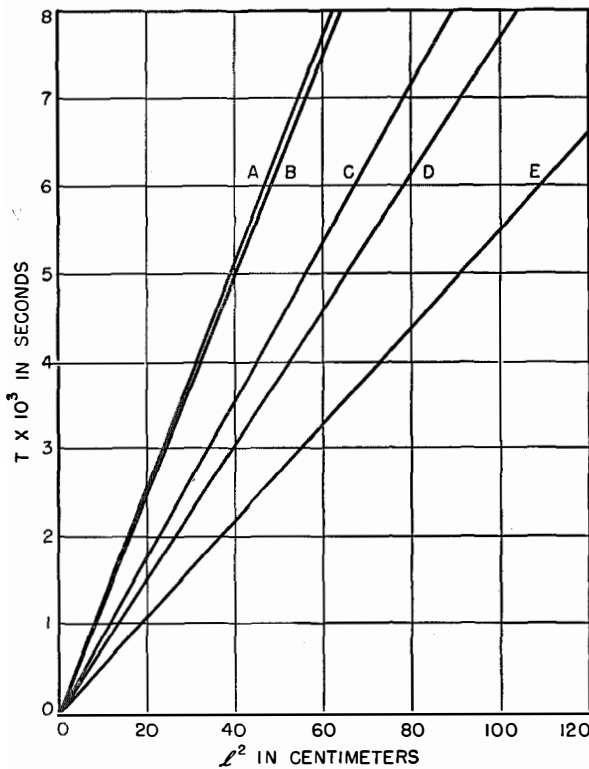


Figure 1—Period of resonant oscillation plotted against the square of the length between insulators for a number of representative wires. A = 5-per-cent chrome-copper of 0.0622-centimetre diameter, B = copper of 0.0622 centimetre, C = nickel of 0.0622 centimetre, D = copper and 5-per-cent chrome-copper of 0.102 centimetre, and E = nickel of 0.1002 centimetre.

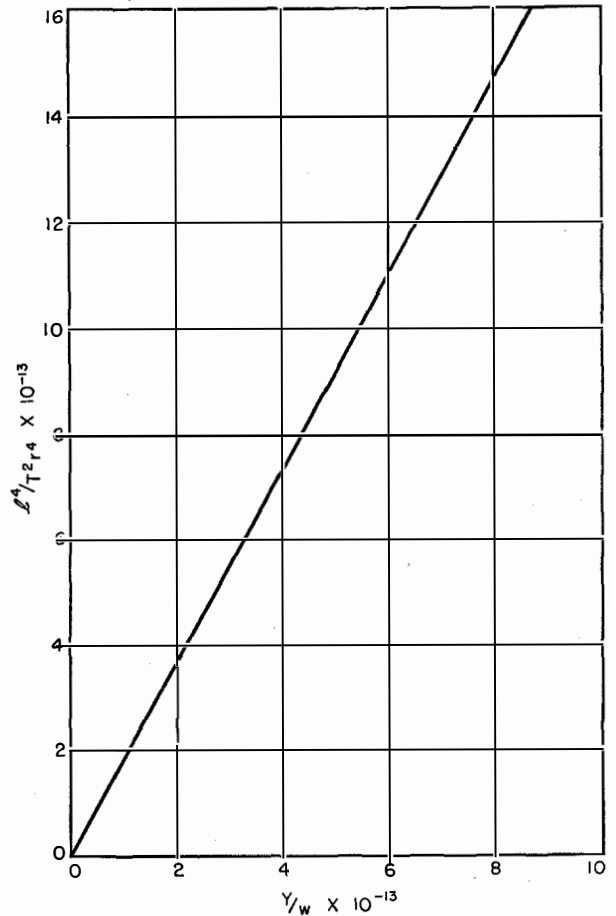


Figure 2—Evaluation of the empirical equation for the resonant frequency of wires supported between insulators.

This equation in itself is not sufficient to define the resonant frequency of a grid support because, firstly, the section of a grid support is modified when the grid is manufactured by the "nick-and-swage" method and, secondly, there will be a certain loading effect due to the weight of the individual lateral wires. The section through the support will be similar to that given in Figure 3.

The mean ratio of X to the diameter for a number of common grids showed that the correction to be applied to the expression for the moment of inertia was

$$I = \frac{\pi r^4 m}{4} \times 0.84. \quad (6)$$

The damping effect of the grid lateral wires attached to the supports may be said to con-

stitute an extra weight \bar{w} per unit length, where half the length of lateral either side of the grid is considered. Hence the total weight per unit length is

$$w(1 + \bar{w}/w). \tag{7}$$

Using (6) and (7) in (4),

$$\frac{1}{f} = T = 2\pi \left\{ \frac{w(1 + \bar{w}/w)l^4}{90.4YI0.84} \right\}^{1/2}, \tag{8}$$

$$\frac{1}{f} = T = 2\pi l^2 \left\{ \frac{(1 + \bar{w}/w)\rho}{19Yr^2} \right\}^{1/2}. \tag{9}$$

Using the values $\rho = 8.8, 8.89, 8.88, 7.8,$ and 8.18 respectively for nickel, copper, 5-per-cent chrome-copper, mild steel, and copper-flashed steel, (9) gives

$$f_{Ni} = \frac{1.3 \times 10^5 \times r}{l^2(1 + \bar{w}/w)^{1/2}}, \tag{10}$$

$$f_{Cu} = \frac{1.088 \times 10^5 \times r}{l^2(1 + \bar{w}/w)^{1/2}}, \tag{11}$$

$$f_{Cr-Cu} = \frac{1.09 \times 10^5 \times r}{l^2(1 + \bar{w}/w)^{1/2}}, \tag{12}$$

$$f_{Fe} = \frac{1.42 \times 10^5 \times r}{l^2(1 + \bar{w}/w)^{1/2}}, \tag{13}$$

$$f_{Cu/Fe} = \frac{1.147 \times 10^5 \times r}{l^2(1 + \bar{w}/w)^{1/2}}, \tag{14}$$

where l and r are in inches.

As examples of the use of these relations, the valve types shown in Table 2 were checked for resonance by practical measurement and correspond with the calculated figures.

TABLE 2
RESONANT FREQUENCIES OF VALVE GRIDS

Valve Type	Grid	Material	Resonant Frequency in Cycles Per Second	
			Calculated	Observed
5763	1	Copper	1570	1580
5763	2	Nickel	2084	2100
6BW6	1	Copper	1880	1900
6BW6	2	Nickel	1890	1910

2.1.2 Lateral Wires

The evaluation of an empirical relation for grid laterals is difficult because of the complexity of grid profiles. It was decided therefore

to approximate all grid profiles either to the arc of a circle or to a rectangle.

The arc of a circle was considered first and the mode of oscillation as if it were a cantilever as shown in Figure 4.

Because the lateral wires of grids are so small, the investigational work was conducted with

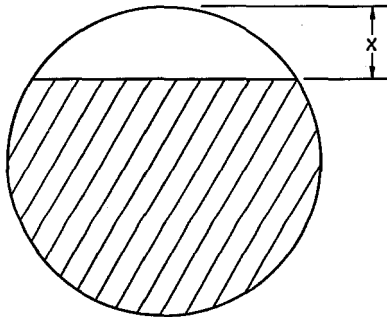


Figure 3—Section through grid support.

nickel wires having diameters of 0.025 and 0.040 inch (0.64 and 1 millimetre). The semi-circle was treated first and the dependence of the time of periodic motion on the square of the radius was investigated. Figure 5 shows R^2

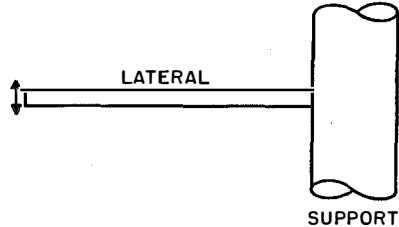


Figure 4—Grid-lateral profile considered as a cantilever.

plotted against T and from this it is clear that T/R^2 is constant. For the various sizes of wire used it was shown further that for nickel

$$Tr/R^2 = 4.086 \times 10^{-5}, \tag{15}$$

where R and r are the radius of the semi-circle and of the wire itself in inches.

It follows therefore that the resonant frequency of a semi-circle of nickel is defined by

$$f_{Ni} = \frac{r \times 10^5}{4.086R^2} \tag{16}$$

If Y' and ρ' are Young's modulus in dynes per square centimetre and the density in

grammes per cubic centimetre, for any other material,

$$f = \frac{r}{19.41R^2} \left(\frac{Y'}{\rho'} \right)^{1/2} \quad (17)$$

The depth of the arc as a function of the time of periodic oscillation was then investigated as shown in Figure 6, where d is taken to the centre of the wire.

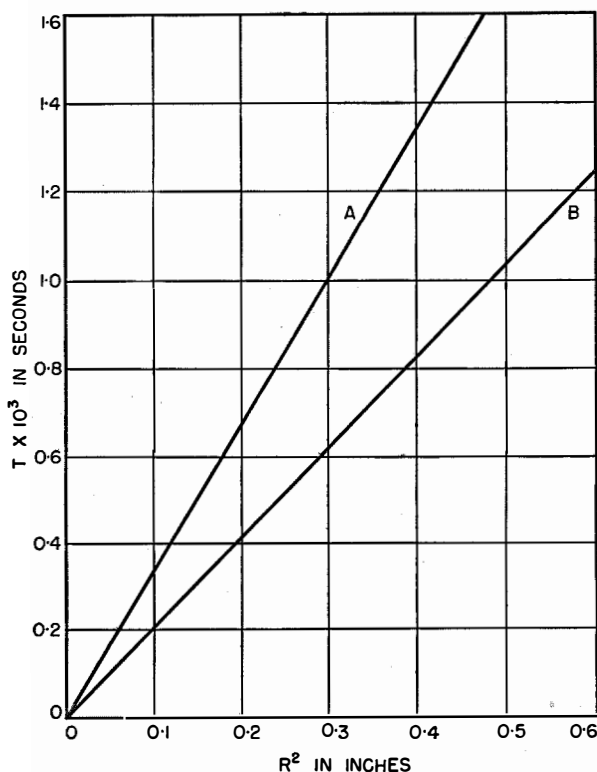


Figure 5—Evaluation of the empirical equation relating the period of oscillation with the square of the radius of a semi-circle. The material is nickel and the diameters are $A = 0.0245$ inch (0.0622 centimetre) and $B = 0.0395$ inch (0.1002 centimetre).

For a constant value of R , d^2 was found to be a linear function of T as may be seen in Figure 7.

$$T = (2.78d^2 + 0.18) \times 10^{-3} \quad (18)$$

for nickel wire of 0.025-inch (0.63-millimetre) diameter.

From the relation

$$d_2 = R_2 d_1 / R_1, \quad (19)$$

the periodic time for similar arcs of different diameters was evaluated. Figure 8. shows T_1

plotted against T_2 for similar arcs of radius 0.568 and 0.70 inch (14.4 and 17.8 millimetres) in nickel wire of 0.025-inch (0.63-millimetre)

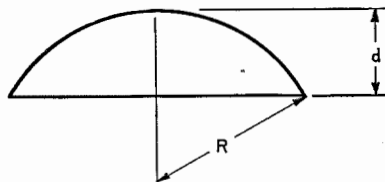


Figure 6—Circular grid profile.

diameter. From the semi-circle relations and this graph it is clear that

$$\frac{T_1}{T_2} = \frac{R_1^2}{R_2^2}$$

and in particular for the two sizes used

$$\frac{R_1^2}{R_2^2} = \frac{1}{1.54} = \frac{T_1}{T_2} \quad (20)$$

From (18) we may proceed as follows.

$$T_1 = (2.78d_1^2 + 0.18) \times 10^{-3}$$

Hence

$$T_2 = (2.78d_1^2 + 0.18)(R_2/R_1)^2 \times 10^{-3}$$

and

$$T_2 = \left\{ 2.78d_2^2 \left(\frac{R_1}{R_2} \right)^2 + 0.18 \right\} (R_2/R_1)^2 \times 10^{-3}$$

and in particular for the radius R_2

$$T_2 = (2.78d_2^2 + 0.558R_2^2) \times 10^{-3} \quad (21)$$

For the sizes of wire used it was clear that

$$T_1 / (2.78d^2 + 0.558R^2) = \text{constant} \quad (22)$$

From which it follows that for nickel wire of any size

$$f_{N1} = \frac{0.81 \times 10^5 \times r}{2.78d^2 + 0.558R^2}, \quad (23)$$

where r , d , and R are in inches. By putting $R = d$, (16) is re-established. For any other material we shall have

$$f = \frac{0.171r}{2.78d^2 + 0.558R^2} \left(\frac{Y}{\rho} \right)^{1/2}, \quad (24)$$

where r is the radius of the wire, d and R are the depth and radius of the arc in inches respectively, Young's modulus for the material is in dynes per

square centimetre, and the density is in grammes per cubic centimetre.

Table 3 shows a comparison between figures calculated from the formula and measured by practical methods.

TABLE 3
RESONANT FREQUENCY OF 6BE6 GRIDS

Grid	Material	Resonant Frequency in Cycles per Second	
		Calculated	Observed
3	Manganese-Nickel	2150	2050-2190
5	Manganese-Nickel	1320	1295-1330

Lastly the rectangular grid profile shown in Figure 9 was investigated. Figures 10 and 11 show the dependence of l_0^2 and L^2 on the periodic time

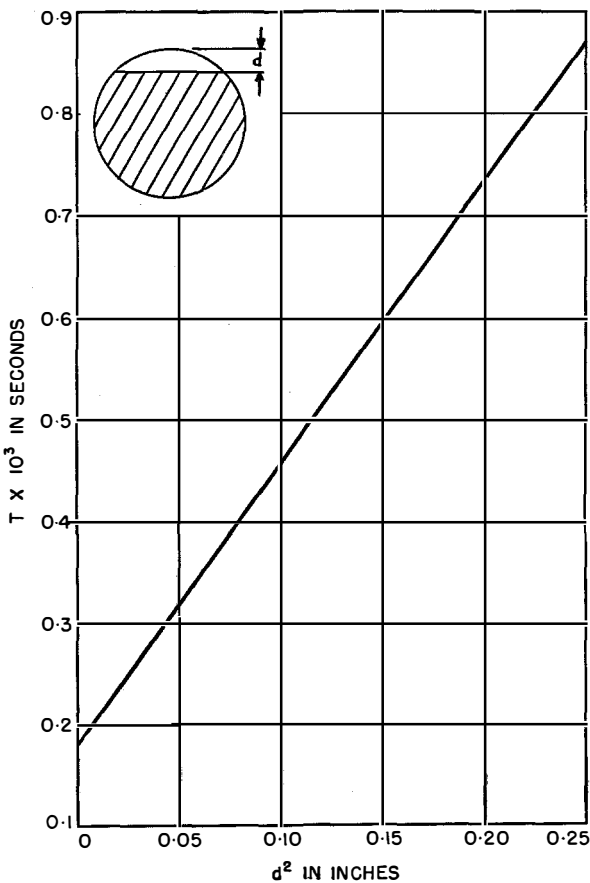


Figure 7—Evaluation of the empirical equation relating the period of oscillation with the square of the depth of an arc of a circle for a nickel wire of 0.0245-inch (0.0622-centimetre) diameter.

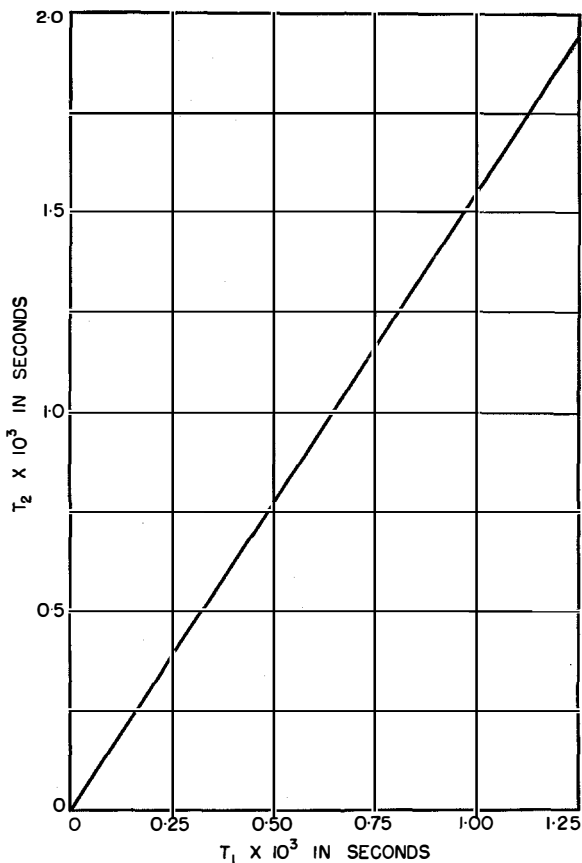


Figure 8—Relation between the periods of resonant oscillations of similar arcs of 0.568- and 0.70-inch (1.44- and 1.78-centimetre) diameter in 0.0245-inch (0.0622-centimetre) wire.

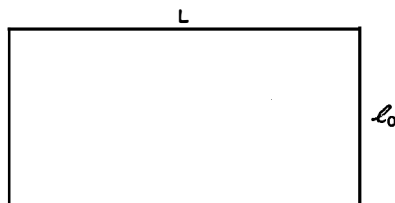


Figure 9—Rectangular grid profile.

for nickel wire of 0.025-inch (0.63-millimetre) diameter. From these the following relations were evaluated.

$$\left. \begin{aligned} T &= 2.9l_0^2 \times 10^{-3} + \text{function}(L) \\ T &= 0.325L^2 \times 10^{-3} + \text{function}(l_0) \end{aligned} \right\} (25)$$

When $l_0 = 0$

$$T = \text{function}(L) = 0.325L^2 \times 10^{-3}.$$

Hence in general for this particular diameter of wire

$$T = 2.9l_0^2 \times 10^{-3} + 0.325L^2 \times 10^{-3}. \quad (26)$$

Using reasoning similar to that used with the circular arc, the expression for the resonant frequency becomes

$$f_{Ni} = \frac{0.81 \times 10^6 \times r}{2.9l_0^2 + 0.325L^2}, \quad (27)$$

and for any other material

$$f = \frac{0.171r}{2.9l_0^2 + 0.325L^2} \left(\frac{Y}{\rho}\right)^{1/2}, \quad (28)$$

where l_0 , L , and r are in inches, Y in dynes per square centimetre, and ρ in grammes per cubic centimetre.

As an example of the use of this expression, a high-slope valve gave for grid 3 a calculated resonance frequency of 1190 cycles per second and an observed value of 1090–1350.

2.2 CATHODE RESONANCE

For a cylindrical rod where r_1 and r_2 are the internal and external radii then

$$I = \frac{\pi(r_1^4 - r_2^4)m}{4}, \quad (29)$$

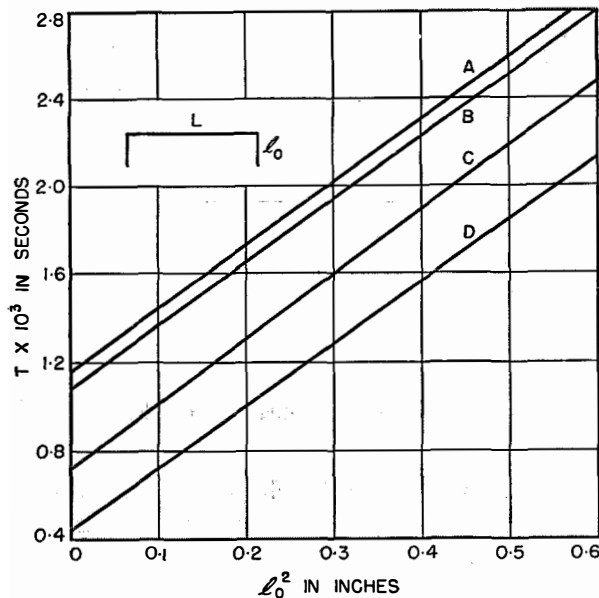


Figure 10—Relation between the period of oscillation and breadth l_0 of a rectangle of nickel wire of 0.0245-inch (0.0622-centimetre) diameter for four values of L , which in curve $A = 1.98$ inches (5.03 centimetres), $B = 1.885$ inches (4.79 centimetres), $C = 1.5$ inches (3.81 centimetres), and $D = 1.15$ inches (2.92 centimetres).

where m is the mass per unit area. Using (4) the resonant frequency is

$$f = \frac{1}{2\pi l^2} \left\{ \frac{22.6Y(r_1^4 - r_2^4)\pi m}{w} \right\}^{1/2}, \quad (30)$$

which reduces to

$$f_{Ni} = \frac{1.42 \times 10^6 (r_1^2 + r_2^2)^{1/2}}{l^2}.$$

Similarly where a and a' are respectively the external and internal dimensions of a rectangular cathode across either of the principal axes and through the centre of gravity of the cross section, then

$$f_{Ni} = \frac{1.64 \times 10^6 (a^2 + aa' + a'^2)^{1/2}}{l^2}, \quad (31)$$

where the dimensions are in inches and the damping effect of the cathode coating is ignored.

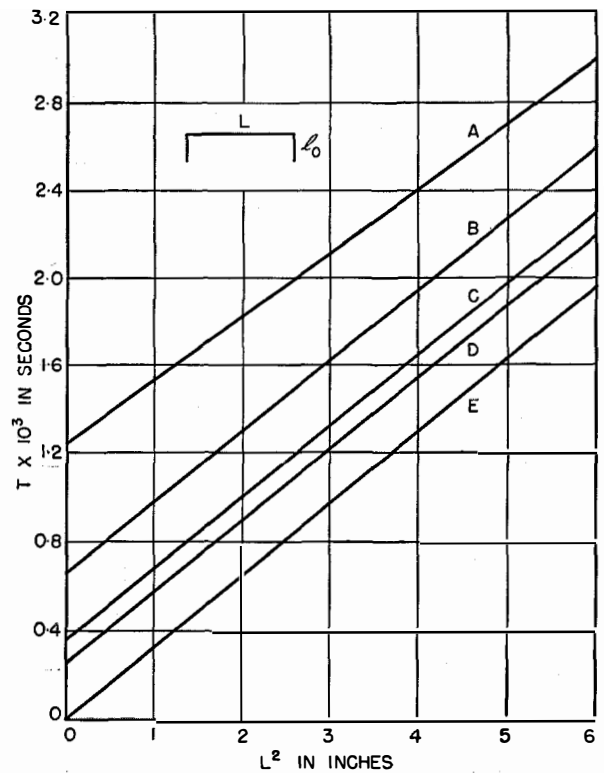


Figure 11—Relation between the period of oscillation and the length L of a rectangle of nickel wire of 0.0245-inch (0.0622-centimetre) diameter for 5 values of l_0 , which in curve $A = 0.65$ inch (1.65 centimetres), $B = 0.48$ inch (1.22 centimetres), $C = 0.35$ inch (0.89 centimetre), $D = 0.30$ inch (0.76 centimetre), and $E = 0$ inches.

If coating weight is considered then the frequency of vibration will be modified by the term

$$(1 + \bar{w}_c/w)^{1/2},$$

where w and \bar{w}_c are the weight of sleeve and the weight of the coating per unit length.

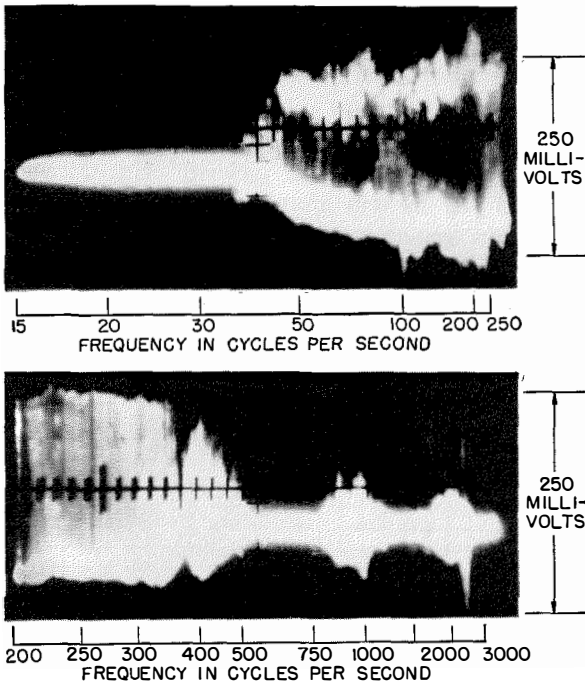


Figure 12—Noise spectrum of a miniature radio-frequency pentode.

3. Measurement of Noise and Resonance

The chief advantage of the relations that have been derived is that they permit the valve to be designed so that the resonant frequency of the electrodes will occur at points other than those at which mechanical vibration is expected. It is still necessary to study the magnitude of the effects of both resonance and loose electrodes on the valve space current.

Figure 12 shows a photographic record of an oscilloscope trace of the noise voltage developed across a 2000-ohm anode load resistor for a noisy miniature radio-frequency pentode operated under normal conditions. The valve was vibrated at a constant acceleration of 2.5g through the frequency spectrum from 0 to 3000 cycles per second. It will be seen that there is a very high continuous noise output from about 40 to 400

cycles per second. This is typical of electrode rattle and in this particular case was due to cathode movement.

While this method of measurement may be satisfactory for individual valves it is not an easy production test. Since the noise may be excited by any low-frequency vibration it is convenient to use a simple mechanical device giving sinusoidal vibrations at 50 cycles per second with an acceleration of about 4g and then to check each valve. This method has advantages over the previous types of test that have always necessitated tapping the valve by an indeterminate amount to excite a disturbance. Results of testing in this way show a very high degree of repeatability. Figure 13 shows the distribution of noise output in a batch of high-slope miniature pentode valves. The effect of design changes may be studied by comparing distributions of this type.

The resonant frequency, which is a design feature, and noise at resonance may be measured by vibrating the valve through the audio-frequency spectrum by the coil-and-magnet method. Resonances or even harmonics are not encountered much above 7000 cycles per second, up to which point the response characteristics of the system are usually satisfactory so that the value of acceleration may be defined. Again, the method consists of measuring the noise output.

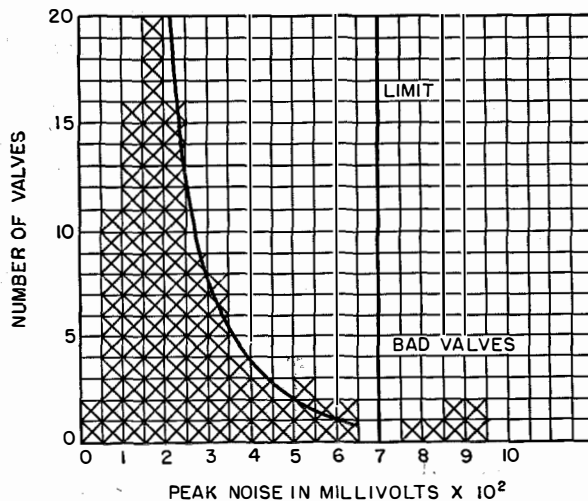


Figure 13—Distribution of noise output across an anode load of 2000 ohms for a batch of 100 high-slope miniature pentode valves.

While the resonant frequency of individual electrodes remains the same from valve to valve the amount of noise varies since it depends on the symmetry of the structure and on the minor damping effects that can occur. Once again the only satisfactory method of attacking the problem is by a quantitative analysis.

Since practically all objectionable valve resonances occur in the audio-frequency spectrum, a form of microphony test is a satisfactory means of assessing the noise because it is more easily applied than the method of varying the frequency of the exciting device and searching for resonant points. When a valve with a high resonance noise is placed in the first stage of an

audio-frequency amplifier terminated by a loudspeaker, it will produce a condition of regenerative feedback. Unless special precautions are taken however, a circuit of this type will tend to become very selective in certain bands. It is important therefore that the valve shall be freely mounted in front of the speaker, which must face free space. Any attempt at producing a test box or making mechanical connections between the valve and the speaker limits the device to a response characteristic that usually invalidates the results. The normal method of measuring is to obtain a level of total gain around the system that is just insufficient to maintain regenerative feedback. If, in addi-

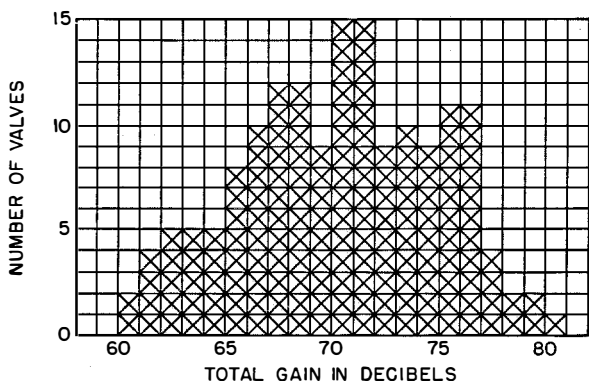


Figure 14—This batch of 158 pentodes of modified design were tested by being placed approximately 8 inches from a loudspeaker in a position giving regenerative feedback. The maximum gain to which the amplifier between the valve and the loudspeaker could be adjusted before oscillations started is indicated. The mean value was 70.3 decibels.

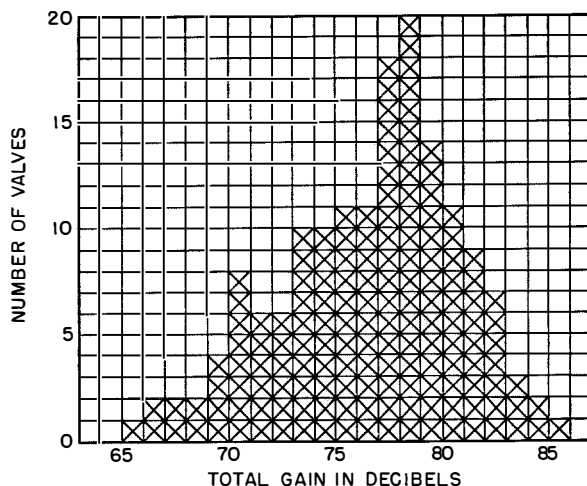


Figure 15—This batch of 163 pentodes were placed 1 foot (30 centimetres) from the loudspeaker and the amplifier gain adjusted to the start of regenerative feedback. The mean value was 76.7 decibels.

TABLE 4
CALCULATED RESONANT FREQUENCIES

Element	Vari- μ Valve		High-Slope Valve	
	Characteristic	Cycles per Second	Characteristic	Cycles per Second
Cathode	Circular	13 720	Rectangular	38 000
Grid 1 Support Lateral	Arc		Rectangular	
	Nickel	3 218	Copper	9 900
Grid 2 Support Lateral	Manganese-Nickel	11 570	Molybdenum	7 500
	Arc		Rectangular	
Grid 3 Support Lateral	Nickel	3 080	Nickel	7 520
	Molybdenum	4 720	Molybdenum	2 500
Grid 3 Support Lateral	Arc		Rectangular	
	Nickel	3 840	Nickel	11 900
	Manganese-Nickel	2 280	Molybdenum	1 190

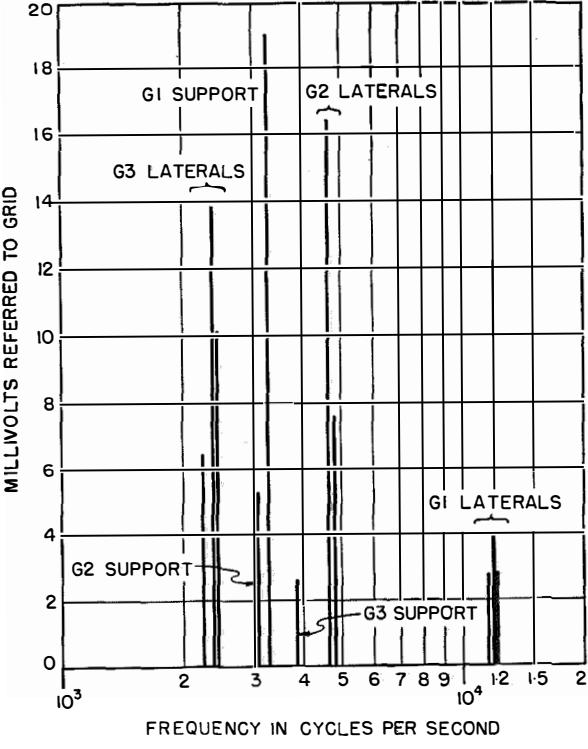


Figure 16—Resonance diagram for a vari- μ radio-frequency pentode.

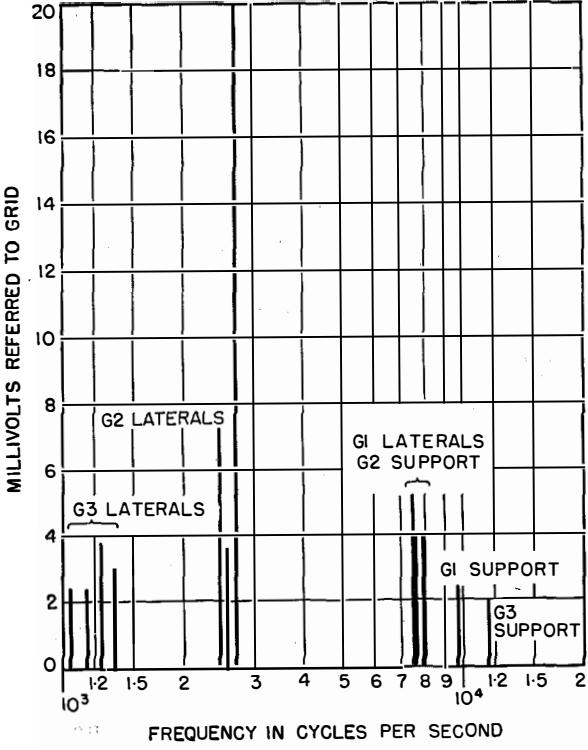


Figure 17—Resonance diagram for a high-slope radio-frequency pentode.

tion, the valve is moved about in front of the speaker until an antinode is found for the particular resonance that it has selected, then a repeatability of ± 1 decibel in about 80 decibels is easily achieved. Figure 14 shows the distribution of gain in a batch of radio-frequency pentodes measured under these conditions. The alternative method of testing all the valves in a fixed position relative to the loudspeaker produces a distribution that is slightly skew (Figure 15). Using this method the results of changes in design to increase the damping effect at resonance is capable of accurate quantitative assessment. In addition, when the gain level is adjusted to a particular test figure the apparatus may be used as a production test for resonance noise.

4. Interpretation of Resonance Diagrams

Figures 16 and 17 are diagrams showing the noise output recorded on samples of straight and vari- μ radio-frequency pentodes. The calculated resonant frequencies are given in Table 4.

From the diagrams it is evident that there are a number of resonances at the natural frequencies of the lateral wires. Visual examination of the high-slope pentode showed that each lateral wire of the suppressor grid had a separate resonance in the band 1020 to 1350 cycles per second, where the calculated value is 1190 cycles per second. Figure 18 shows this feature diagrammatically.

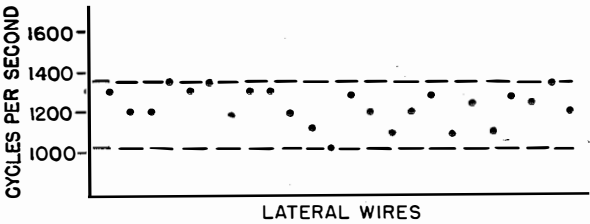


Figure 18—Resonant frequencies of individual lateral wires of grid 3 in a high-slope pentode. Maximum and minimum frequency limits are indicated by dashed lines.

At each of the resonances a check was made on the effect of increasing the acceleration. Figure 19 shows a typical graph of one of the resonances. In all cases it was found that the noise increased approximately with the square root of the acceleration.

5. Design Improvements

Noise produced by electrode rattle may be overcome easily, but excessive noise due to electrodes resonating can only be avoided by basic design of the structure.

A general improvement in rattle noise will nearly always result from a reduction of the tolerances on the insulator holes into which the electrodes fit. This is especially important at the top end of the structure because the movement is not restricted by the connecting bars and tapes as it is at the bottom. The direct connections of the pin to the electrode in the case of miniature valves also helps. The additional rigidity that is necessary for reliable valves is obtained by locking the cathode and grids in the top insulator by means of special pips, beads, or stakes formed on the electrodes, or better by using tapes that are clamped to the insulators and then welded to the electrode. Figure 20 shows the rattle-noise output in the case of a reliable valve during initial development, after the initial precautions had been taken, and finally when all precautions had been taken.

Apart from the fact that it is desirable to make the resonant frequencies of the electrodes as

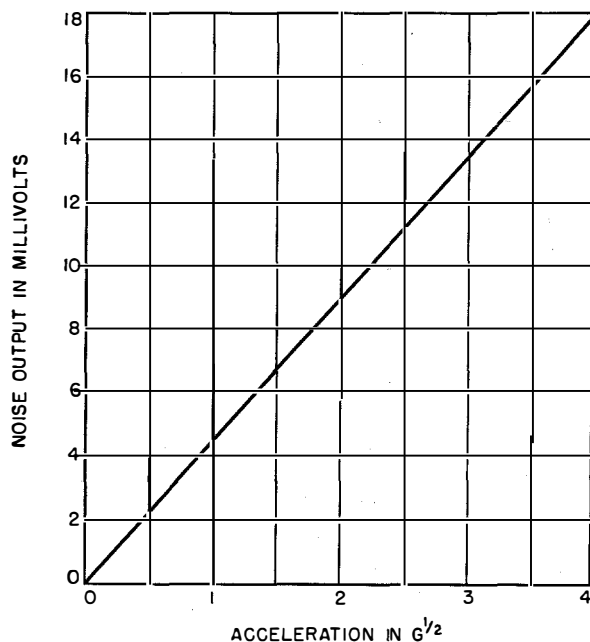


Figure 19—Noise output plotted against acceleration at a frequency of 2400 cycles per second for a lateral wire of grid 3 of a high-slope pentode.

high as possible because they are not so liable to excitation by normal mechanical vibrations, the amplitude of the electrode movement will be proportionally less with the time of periodic motion for constant excitation.

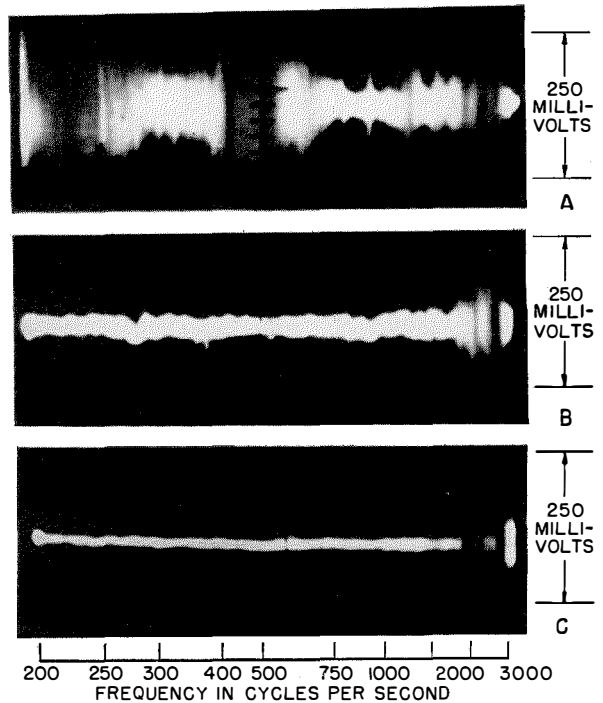


Figure 20—Noise spectra for radio-frequency-pentode designs. *A* = normal commercial valve, *B* = results of early design efforts, and *C* = final reliable valve.

From the point of view of the supporting members and electrodes held between the insulators the frequency will vary inversely with the square of the length, proportionally with the diameter, and with the square root of Young's modulus. If the supports are fixed rigidly at each end instead of being free in the insulators the resonant frequency is given by

$$\frac{1}{f} = T = \frac{2\pi l^2}{r} \left(\frac{\rho}{62.8Y} \right)^{1/2}. \quad (32)$$

The frequency is actually increased by 1.67 times compared to the non-rigid fixing.

The resonant frequency of the lateral wires may be increased only by using small values of major axis and large diameters of wire. Except for suppressor grids however, the frequency of lateral wires of normal valves is well above 1000 cycles per second.

6. *Conclusions*

It has been shown how the resonant frequency or frequencies of valve electrodes may be calculated and indication has been given respecting their usefulness in basic valve design.

Present trends are to produce valves that will not have resonant frequencies or rattle noises at frequencies so low that they are excited by mechanical disturbances but there is a need

for more research into the field of impacts and non-linear accelerations in order that a clearer picture of the precise requirements for future designs can be obtained.

7. *Acknowledgment*

The authors thank Standard Telephone and Cables Limited and the Admiralty for permission to publish this information and acknowledge the assistance given by Mr. E. G. Rowe.

Wide-Frequency-Range Tuned Helical Antennas and Circuits

By A. G. KANDOIAN and WILLIAM SICHAK
Correction for Volume 29, Pages 294-299; December, 1953

THE second-from-last sentence in section 4.2 on page 297 should be, "The solid curves are calculated using (12) above." The reference to (9) is incorrect.

Some Wave Properties of Helical Conductors

By J. H. BRYANT

Federal Telecommunication Laboratories, a division of International Telephone and Telegraph Corporation; Nutley, New Jersey

THE wave properties of a helically conducting cylinder in free space have been studied in detail.¹ In delay lines using spiraled conductors as well as in some traveling-wave-tube applications, the wave properties of the helical structure are modified by the presence of additional coaxial conductors.

The factors of interest in traveling-wave-tube work are the velocity of propagation and the impedance function $E_z^2/\beta^2 P$ (see section 6 for glossary of symbols) relating the longitudinal field to the total power flowing. This latter field determines the degree of interaction of the wave and the moving electron stream.

The problem considered is illustrated in Figure 1, which shows the infinitely thin helically conducting cylinder of radius a and coaxial inner and outer uniformly conducting cylinders of radii c and b , respectively. Four conditions are possible depending on the presence, absence, or combination of conducting cylinders. These conditions are considered separately in the subsequent sections.

1. Helix in Free Space

The wave properties of a helical conductor in free space have been adequately covered in the literature. The results are recorded here for information and comparison with other conditions. For this condition, where $c = 0$ and $b = \infty$, the radial propagation constant γ is given by

$$(\gamma a)^2 \frac{I_0(\gamma a) K_0(\gamma a)}{I_1(\gamma a) K_1(\gamma a)} = (ka \cot \psi)^2. \quad (1)$$

The factor $F(\gamma a)$ in the impedance parameter, $(E_z^2/\beta^2 P)^{1/2} = (\beta/k)^{1/2} (\gamma/\beta)^{1/2} F(\gamma a)$, is given by

$$F(\gamma a) = \left[\frac{\gamma a}{240} \frac{I_0(\gamma a)}{K_0(\gamma a)} \right] \left[\left(\frac{I_1(\gamma a)}{I_0(\gamma a)} - \frac{I_0(\gamma a)}{I_1(\gamma a)} \right) + \left(\frac{K_0(\gamma a)}{K_1(\gamma a)} - \frac{K_1(\gamma a)}{K_0(\gamma a)} \right) + \frac{4}{\gamma a} \right]^{1/2}. \quad (2)$$

¹ J. R. Pierce, "Traveling Wave Tubes," D. Van Nostrand Company, New York, New York; 1950.

² L. N. Loshakov and E. B. O'Derogge, "On the Theory of the Coaxial Spiral Line," *Radiotekhnika* (Moscow), volume 3, pages 11-20; March/April, 1948.

2. Helical Conductor Inside a Coaxial Conductive Cylinder

This condition is the one most likely to be met in practice. For this condition, $c = 0$ and b has a

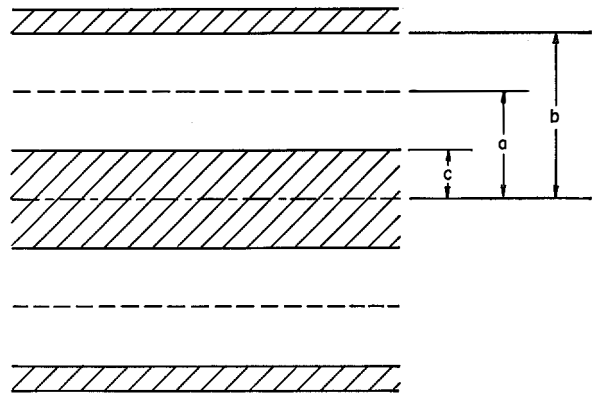


Figure 1—Helically conducting cylinder with inner and outer coaxial conductive cylinders.

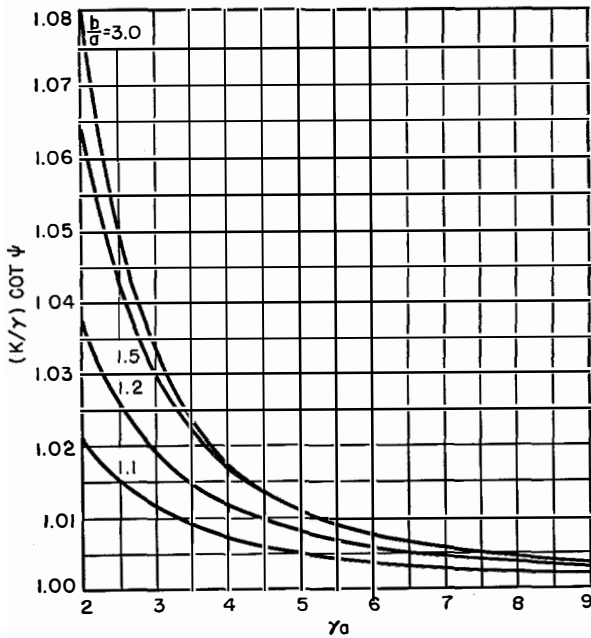
finite value. The radial propagation constant γ is given² by

$$\left(\frac{k}{\gamma} \cot \psi \right)^2 = \frac{I_0(\gamma a) K_0(\gamma a)}{I_1(\gamma a) K_1(\gamma a)} \left[\frac{1 - \frac{I_0(\gamma a) K_0(\gamma b)}{K_0(\gamma a) I_0(\gamma b)}}{1 - \frac{I_1(\gamma a) K_1(\gamma b)}{K_1(\gamma a) I_1(\gamma b)}} \right]. \quad (3)$$

The solution is shown plotted in Figure 2 with b/a as a parameter. As can be seen, the effect is to reduce the low-frequency dispersion.

The factor $F(\gamma a, \gamma b)$ in the impedance parameter is given by (4).

$$F(\gamma a, \gamma b) = \left\{ \frac{(\gamma a)^2}{240} \left[1 + \frac{I_0^2(\gamma a)}{R I_1^2(\gamma a)} \right] \left[M(\gamma a) \right] + I_0^2(\gamma a) \left[\left(\frac{K_0^2}{H} + \frac{K_1^2}{J R} \right) \left(\frac{b^2}{a^2} M(\gamma b) - M(\gamma a) \right) \right. \right. \\ \left. \left. + \left(\frac{I_0^2}{H} + \frac{I_1^2}{J R} \right) \left(\frac{b^2}{a^2} N(\gamma b) - N(\gamma a) \right) + 2 \left(\frac{I_0 K_0}{H} - \frac{I_1 K_1}{J R} \right) \left(\frac{b^2}{a^2} P(\gamma b) - P(\gamma a) \right) \right] \right\}^{-1/2}, \quad (4)$$



where I_0 , I_1 , and I_2 are Bessel functions of an imaginary argument of the first kind of order zero, one, and two, respectively; and K_0 , K_1 , and K_2 are Bessel functions of an imaginary argument of the second kind of order zero, one, and two, respectively.

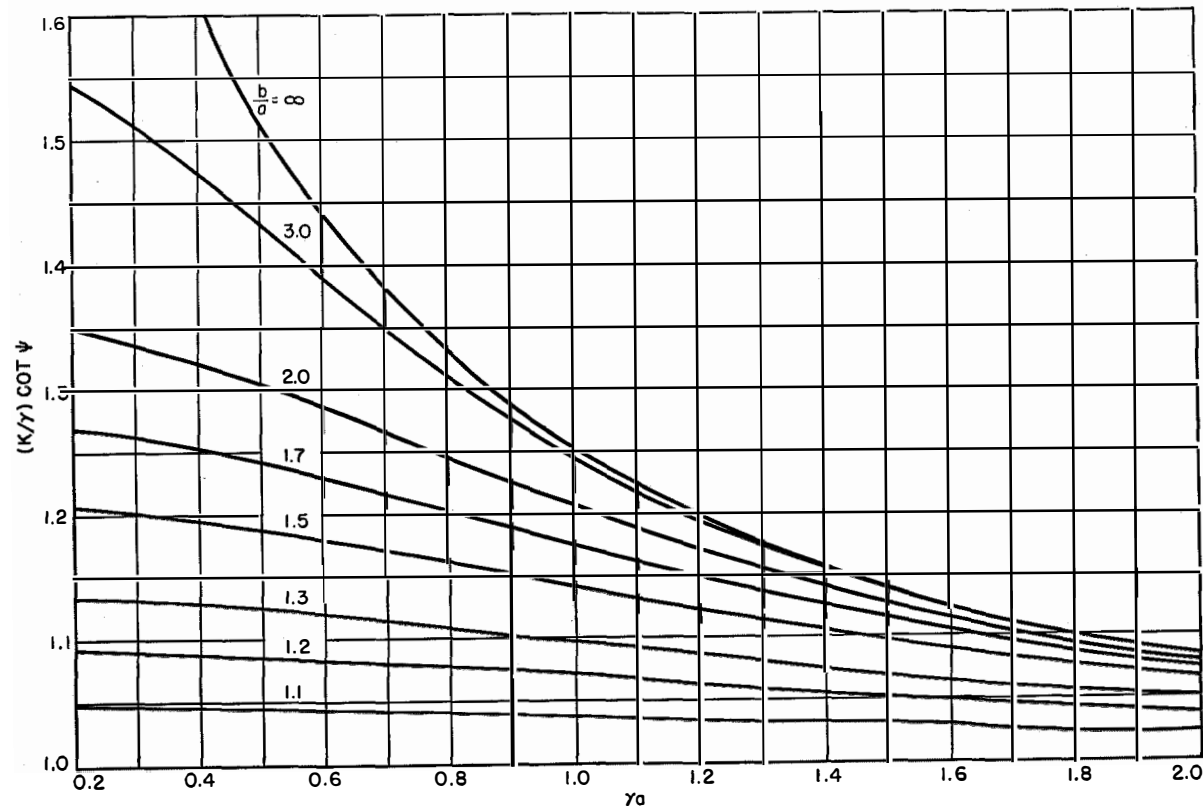
The broken-line underscoring denotes the argument γa for the functions and the solid-line underscoring denotes the argument γb .

The quantities H , J , R , $M(x)$, $N(x)$, and $P(x)$ are defined by the following equations.

$$H \equiv [I_0(\gamma a)K_0(\gamma b) - I_0(\gamma b)K_0(\gamma a)]^2$$

$$J \equiv [I_1(\gamma a)K_1(\gamma b) - I_1(\gamma b)K_1(\gamma a)]^2$$

Figure 2—Below and at left, $(k/\gamma) \cot \psi$, a quantity proportional to velocity, plotted as a function of γa , a quantity proportional to frequency, for a helically conductive cylinder within a coaxial conductive cylinder.



$$R \equiv \frac{I_0(\gamma a)K_0(\gamma a)}{I_1(\gamma a)K_1(\gamma a)} \left[\frac{1 - \frac{I_0(\gamma a)K_0(\gamma b)}{K_0(\gamma a)I_0(\gamma b)}}{1 - \frac{I_1(\gamma a)K_1(\gamma b)}{K_1(\gamma a)I_1(\gamma b)}} \right]$$

$$M(x) \equiv I_1^2(x) - I_0(x)I_2(x)$$

$$N(x) \equiv K_1^2(x) - K_0(x)K_2(x)$$

$$P(x) \equiv I_1(x)K_1(x) + I_2(x)K_2(x).$$

Figure 3 shows $F(\gamma a, \gamma b)$ as a function of γa for various radii of the surrounding cylinder. The effect of the surrounding cylinder has been to reduce the impedance parameter as b/a is decreased. The physical interpretation of this is that as b/a is reduced, more of the radio-frequency energy flows between the helix and the cylinder, thus reducing E_z^2 on the axis.

The derivations of (3) and (4) are given in the appendix.

3. Helical Conductor Surrounding a Coaxial Conductive Cylinder

For this condition, radius c is finite and less than a , while b is infinite. The radial propagation

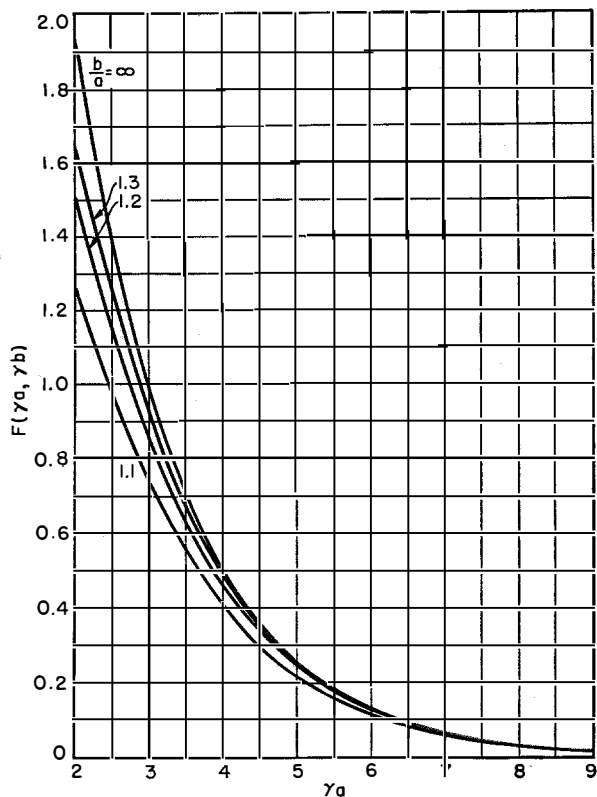
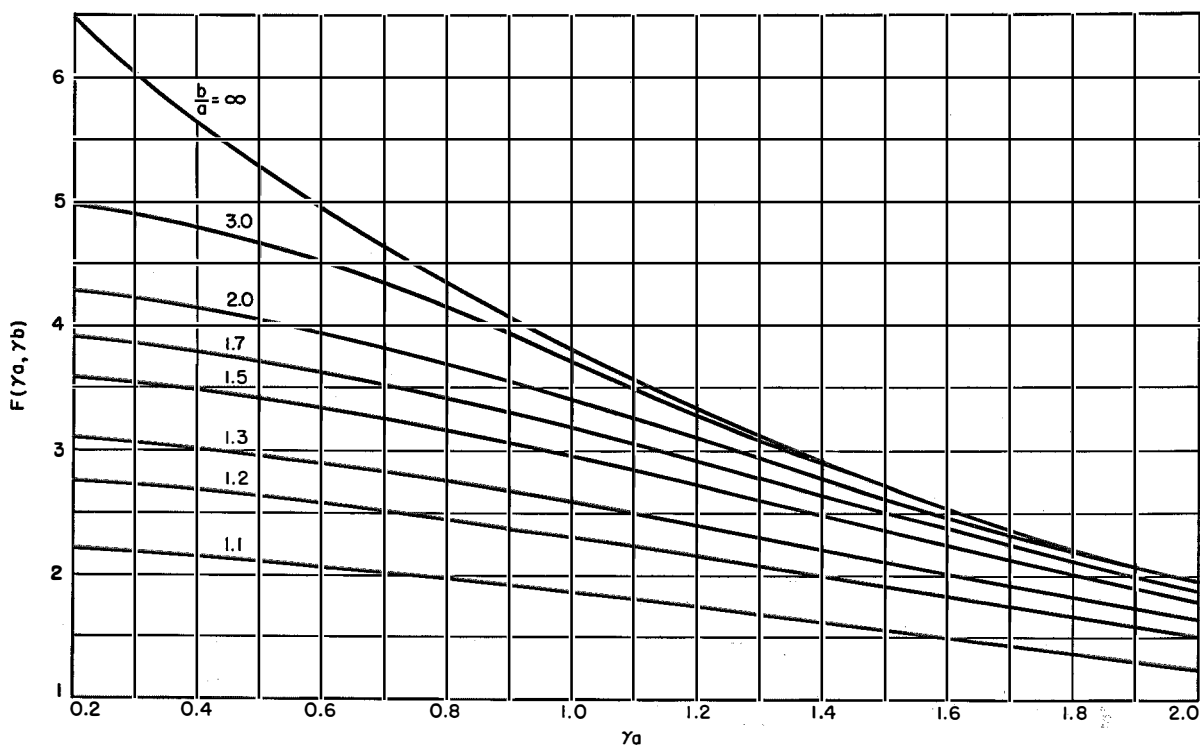


Figure 3—Above and below, impedance function $F(\gamma a, \gamma b)$ plotted against γa for a helically conductive cylinder within a coaxial conductive cylinder.



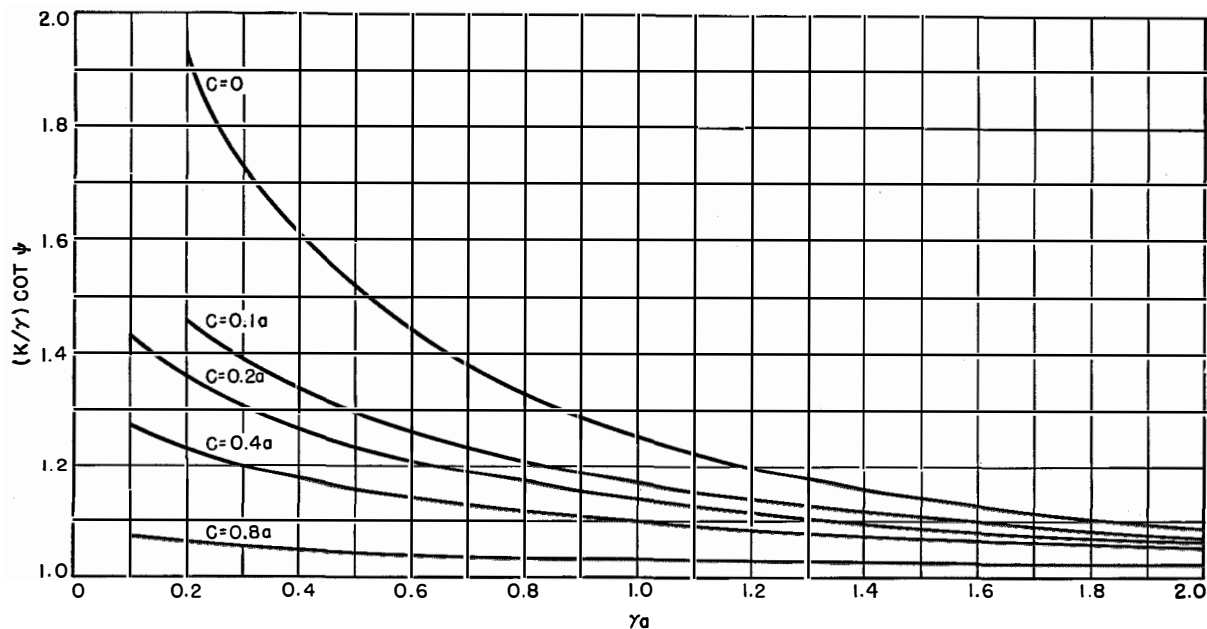


Figure 4— $(k/\gamma) \cot \psi$, a quantity proportional to velocity, plotted as a function of γa , a quantity proportional to frequency, for a helically conductive cylinder with an inner coaxial conductive cylinder.

constant is given³ by

$$\left(\frac{k}{\gamma} \cot \psi\right)^2 = \frac{I_0(\gamma a) K_0(\gamma a)}{I_1(\gamma a) K_1(\gamma a)} \left[\frac{1 - \frac{I_0(\gamma c) K_0(\gamma a)}{K_0(\gamma c) I_0(\gamma a)}}{1 - \frac{I_1(\gamma c) K_1(\gamma a)}{K_1(\gamma c) I_1(\gamma a)}} \right] \quad (5)$$

The solution is shown plotted in Figure 4 with b/a as a parameter.

4. Helical Conductor Between Coaxial Conductive Cylinders

For this condition, radius c is finite and less than a , while b is finite and greater than a . The radial propagation constant is given by

$$\left(\frac{k}{\gamma} \cot \psi\right)^2 = \frac{I_0(\gamma a) K_0(\gamma a)}{I_1(\gamma a) K_1(\gamma a)} \frac{I_0(\gamma b) K_1(\gamma b)}{I_1(\gamma b) K_0(\gamma b)} \frac{I_1(\gamma c) K_0(\gamma c)}{I_0(\gamma c) K_1(\gamma c)} \times \left[\frac{\left(1 - \frac{I_0(\gamma a) K_0(\gamma b)}{K_0(\gamma a) I_0(\gamma b)}\right) \left(1 - \frac{I_0(\gamma c) K_0(\gamma a)}{K_0(\gamma c) I_0(\gamma a)}\right) \left(1 - \frac{I_1(\gamma b) K_1(\gamma c)}{I_1(\gamma c) K_1(\gamma b)}\right)}{\left(1 - \frac{I_1(\gamma a) K_1(\gamma b)}{K_1(\gamma a) I_1(\gamma b)}\right) \left(1 - \frac{I_1(\gamma c) K_1(\gamma a)}{K_1(\gamma c) I_1(\gamma a)}\right) \left(1 - \frac{I_0(\gamma b) K_0(\gamma c)}{I_0(\gamma c) K_0(\gamma b)}\right)} \right] \quad (6)$$

³O. Doehler and W. Kleen, "Effect of the Transverse Electric Vector on the Delay Line of a Traveling-Wave Tube," *Annales de Radioélectricité*, volume 4, pages 117-130; 1949.

The solution is shown plotted in Figure 5 with $c:a:b$ as a parameter.

5. Acknowledgments

The form of the expression given in (4) is due to Mr. V. R. Saari. The computations for the curves were carried out by Mrs. E. J. White.

6. Glossary of Symbols

- a = mean radius of helically conductive cylinder
- b = inner radius of outer conductive cylinder
- c = outer radius of inner conductive cylinder
- c = velocity of light
- E = electric field along the axis indicated by the subscript

I = modified Bessel function of the first kind and of the order indicated by the subscript

$k = \omega/c$

K = modified Bessel function of the second kind and of the order indicated by the subscript

P = total power flowing

v = axial phase velocity

$\beta = \omega/v$

$\gamma = (\beta^2 - k^2)^{1/2}$ = radial propagation constant

ψ = pitch angle between helix and a circumference

$\omega = 2\pi f$ = radian frequency.

parameter defined as

$$(E_z^2/\beta^2 P)^{1/2}. \quad (1)$$

The field components representing solutions of the wave equation in cylindrical coordinates for a plane wave having circular symmetry and propagating in the z direction with velocity

$$v = \omega/\beta \quad (2)$$

for the model of Figure 1, with the center conductor removed, with lossless conductors, and with space having a dielectric constant equal to that of vacuum are

Inside radius a , $r \leq a$,

$$H_{z1} = B_1 I_0(\gamma r) \quad (3)$$

$$E_{z3} = B_3 I_0(\gamma r) \quad (4)$$

$$H_{\phi 3} = B_3 \frac{j\omega\epsilon}{\gamma} I_1(\gamma r) \quad (5)$$

$$H_{r1} = B_1 \frac{j\beta}{\gamma} I_1(\gamma r) \quad (6)$$

$$E_{\phi 1} = -B_1 j \frac{\omega\mu}{\gamma} I_1(\gamma r) \quad (7)$$

$$E_{r3} = B_3 \frac{j\beta}{\gamma} I_1(\gamma r). \quad (8)$$

7. Appendix—Wave Propagation on a Helical Conductor Surrounded by a Coaxial Conductive Cylinder⁴

The problem of propagation on a helical conductor has been treated in detail.¹ In many applications of helical delay lines as well as traveling-wave tubes, the helix is surrounded by a conductive cylinder. We are interested in the effect of a uniformly conductive cylinder on the phase velocity of the wave and on the impedance

⁴ Similar results for propagation constants using a different approach were obtained by W. Sichak in, "Coaxial Line with Helical Inner Conductor," soon to be published in *Proceedings of the IRE*.

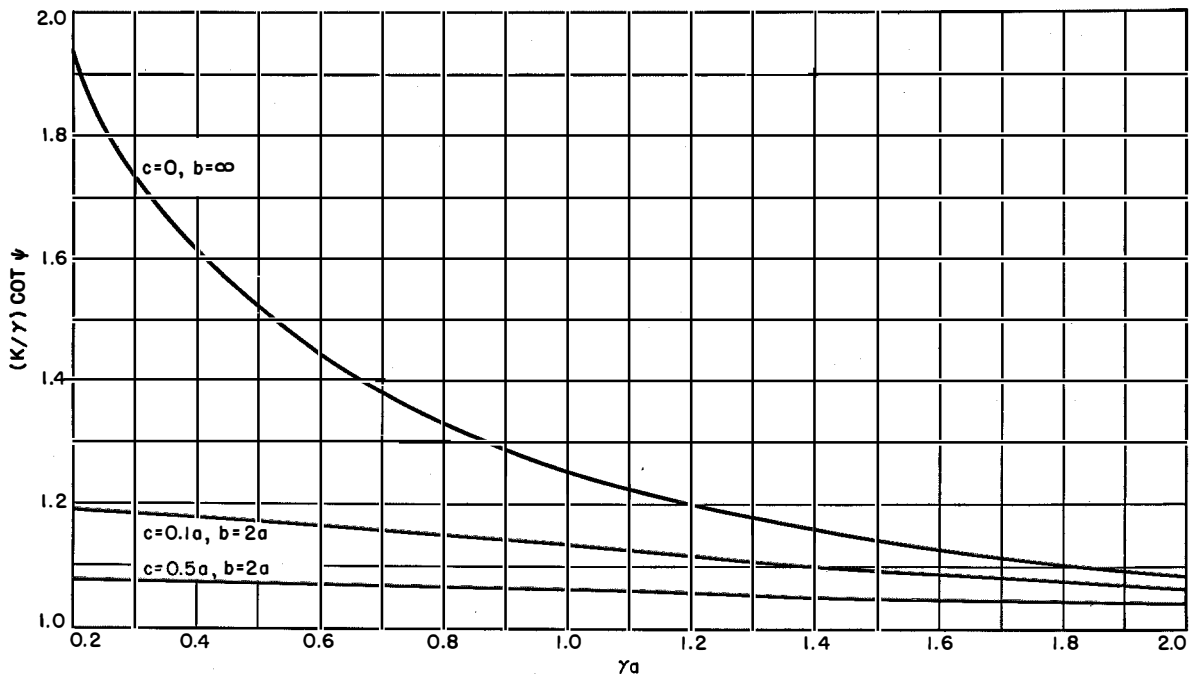


Figure 5— $(k/\gamma) \cot \psi$, a quantity proportional to velocity, plotted as a function of γa , a quantity proportional to frequency, for a helically conductive cylinder between two coaxial conductive cylinders.

Outside radius a , $r \leq a \leq b$

$$H_{z2} = B_2[I_0(\gamma r)K_1(\gamma b) + K_0(\gamma r)I_1(\gamma b)] \quad (9)$$

$$E_{z4} = B_4[I_0(\gamma r)K_0(\gamma b) - K_0(\gamma r)I_0(\gamma b)] \quad (10)$$

$$H_{\phi 4} = -B_4 \frac{j\omega\epsilon}{\gamma} \times [I_1(\gamma r)K_0(\gamma b) + K_1(\gamma r)I_0(\gamma b)] \quad (11)$$

$$H_{r2} = -B_2 j \frac{\beta}{\gamma} \times [I_1(\gamma r)K_1(\gamma b) - K_1(\gamma r)I_1(\gamma b)] \quad (12)$$

$$E_{\phi 2} = B_2 j \frac{\omega\mu}{\gamma} \times [I_1(\gamma r)K_1(\gamma b) - K_1(\gamma r)I_1(\gamma b)] \quad (13)$$

$$E_{r4} = -B_4 j \frac{\beta}{\gamma} \times [I_1(\gamma r)K_0(\gamma b) + K_1(\gamma r)I_0(\gamma b)], \quad (14)$$

where

$$\left. \begin{aligned} \gamma &= (\beta^2 - k^2)^{1/2} \\ \beta &= \omega/v \\ k &= \omega/c \end{aligned} \right\} (15)$$

and all field components [(3) through (14)] are multiplied by $\exp [j(\omega t - \beta z)]$.

The boundary conditions to be satisfied at the cylinder of radius a are as follows.

First,

$$E_{z3} \sin \psi + E_{\phi 1} \cos \psi = 0 \quad (16)$$

$$E_{z4} \sin \psi + E_{\phi 2} \cos \psi = 0. \quad (17)$$

Second,

$$E_{z3} = E_{z4} \quad (18)$$

$$E_{\phi 1} = E_{\phi 2}. \quad (19)$$

Third,

$$H_{z1} \sin \psi + H_{\phi 3} \cos \psi = H_{z2} \sin \psi + H_{\phi 4} \cos \psi. \quad (20)$$

These boundary conditions applied to (3) through (14) yield an expression for the determination of the propagation constant γ .

$$\left(\frac{k}{\gamma \cot \psi} \right)^2 = \frac{I_0(\gamma a)K_0(\gamma a)}{I_1(\gamma a)K_1(\gamma a)} \left[\frac{1 - \frac{I_0(\gamma a)K_0(\gamma b)}{K_0(\gamma a)I_0(\gamma b)}}{1 - \frac{I_1(\gamma a)K_1(\gamma b)}{K_1(\gamma a)I_1(\gamma b)}} \right]. \quad (21)$$

The field components in terms of a common amplitude factor B are as follows.

Inside the helix, $r \leq a$

$$E_z = BI_0(\gamma r) \quad (22)$$

$$E_r = jB \frac{\beta}{\gamma} I_1(\gamma r) \quad (23)$$

$$E_\phi = -B \frac{I_0(\gamma a)}{I_1(\gamma a)} \frac{1}{\cot \psi} I_1(\gamma r) \quad (24)$$

$$H_z = -j \frac{B \gamma I_0(\gamma a)}{K k I_1(\gamma a)} \frac{1}{\cot \psi} I_0(\gamma r) \quad (25)$$

$$H_r = \frac{B \beta I_0(\gamma a)}{K k I_1(\gamma a)} \frac{1}{\cot \psi} I_1(\gamma r) \quad (26)$$

$$H_\phi = j \frac{B k}{K \gamma} I_1(\gamma r). \quad (27)$$

Outside the helix, $a \leq r \leq b$

$$E_z = BI_0(\gamma a) \times \left[\frac{I_0(\gamma r)K_0(\gamma b) - K_0(\gamma r)I_0(\gamma b)}{I_0(\gamma a)K_0(\gamma b) - K_0(\gamma a)I_0(\gamma b)} \right] \quad (28)$$

$$E_r = jB \frac{\beta}{\gamma} I_0(\gamma a) \times \left[\frac{I_1(\gamma r)K_0(\gamma b) + K_1(\gamma r)I_0(\gamma b)}{I_0(\gamma a)K_0(\gamma b) - K_0(\gamma a)I_0(\gamma b)} \right] \quad (29)$$

$$E_\phi = -BI_0(\gamma a) \frac{1}{\cot \psi} \times \left[\frac{I_1(\gamma r)K_1(\gamma b) - K_1(\gamma r)I_1(\gamma b)}{I_1(\gamma a)K_1(\gamma b) - K_1(\gamma a)I_1(\gamma b)} \right] \quad (30)$$

$$H_z = -j \frac{B \gamma}{K k} I_0(\gamma a) \frac{1}{\cot \psi} \times \left[\frac{I_0(\gamma r)K_1(\gamma b) + K_0(\gamma r)I_1(\gamma b)}{I_1(\gamma a)K_1(\gamma b) - K_1(\gamma a)I_1(\gamma b)} \right] \quad (31)$$

$$H_r = \frac{B \beta}{K k} I_0(\gamma a) \frac{1}{\cot \psi} \times \left[\frac{I_1(\gamma r)K_1(\gamma b) - K_1(\gamma r)I_1(\gamma b)}{I_1(\gamma a)K_1(\gamma b) - K_1(\gamma a)I_1(\gamma b)} \right] \quad (32)$$

$$H_\phi = -j \frac{B k}{K \gamma} I_0(\gamma a) \times \left[\frac{I_1(\gamma r)K_0(\gamma b) + K_1(\gamma r)I_0(\gamma b)}{I_0(\gamma a)K_0(\gamma b) - K_0(\gamma a)I_0(\gamma b)} \right], \quad (33)$$

where

$$K = (\mu/\epsilon)^{1/2} = 120\pi, \text{ ohms} \quad (34)$$

and all field components [(22) through (33)] are multiplied by $\exp [j(\omega t - \beta z)]$.

The impedance parameter may now be evaluated by use of these field components. The power associated with the propagation is given by

$$P = \frac{1}{2} R_e \int E \times H^* d\tau \quad (35)$$

taken over a plane normal to the axis of propagation. This is

$$P = \pi R_e \left[\int_0^a (E_r H_\phi^* - E_\phi H_r^*) r dr + \int_a^b (E_r H_\phi^* - E_\phi H_r^*) r dr \right]. \quad (36)$$

This yields

$$P = E_z^2(0) \frac{\pi}{2K} \frac{\beta a k a}{\gamma^2} \left\{ \left[1 + \frac{I_0^2(\gamma a)}{I_1^2(\gamma a) R} \right] \left[\frac{a^2}{2} M(\gamma a) \right] + \left[\frac{HK_0^2(\gamma b)}{R} + \frac{JK_1^2(\gamma b)}{R} \right] \right. \\ \times \left[\frac{b^2}{2} M(\gamma b) - \frac{a^2}{2} M(\gamma a) \right] + \left[\frac{HI_0^2(\gamma b)}{R} + \frac{JK_1^2(\gamma b)}{R} \right] \left[\frac{b^2}{2} N(\gamma b) - \frac{a^2}{2} N(\gamma a) \right] \\ \left. + 2 \left[\frac{HI_0(\gamma b) K_0(\gamma b)}{R} - \frac{J}{R} I_1(\gamma b) K_1(\gamma b) \right] \left[\frac{b^2}{2} P(\gamma b) - \frac{a^2}{2} P(\gamma a) \right] \right\}. \quad (37)$$

Defining the impedance function as

$$(E_z^2/\beta^2 P)^{1/4} = (\beta/k)^{1/4} (\gamma/\beta)^{1/4} F(\gamma a, \gamma b) \quad (38)$$

gives

$$F(\gamma a, \gamma b) = \left\{ \frac{(\gamma a)^2}{240} \left\{ \left[1 + \frac{I_0^2(\gamma a)}{R I_1^2(\gamma a)} \right] \left[M(\gamma a) \right] + I_0^2(\gamma a) \left[\left(\frac{K_0^2}{H} + \frac{K_1^2}{JR} \right) \left(\frac{b^2}{a^2} M(\gamma b) - M(\gamma a) \right) \right. \right. \right. \\ \left. \left. + \left(\frac{I_0^2}{H} + \frac{I_1^2}{JR} \right) \left(\frac{b^2}{a^2} N(\gamma b) - N(\gamma a) \right) + 2 \left(\frac{I_0 K_0}{H} - \frac{I_1 K_1}{JR} \right) \left(\frac{b^2}{a^2} P(\gamma b) - P(\gamma a) \right) \right] \right\}^{-1/4}. \quad (39)$$

Determination of Reflection Coefficients and Insertion Loss of a Waveguide Junction*

By G. A. DESCHAMPS

Federal Telecommunication Laboratories, a division of International Telephone and Telegraph Corporation; Nutley, New Jersey

REFLECTION and transmission coefficients are important parameters of a waveguide junction. It is shown that these parameters in phase as well as in magnitude may be read directly from a graph. A short-circuit is moved in one of two waveguides that are connected by the junction, and the corresponding reflection coefficient is measured in the other waveguide as in a standard method. The positions of the short-circuit, however, are taken equally spaced every $\frac{1}{8}$ th of a wavelength. When plotted in the complex plane, the corresponding reflection coefficients fall on a circle and the chords joining opposite points intersect at a point that is simply related to the desired parameters.

When very accurate measurements are desired, 8 or even 16 short-circuit positions spaced at $\frac{1}{16}$ th or $\frac{1}{32}$ nd wavelength can be used. The quality of the chord intersection then gives a control of the experiment by showing systematic or random errors. When the intersection is not perfect because of random errors, a method of averaging is described that reduces these errors.

• • •

1. Introduction

The best description of a waveguide junction from the viewpoint of power relations is the scattering matrix.¹ For the elements of this matrix, s_{11} is the reflection coefficient at terminal 1 when line 2 is matched, s_{22} is the reflection coefficient at terminal 2 when line 1 is matched, and s_{12} is the transmission coefficient from 1 to 2. Terminals 1 and 2 are some arbitrarily specified points in the two transmission lines (Figure 1), and it is understood that the two waveguides or transmission lines can carry only one mode. The

* Reprinted from *Journal of Applied Physics*, volume 24, pages 1046-1050; August, 1953. This work was sponsored by the Wright-Patterson Air Force Base; Dayton, Ohio.

¹ C. G. Montgomery, R. H. Dicke, and E. M. Purcell, "Principles of Microwave Circuits," McGraw-Hill Book Company, Incorporated, New York, New York; 1948; page 146.

transmission coefficient s_{21} is equal to s_{12} when reciprocity applies, as will be assumed here. The insertion loss

$$(s_{12})_{db} = -20 \log_{10} |s_{12}| \quad (1)$$

is a measure of the efficiency of the junction.

The junction is generally described by some equivalent circuit, which is obtained by impedance measurements and from which the scattering coefficients would have to be deduced. The present method gives them more directly by interpreting the bilinear relation

$$w' = T(w) \quad (2)$$

between a reflection coefficient w at terminal 2 and its image w' at terminal 1.

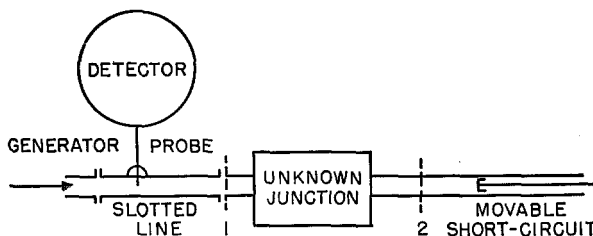


Figure 1—Experimental setup.

2. Measurement Procedure

The experimental procedure is a slight modification of the conventional method.² A short-circuit is moved in line 2 and produces at terminal 2 a reflection coefficient of unit amplitude and known phase. Measuring the standing waves in line 1 will give the corresponding reflection coefficient w' at terminal 1. (See Figure 1.)

Instead of moving the short-circuit in line 2 arbitrarily, we displace it in equal steps, for instance, $\frac{1}{16}$ -wavelength intervals. Thus the reflection coefficient w takes values w_1, w_2, \dots, w_8 , which form a regular polygon on the unit

² N. Marcuvitz, "Waveguide Handbook," McGraw-Hill Book Company, Incorporated, New York, New York; 1951; pages 130-138.

circle Γ in the w plane (Figure 2A). The images by the transformation T , characteristic of the junction, fall on a circle Γ' inside Γ as shown in Figure 2B.

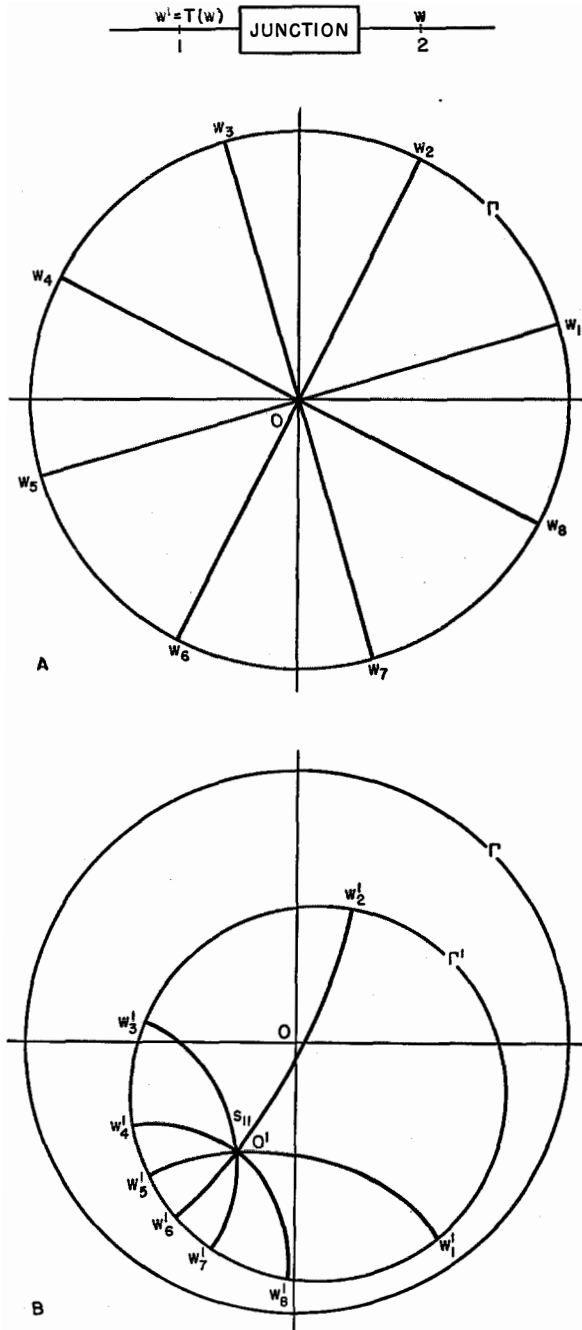


Figure 2—Unit circle Γ and its image Γ' by the transformation T , characteristic of the junction. *A*—Reflection coefficient w at terminal 2. *B*—Reflection coefficient w' at terminal 1.

The diameters of the unit cycle Γ become circles orthogonal to Γ' and passing through the point O' , the image of O . The point O' , called the iconocenter³ of Γ' , plays an important part in the interpretation of the results.

3. Reflection Coefficient s_{11}

Determination of the reflection coefficient s_{11} is equivalent to the construction of the iconocenter, since obviously the complex number corresponding to O' is

$$T(O) = s_{11}. \quad (3)$$

The point O' may be obtained by drawing the circles shown in Figure 2B. However, it is simpler to proceed as follows. The chords $w_1'w_6'$, $w_2'w_5'$, $w_3'w_7'$, $w_4'w_8'$, have a common crossover point \bar{O} . If as in Figure 3 the perpendiculars CL and

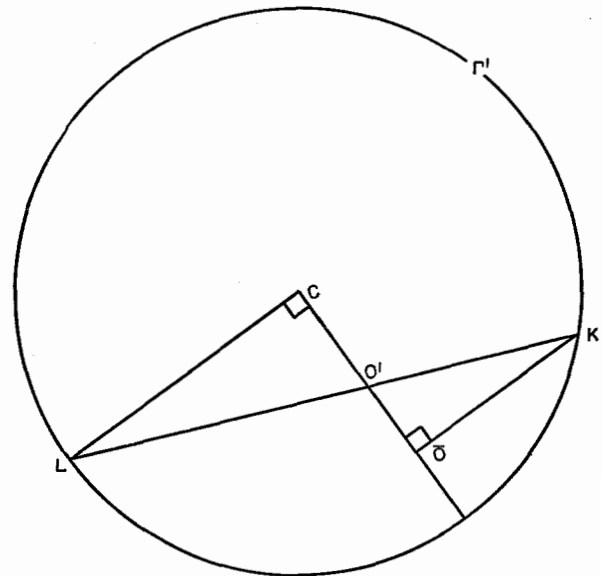


Figure 3—Relation between the iconocenter and the crossover point.

$\bar{O}K$ are drawn to the radius $C\bar{O}$ of circle Γ' , the point O' will be the intersection of $C\bar{O}$ and LK .

The existence of the crossover point and its relation to the iconocenter may be proved by considering the sphere S having Γ' as its equator (Figure 4). By stereographic projection from the pole L , any circle γ' passing through O' and orthogonal to Γ' is transformed into a circle γ

³ From the Greek $\epsilon\iota\kappa\omega\upsilon\upsilon$ for image. The point O' is not defined uniquely by the circle Γ' but depends on how the images w_i' are distributed on it.

on S , also orthogonal to Γ' and passing through the stereographic projection K of O' . By projection on the plane of the equator, this circle becomes a straight line $\bar{\gamma}$, which goes through the projection \bar{O} of K . The construction in Figure 3 is a reproduction of $LCO'K\bar{O}$ on the plane of Γ' obtained for instance by rotation through 90 degrees about CO' .

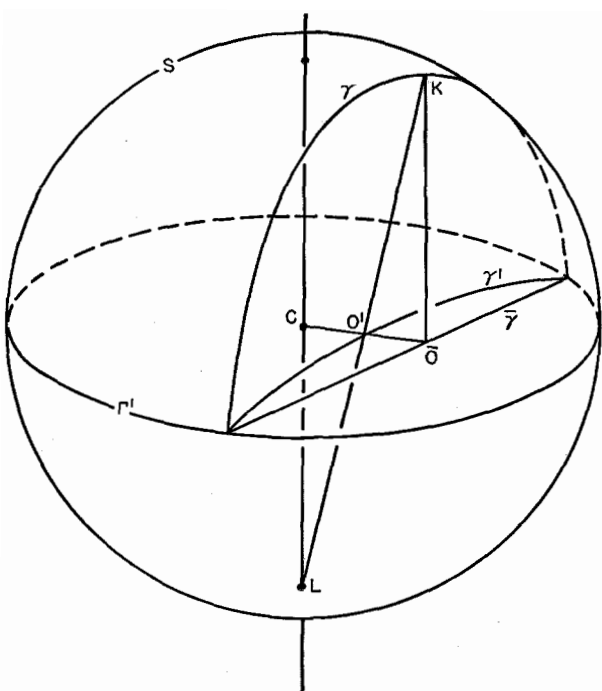


Figure 4—Transformation from the crossover point to the iconocenter.

It is to be noted that s_{11} is obtained correctly by the present method even if the short-circuit is not perfect. The circle Γ is then replaced by a circle concentric to it and therefore its image has the same iconocenter O' as before.

If a matched load is available in line 2, the point O' can also be obtained by direct measurement of the corresponding input reflection coefficient in line 1.

4. Power Relations

The power relations that are expressed by the absolute values of the scattering coefficients can be deduced from the iconocenter O' , the center C , and the radius R of the image circle Γ' . The

equations proved in Section 4 are

$$|s_{11}| = OO', \tag{4}$$

$$|s_{22}| = CO'/R, \tag{5}$$

$$|s_{12}|^2 = R(1 - |s_{22}|^2). \tag{6}$$

An alternative form of (6) deduced by elementary geometry is

$$|s_{12}| = O'H/R^{1/2}, \tag{7}$$

where $O'H$ is perpendicular to CO' and H is on Γ' (Figure 5). Introducing the notation $(x)_{db}$ to mean $-20 \log_{10}|x|$, we find the insertion loss

$$(s_{12})_{db} = (O'H)_{db} - \frac{1}{2}(R)_{db}. \tag{8}$$

These results do not depend on the choice of the terminal planes for the junction.⁴

When a wave of unit amplitude is incident on side 2 of the junction and the transmission line connected to 1 is matched, the power $|s_{22}|^2$ is

⁴They are "distant invariant" in the sense given on page 137 of footnote reference 2.

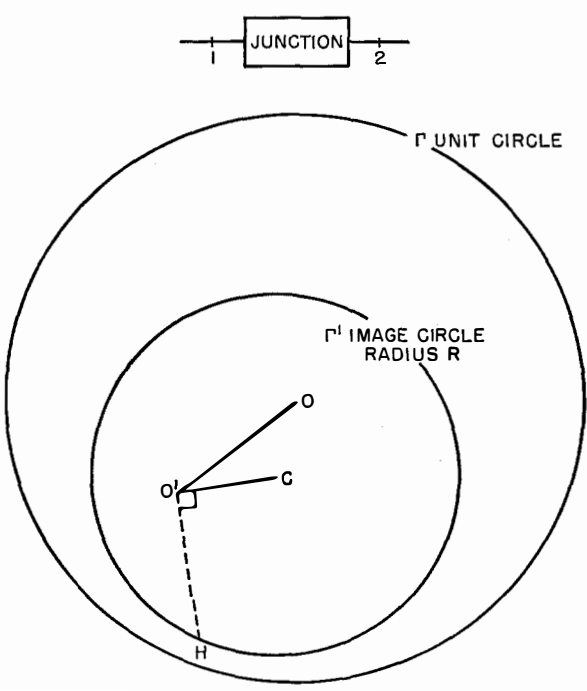


Figure 5—Power relations. The magnitudes of the reflection coefficient on sides 1 and 2 of the junction are, respectively, $|s_{11}| = OO'$ and $|s_{22}| = CO'/R$. The magnitude of the transmission coefficient is $|s_{12}| = O'H/R^{1/2}$ or in decibels the insertion loss is $(s_{12})_{db} = (O'H)_{db} - \frac{1}{2}(R)_{db}$.

reflected and $|s_{12}|^2$ is transmitted. Therefore, R indicates, according to (6), the fraction of the net incident power $1 - |s_{22}|^2$ that is transmitted.⁵

5. Phase Relations

Before considering the phases of s_{22} and s_{12} , it is convenient to introduce the transformation Θ , which is the result of a negative inversion of center O' leaving Γ' invariant followed by a negative inversion of center C also leaving Γ' invariant. The effect of Θ on the points of Γ' is quite simple; it is a projection of center O' followed by a projection of center C and transforms M' into M'' , for instance, as illustrated in Figure 6. Θ is a bilinear transformation that carries O' into C and, therefore, it also carries the circles orthogonal to Γ' and passing through O' into the diameters of Γ' . Since the transformation is conformal, these diameters form between them the same angles as the original diameters of Γ .

The use of Θ makes it possible to extend the transformation T to points of Γ for which a measurement has not been made. For instance, if the point $P(w = +1)$ is not one of the w_i , we find its image by considering $w_1'' = \Theta(w_1')$ and observing that the angle between P'' and w_1'' on Γ' must equal the angle between $+1$ and w_1 on

⁵ This interpretation of R is found in W. Altar, "Q Circles—Means of Analysis of Resonant Microwave Systems," *Proceedings of the IRE*, volume 35, pages 355-361 and pages 478-484; April and May, 1947; also in A. L. Cullen, "Measurement of Microwave-Transmission Efficiency," *Wireless Engineer*, volume 26, pages 255-257; August, 1949.

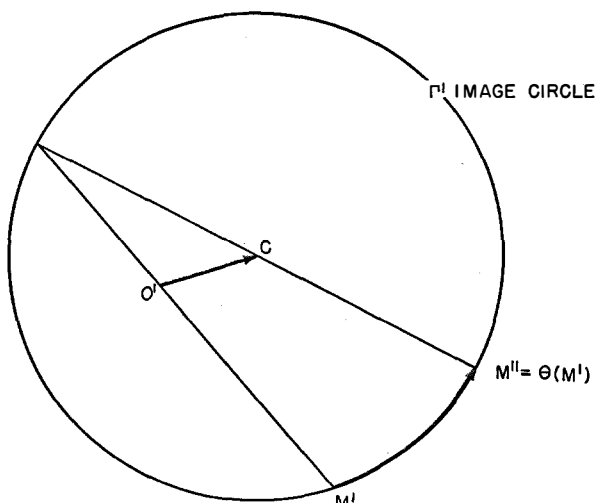


Figure 6—The transformation Θ .

Γ . We can construct P'' from this property and then P' by applying Θ^{-1} .

As shown in the next section, the phase σ_2 of s_{22} is then the angle between the vectors $O'C$ and CP'' (Figure 7),

$$\sigma_2 = (\angle O'C, CP''). \quad (9)$$

The phase⁶ σ_{12} of the transmission coefficient s_{12} is

$$\sigma_{12} = \frac{1}{2}(\angle OP, CP''). \quad (10)$$

It is to be noted that the sign of s_{12} cannot be determined by the present method and this is reflected in (10), which gives σ_{12} only modulo π .

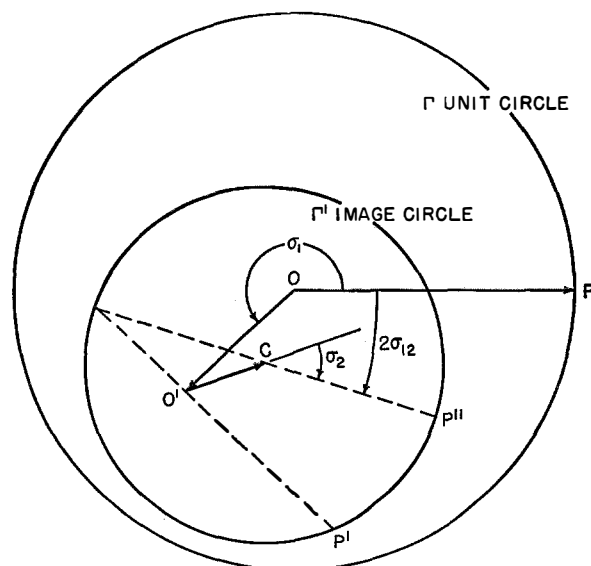


Figure 7—Phase relations. The phases of the scattering coefficients s_{11} , s_{22} , s_{12} are, respectively, σ_1 , σ_2 , σ_{12} .

6. Relations Between Image Circle and Scattering Coefficients

The transformation T is given explicitly by

$$w' = T(w) = s_{11} + s_{12}^2 w / (1 - s_{22} w). \quad (11)$$

One verifies immediately that

$$T(O) = s_{11}.$$

To find the other relations, first assume that the terminals have been chosen at $1'$ and $2'$

⁶ The angles in (9) and (10) are directed angles between directed segments or vectors. Changing the sense of one of these vectors or their order would give an incorrect result.

(Figure 8) so as to make both s_{11} and s_{22} real and positive.

The point C and the point at infinity are inverse with respect to Γ' , and therefore $T^{-1}(C)$ and $T^{-1}(\infty) = s_{22}^{-1}$ are inverse with respect to the unit circle Γ . The inverse of the point $1/s_{22}$ being the point $s_{22}^* = s_{22}$, the affix⁷ of C will be

$$w_C = T(s_{22}) = s_{11} + s_{22} s_{12}^2 / (1 - s_{22}^2). \quad (12)$$

The image P' of the point P ($w = +1$) corresponds to

$$w_1 = T(1) = s_{11} + s_{12}^2 / (1 - s_{22}^2). \quad (13)$$

The affix of CP' is, therefore,

$$w_1 - w_C = s_{12}^2 / (1 - s_{22}^2), \quad (14)$$

where the phase angle is twice that of s_{12} and where the absolute value is the radius R of the image circle Γ' ,

$$R = |s_{12}|^2 / (1 - s_{22}^2). \quad (15)$$

The affix of $O'C$ is

$$w_C - s_{11} = s_{22} s_{12}^2 / (1 - s_{22}^2).$$

⁷ The affix of a point or of a vector in the complex plane is the complex number corresponding to that point or that vector.

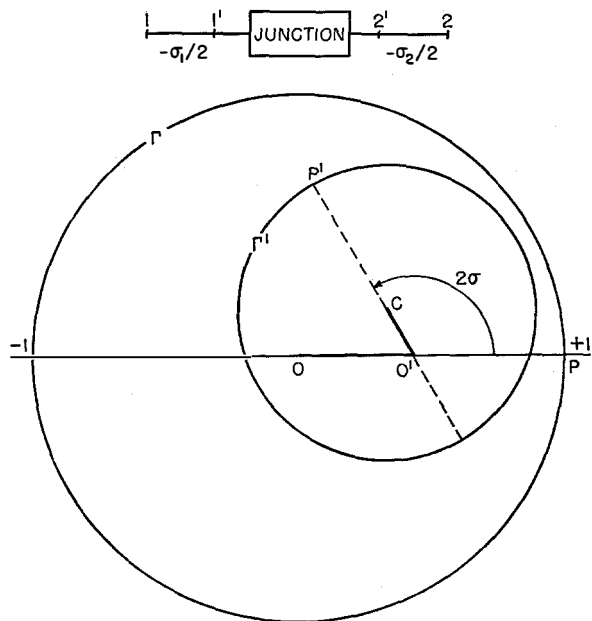


Figure 8—Image circle when both reflection coefficients are real and positive. (Junction between terminals $1'$ and $2'$.)

It has the same phase 2σ as $w_1 - w_C$, and therefore the points $O'CP'$ are on a straight line as in Figure 8 and also

$$s_{22} = O'C/R. \quad (16)$$

It remains to show what happens when s_{11} and s_{22} have the phases σ_1 and σ_2 , respectively. The junction is now considered between its terminals 1 and 2 instead of $1'$ and $2'$ and the lengths of line $11'$ and $22'$ are, respectively, $-(\sigma_1/2)$ and $-(\sigma_2/2)$ radians.

The effect of the line on side 1 is to rotate the circle Γ' and the points on it about the point O through the angle σ_1 (Figure 9). The effect on

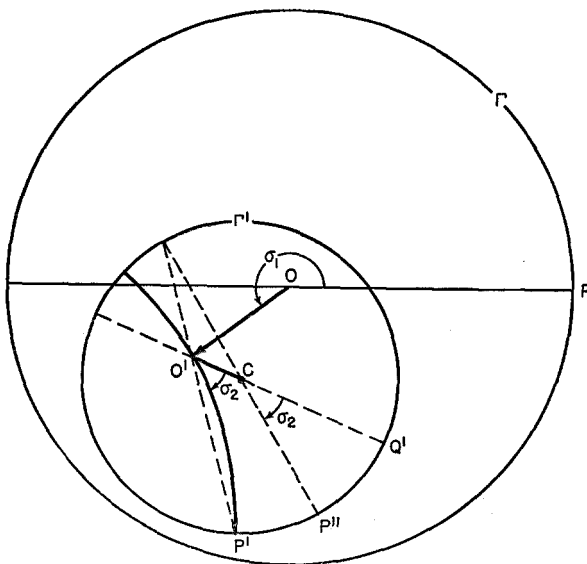


Figure 9—Transformation of the image circle (Figure 7) when the junction is referred to its actual terminals 1 and 2 .

side 2 is to rotate the points on the unit circle Γ through the angle σ_2 before they undergo the above transformation. The image of P ($w = +1$) instead of being the point Q' on $O'C$ produced, as it would be if $\sigma_2 = 0$, is the point P' . Therefore σ_2 is the angle between $O'C$ and the arc of a circle $O'P'$, image of OP . Applying the conformal transformation Θ considered in section 5, this angle becomes (CQ', CP'') or $(O'C, CP'')$ as indicated in (9).

For the phase σ_{12} of s_{12} , we have to add $\sigma_1/2$, $\sigma_2/2$, and σ :

$$\left. \begin{aligned} 2\sigma_{12} &= \sigma_1 + \sigma_2 + 2\sigma \\ &= (\text{OP}, \text{OO}') + (\text{O}'\text{C}, \text{CP}'') + (\text{OO}', \text{O}'\text{C}) \\ &= (\text{OP}, \text{CP}''), \end{aligned} \right\} (17)$$

which justifies (10).

Equations (6) and (5) result from (15) and (16) by replacing s_{22} by its absolute value if we note that the length $O'C$ and R are not changed by the introduction of the lines $11'$ and $22'$.

7. Approximate Relations

When a rapid evaluation is desired, it is sufficient to take four positions of the short-circuit at intervals $\frac{1}{8}$ -th-wavelength apart. Three positions would be sufficient and, even if taken arbitrarily, could be used to construct the iconocenter. However the simplification in interpreting the measurement justifies taking an extra reading.

The following remarks help in computing the scattering coefficients. If the crossover point is not more than $R/4$ away from the center C of the circle Γ' , the phase angles on Γ' can be obtained with less than 1 degree of error by measuring them directly from the crossover point \bar{O} . The iconocenter is then practically the middle of $C\bar{O}$ with less than 1.5 percent error on CO' . Finally when s_{22} is small, (5) reduces to $|s_{12}| \approx R^{2/4}$.

8. Precision Measurement

If on the other hand very accurate results are desired, it becomes advisable to use 8 or even 16 points equally spaced on the circle Γ . Then, two controls on the quality of the experiments are available: The image points should fall on a circle and the 4 (or 8) chords should intersect at a single crossover point. When these two tests do not succeed exactly and the obvious reasons for systematic errors⁸ have been checked, the residual random errors can be minimized by a double-averaging procedure. The first one, which applies to the conventional method as well,

⁸ Some of the errors are detected by the two tests. Accidental errors show up as stray points. Strong attenuation in line 2 produces a circle that does not close or rather an arc of a spiral. Nonuniform lines produce bad crossover. An error in the wavelength gives chords tangent to a small ellipse instead of intersecting.

consists of passing the best circle through the w_i' points. The other is based on estimating the crossover point, then applying the transformation Θ and measuring the phases of the points w_i'' on Γ' . These should be equal to the phases of the original w_i . The plot of one phase *versus* the other should be a straight line with a 45-degree slope. If no systematic trend is observed, which would indicate a bad choice of crossover point, the fitting of a straight line (by the least-square method, for instance) gives a good representative point (P' image of P , for instance) for the set of experimental data.

9. Conclusions

The method of analysis presented here differs from the conventional one^{2,9,10} in the use it makes of the strong relation that exists between the points on the circle and their images by a bilinear transformation. In a disguised way, it uses the invariance of the cross-ratio.¹¹ This affords a new control on the measurement and a means of averaging by fitting a *straight line* to the experimental results properly treated.

In the conventional method applied to lossless structures, one would fit to these results a tangent relation while for lossy structures the procedure is more complicated. In the present method, the consideration of lossy structures does not introduce any difficulties.

For ordinary measurements, the experiment is practically the same but its interpretation is reduced to a minimum: drawing of a few straight lines and direct reading of angles and distances. It gives immediately the most important parameters of the junction transmission and reflection coefficients, independently of any equivalent circuit representation and of a more-or-less-arbitrary convention for the characteristic impedances of the waveguides.

⁹ A. Weissfloch, "Ein Transformationssatz ueber verlustlose Vierpole und seine Anwendung auf die experimentelle Untersuchung von Dezimeter- und Zentimeterwellen-Schaltungen," *Hochfrequenztechnik und Elektroakustik*, volume 60, pages 57-73; September, 1942; brief English abstract in *Wireless Engineer*, volume 20, page 135; March, 1943.

¹⁰ N. Marcuvitz, "On Representation and Measurement of Waveguide Discontinuities," *Proceedings of the IRE*, volume 30, pages 728-735; June, 1948.

¹¹ It follows that the same method is applicable to find the analytic expression of any bilinear transformation even when the scattering interpretation does not apply. This covers problems on interference, polarization transformers, etc.

New High-Frequency Proximity-Effect Formula*

By A. C. SIM

Standard Telecommunication Laboratories, Limited; London, England

ACCURATE formulae for the high-frequency resistance and inductance of a pair of parallel circular conductors connected in series have been presented in the past, but they are all very complicated. The present work derives a new asymptotic formula that is valid whenever the effect is so severe that the resistance is more than doubled. The formula is rigorous and very simple and has been derived by means of a new approach to the problem.

. . .

1. Introduction

Since the first, and very exhaustive, analysis of the problem by G. Mie¹ in 1900 a large number of papers has been published, most of which ignore previous work and, in consequence, arrive at formulae possessing severe limitations. Arnold,² however, surveyed this work, selected Butterworth's solution³ as the most fruitful, and proceeded to extend and develop it. The result has been the presentation^{4,5} of a formula that is valid and accurate over the entire physical range of the problem.

The need for a further investigation of the problem is evident from the complexity of Arnold's formula. A new formula, even though it may not be valid for all possible cases, can be of value if it is really simple and its range of validity is readily found.

* Reprinted from *Wireless Engineer*, volume 30, pages 204-207; August, 1953.

¹G. Mie, "Elektrische Wellen an Zwei Parallelen Drahten," *Annalen der Physik*, volume 2, pages 201-249; 1900.

²A. H. M. Arnold, "Alternating-Current Resistance of Parallel Conductors of Circular Cross-Section," *Journal of the Institution of Electrical Engineers*, volume 77, pages 49-58; October, 1935.

³S. Butterworth, "Eddy-Current Losses in Cylindrical Conductors with Special Applications to the Alternating-Current Resistance of Short Coils," *Philosophical Transactions of the Royal Society of London*, volume 222A, pages 57-100; September, 1921.

⁴A. H. M. Arnold, "Proximity Effect in Solid and Hollow Round Conductors," *Journal of the Institution of Electrical Engineers*, Part 2, volume 88, pages 349-359; August, 1941.

⁵A. H. M. Arnold, "Alternating-Current Resistance of Non-Magnetic Conductors," Her Majesty's Stationery Office, London, England; 1946.

Previous workers in the field have either employed Maxwell's equations or used an integral equation. The present author has found that the amalgamation of both approaches leads most readily to a final result, and the method is, moreover, easily extended to other related but more difficult problems.

In addition it has been found that the general resistance formula obtained by means of Poynting's theorem, which has been universally employed in the past, necessitates a large amount of unnecessary algebraical and analytical labour. The author has developed a new impedance equation that leads more directly to the final result, and without which the new formula to be presented would have been difficult to derive.

2. Impedance Formula

From the symmetry of the problem only the field components \mathcal{E}_z , H_ρ , H_ϕ , will exist provided displacement currents are negligible. If ρ is a dimensionless radial co-ordinate, $\rho = r/a$ where a is the outer radius of the conductors and r is an arbitrary radius, and if ϕ is an angular co-ordinate (Figure 1), and ξ is a parameter defined by

$$\xi^2 = j\omega\mu\sigma a^2, \quad (1)$$

where ω is the angular frequency of the current, μ the permeability of the conductors and the medium surrounding them, and σ is the conductivity of the conductors, all in rationalized metre-kilogram-second units; then a solution of Maxwell's equations shows that the electric field can be expressed in the form:—

$$\mathcal{E}_z = \sum_{n=0}^{\infty} \{M_n I_n(\xi\rho) + M_n' K_n(\xi\rho)\} \cos(n\phi), \quad (2)$$

where M_n and M_n' are constants of integration, and I_n and K_n are the modified Bessel functions. The magnetic field can be found from \mathcal{E}_z by means of Maxwell's equations:—

$$\left. \begin{aligned} H_\rho &= \frac{j}{\mu\omega a \rho} \frac{\partial \mathcal{E}_z}{\partial \phi}, \\ \text{and} \\ H_\phi &= \frac{-j}{\mu\omega a} \frac{\partial \mathcal{E}_z}{\partial \rho}. \end{aligned} \right\} (3)$$

If, in Figure 1, P' and P'' are roving points in each conductor with co-ordinates ρ' , ϕ' and ρ'' , ϕ'' ; and p' , q' and p'' , q'' are the corresponding distances indicated in the diagram, then Curtis'⁶ integral equation as modified by Manneback,⁷ shows that the electric field must also satisfy the equation:—

$$\mathcal{E}_z = \left\{ \mathcal{E}_0 - \frac{\xi^2}{2\pi} \int_k^1 \int_0^{2\pi} \rho' \mathcal{E}_z' \log(p'/q') d\rho' d\phi' + \frac{\xi^2}{2\pi} \int_k^1 \int_0^{2\pi} \rho'' \mathcal{E}_z'' \log(p''/q'') d\rho'' d\phi'' \right\}, \quad (4)$$

where \mathcal{E}_0 is the value of \mathcal{E}_z at the point P_0 , \mathcal{E}_z' and \mathcal{E}_z'' the values at P' and P'' , and $k = b/a$ is the ratio of inner-to-outer radii.

By substituting the series (2) into (4), the constants M_n and M_n' can be determined, and it is found that the value of \mathcal{E}_z at the point Q is given by

$$\mathcal{E}_z = I R_0 \frac{\xi^2}{2} \left\{ \chi_0 + \sum_{n=1}^{\infty} \frac{\alpha^n A_n}{n} (1 - \chi_n) \right\} \quad \left. \vphantom{\mathcal{E}_z} \right\} (5)$$

$(\rho = 1, \phi = 0),$

where $R_0 = 1/\pi\sigma a^2$, I is the total current, and the constants A_n are defined by

$$A_n = \left\{ 1 + \sum_{m=1}^{\infty} \binom{n+m-1}{m} \alpha^{2m} \chi_m A_m \right\}, \quad (6)$$

⁶ H. L. Curtis, "An Integration Method of Deriving the Alternating-Current Resistance and Inductance of Conductors," *Bureau of Standards Scientific Papers*, volume 16, pages 93-124; April, 1920.

⁷ C. Manneback, "An Integral Equation for Skin Effect in Parallel Conductors," *Journal of Mathematics and Physics*, volume 1, pages 124-146; 1921.

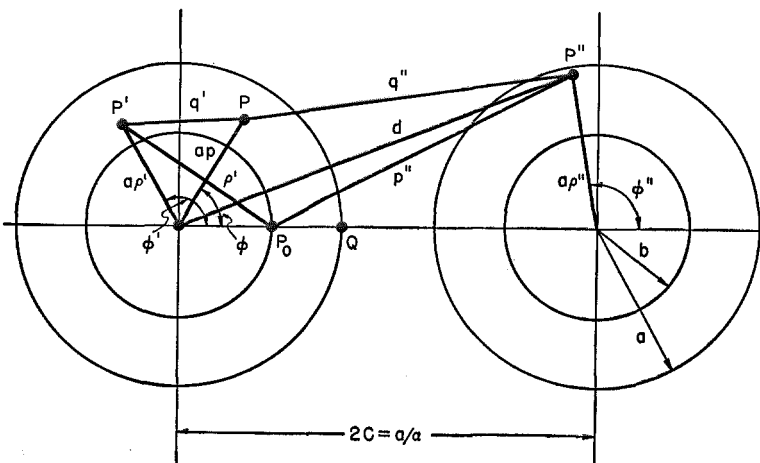


Figure 1—Section through two parallel conductors with the geometrical construction used in the analysis.

where $\binom{n}{m} = \frac{n!}{(n-m)!m!}$ is the binomial coefficient,

$$\chi_n \equiv \left\{ \frac{I_{n+1}(\xi)K_{n+1}(k\xi) - I_{n+1}(k\xi)K_{n+1}(\xi)}{I_{n-1}(\xi)K_{n+1}(k\xi) - I_{n+1}(k\xi)K_{n-1}(\xi)} \right\},$$

and

$$\chi_0 \equiv \left\{ \frac{I_0(\xi)K_1(k\xi) + I_1(k\xi)K_0(\xi)}{I_1(\xi)K_1(k\xi) - I_1(k\xi)K_1(\xi)} \right\} / \xi. \quad (7)$$

Similarly, the magnetic intensity perpendicular to the plane containing the conductor axes and external to the conductor is found to be

$$H_\phi = \frac{I}{2\pi a} \times \left[\rho^{-1} + \sum_{n=1}^{\infty} \alpha^n A_n \{ \rho^{(n-1)} + \rho^{-(n+1)} \} \chi_n \right] \quad \left. \vphantom{H_\phi} \right\} (8)$$

$(\rho \geq 1, \phi = 0).$

Thus the flux linking the point Q , which must equal half the flux passing between the conductors, is

$$\Phi = \mu a \int_1^{\alpha/2} H_\phi d\rho = \frac{\mu I}{2\pi} \left[\log(1/2\alpha) + \sum_{n=1}^{\infty} \frac{\alpha^n A_n}{n} \{ 1 - (2\alpha)^n \} \{ \chi_n + (2\alpha)^{-n} \} \right]. \quad (9)$$

The total voltage drop at Q must be $(\mathcal{E}_z + j\omega\Phi)$ per unit length of conductor, and this must be half the applied voltage per unit length of the system. It follows that the impedance per unit length is

$$Z = R_0 \xi^2 \left[\chi_0 + \log(1/2\alpha) + \sum_{n=1}^{\infty} \frac{A_n}{n} \{ 2^{-n} - (2\alpha^2)^n \chi_n \} \right]. \quad (10)$$

Now, from (6), if x is an arbitrary variable sufficiently

small,

$$\begin{aligned} \sum_{n=1}^{\infty} \frac{x^n A_n}{n} &= \left\{ -\log(1-x) \right. \\ &+ \sum_{n=1}^{\infty} \sum_{m=1}^{\infty} \binom{n+m-1}{m} \frac{x^n \alpha^{2m}}{n} \chi_m A_m \left. \right\} \\ &= \left\{ -\log(1-x) \right. \\ &+ \sum_{m=1}^{\infty} \sum_{n=1}^{\infty} \binom{m+n-1}{n} \frac{x^n \alpha^{2m}}{m} \chi_m A_m \left. \right\} \\ &= \left[-\log(1-x) \right. \\ &+ \sum_{m=1}^{\infty} \{1 - (1-x)^{-m}\} \frac{\alpha^{2m}}{m} \chi_m A_m \left. \right]. \quad (11) \end{aligned}$$

By letting $x = 1/2$, and substituting the result into (10), there follows:—

$$Z = R_0 \xi^2 \left\{ \chi_0 + \log(1/\alpha) - \sum_{m=1}^{\infty} \frac{\alpha^{2m}}{m} \chi_m A_m \right\}. \quad (12)$$

It can be seen from (6) that this series is identical with the coefficient of n in the expansion of A_n in powers of n , and it follows that if

$$A_n = \kappa^n \{1 + n \cdot \kappa_1 + n^2 \cdot \kappa_2 + \dots\}, \quad (13)$$

then

$$Z = R_0 \xi^2 \{ \chi_0 + \log(1/\alpha\kappa) - \kappa_1 \}. \quad (14)$$

This is the final impedance formula.

3. Integration Constants

Equation (14) may be checked by solving (6) in powers of α , and extracting the coefficient κ_1 , when the formula, previously found by Arnold⁸ and others, using a relatively tedious method, is confirmed. To obtain a new and very simple formula, an asymptotic form of A_n must be found.

When ξ is very large, the function χ_n approximates to

$$\chi_n \approx I_{n+1}(\xi)/I_{n-1}(\xi), \quad (15)$$

and is thus independent of k , provided

$$\exp\{-2(1-k)|\xi|\} \ll 1.$$

This simplified function (Butterworth's function⁸), can be seen to satisfy the equation

$$\left\{ \frac{d\chi_n}{d\xi} + \frac{\xi}{2n} (1 + \chi_n)^2 + \frac{2n}{\xi} \chi_n \right\} = 0 (k=0), \quad (16)$$

⁸ S. Butterworth, "On the Evaluation of Certain Combinations of the Ber, Bei, and Allied Functions," *Proceedings of the Physical Society*, volume 25, pages 294-297; 1913.

which may be solved by successive approximations (starting with $\chi_n \approx 1$), to give⁹

$$\begin{aligned} \chi_n \sim & \{1 - 2n \cdot \xi^{-1} + n(2n-1) \cdot \xi^{-2} \\ & - \frac{1}{4} n(2n-1)(2n-3) \cdot \xi^{-3} \\ & + \frac{1}{4} n(2n-1)(2n-3) \cdot \xi^{-4} + \dots\}. \quad (17) \end{aligned}$$

By substituting this into (6) and assuming that A_n possesses a similar form, it is found after considerable reduction that

$$\begin{aligned} A_n \sim & \frac{\{1 - (1 - 4\alpha^2)^{1/2}\}^n}{(2\alpha^2)^n} \left[1 - \frac{(1-\lambda)}{\lambda} n \xi^{-1} \right. \\ & + \left\{ \frac{(1-\lambda)(1+\lambda-\lambda^2)}{2\lambda^3} \cdot n + \frac{(1-\lambda)^2}{2\lambda^2} n^2 \right\} \xi^{-2} \\ & - \left\{ \left(\frac{3\lambda^4(1-\lambda) + 2(2-5\lambda^2+3\lambda^4)}{8\lambda^5} \right) n \right. \\ & + \left. \left\{ \frac{(1-\lambda)^2}{4\lambda^4} (1-3\lambda^2) + \frac{3(1+\lambda)^2}{(3+\lambda^2)} \right\} n^2 \right. \\ & \left. \left. + \frac{(1-\lambda)^3}{2\lambda^3(3+\lambda^2)} n^3 \right\} \xi^{-3} + \dots \right], \quad (18) \end{aligned}$$

in which $\lambda \equiv (1 - 4\alpha^2)^{1/2}$. Thus

$$\kappa = \{1 - (1 - 4\alpha^2)^{1/2}\} / 2\alpha^2$$

and

$$\begin{aligned} \kappa_1 \sim & \left[-\frac{(1-\lambda)}{\lambda\xi} + \frac{(1-\lambda)(1+\lambda-\lambda^2)}{2\lambda^3\xi^2} \right. \\ & \left. - \frac{\{3\lambda^4(1-\lambda) + 2(2-5\lambda^2+3\lambda^4)\}}{8\lambda^5\xi^3} + \dots \right]. \end{aligned}$$

4. The New Formula

If $\beta = (1 - 4\alpha^2)^{-1/2}$, it follows from (14) that

$$\begin{aligned} Z \sim R_0 \left\{ \xi^2 \log(1/\alpha\kappa) + \beta \cdot \xi + \beta(1 - \frac{1}{2}\beta^2) \right. \\ \left. + \frac{\beta}{8\xi} (9 - 10\beta^2 + 4\beta^4) + \dots \right\}, \quad (19) \end{aligned}$$

where $R_0 = 1/\pi\sigma a^2$ = the direct-current resistance of solid conductors of radius a . Extracting the real and imaginary parts gives

$$\begin{aligned} R'/R \sim (1 - k^2) \left\{ \frac{\beta|\xi|}{2\sqrt{2}} + \frac{\beta(2 - \beta^2)}{4} \right. \\ \left. + \frac{\beta(9 - 10\beta^2 + 4\beta^4)}{16\sqrt{2}|\xi|} + \dots \right\}, \quad (20) \end{aligned}$$

⁹ The sign \sim is used here in its conventional sense of "asymptotically equal to," which means that the formula is not accurate, but becomes more accurate as ξ becomes larger. The error is less than the last term included, and summation should be terminated at the smallest term.

where R is the direct-current resistance of the hollow conductors, and k is the ratio of inner-to-outer radii; and

$$L' \sim \frac{\mu}{\pi} \left\{ \frac{1}{2} \log \left(\frac{\beta + 1}{\beta - 1} \right) + \frac{\beta}{\sqrt{2}|\xi|} - \frac{\beta(9 - 10\beta^2 + 4\beta^4)}{9\sqrt{2}|\xi|^3} + \dots \right\}. \quad (21)$$

Note that $|\xi| = (\mu\sigma\omega a)^{1/2} = (\mu\omega/\pi R_0)^{1/2}$; $\mu = 4\pi \times 10^{-7}$ for free space if L' is measured in henrys per metre.

5. Validity

The resistance formula can be compared numerically with Arnold's formula, and in this way the corresponding values of β and $|\xi|$ determined for a given error Δ . Figure 2 gives a set of iso-error curves for (20) for values of β up to 2.5. The corresponding conductor spacings are illustrated and it can be seen that β is not likely to exceed this limit in practice.

Figure 2 gives the error in the case of a solid conductor, and when hollow wires are used, a further condition is necessary:—

$$|\xi| \geq \delta/(1 - k), \quad (22)$$

where δ is plotted against Δ in Figure 3.

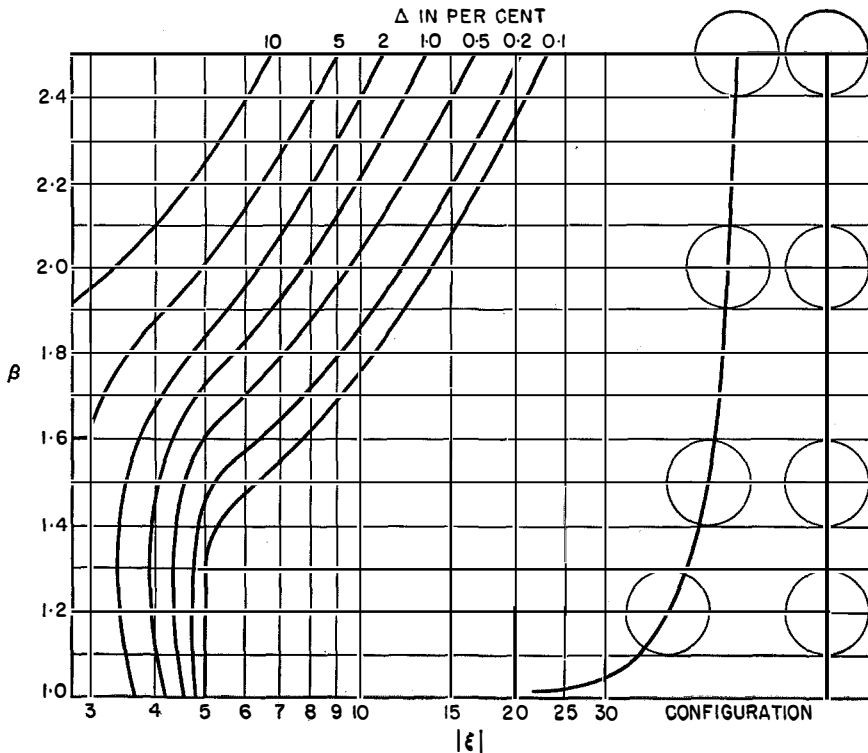


Figure 2—Iso-error curves for equation (20) for a solid conductor.

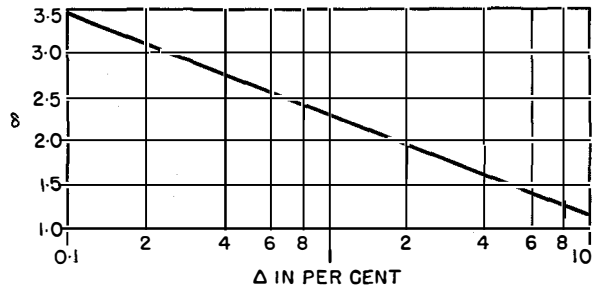


Figure 3—Values of δ to be used in equation (22) for a hollow conductor.

In general it is found that (20) is useful when the skin effect is sufficiently serious for R'/R to exceed 2. When $|\xi| \geq 3$ the accuracy of the formula can be improved to a large extent by estimating the error Δ from Figure 2 and noting that the formula is always pessimistic in this range.

The error in the inductance formula will be less serious since L' does not vary over an infinite range with frequency. A comparison with Arnold's inductance formula¹⁰ reveals analytical disagreement but a little experiment suggests that Arnold's error will not exceed 2.7 per cent, and becomes negligible at low frequencies and when $\beta < 2$. By comparing (20) and (21), it can be seen that the percentage error in the quantity

$$\left\{ \frac{\pi L'}{\mu} - \frac{1}{2} \log \left(\frac{\beta + 1}{\beta - 1} \right) \right\}$$

is of the order of $|\xi|$ times the error in R' for the same β and $|\xi|$.

6. Acknowledgments

This work has been accelerated by illuminating discussions with Mr. L. Lewin.

¹⁰ A. H. M. Arnold, "Inductance of Wires and Tubes," *Journal of the Institution of Electrical Engineers*, Part 2, volume 93, pages 532-540; December, 1946.

United States Patents Issued to International Telephone and Telegraph System, August-October, 1953

UNITED STATES patents numbering 60 were issued between August 1 and October 31, 1953 to companies in the International System. The inventors, titles, and numbers of these patents are given below; summaries of several that are of more-than-usual interest are included. In cases where equivalent Canadian patents have already issued, their numbers are given in parenthesis.

- R. S. Bailey, Traveling-Wave-Amplifier Device, 2,654,004.
- E. Baum, Pulse Demodulating System, 2,654,027.
- M. C. Bloom and J. P. Levy, Electrodeposition of Selenium, 2,649,410.
- P. C. Borel and M. R. Mauge, Automatic Switching System, 2,651,681.
- O. J. J. Brack and G. X. Lens, Selecting-and-Controlling Mechanism for Movable Parts, 2,653,486.
- W. Brandt, Signal Receiver Circuit, 2,657,308.
- F. H. Bray, M. T. Wilson, D. H. Ormond, and S. G. W. Johnstone, Dual-Use Register Sender, 2,651,680.
- E. M. Buyer, Pulse Keying System, 2,651,753.
- T. H. Clark, Electron Switch Control System, 2,654,049.
- A. G. Clavier, Beam Traveling-Wave-Amplifier Tube, 2,654,047 (582,551).
- A. G. Clavier and E. C. de Faymoreau, Traveling-Wave Amplifier, 2,651,686 (571,913).
- G. Deakin, Multipotential-Type Register Controller, 2,654,000.
- R. H. Dunn, Electric Signalling System, 2,649,580.
- C. W. Earp, Radio Direction Finder, 2,651,774 (611,234).
- H. F. Engelmann, Radio-Frequency Antenna, 2,654,842 (632,697).
- H. Feissel, Pulse-Code-Modulation Demodulator, 2,651,716 (578,935).
- L. G. Fischer, Radio-Frequency Amplitude Control Device, 2,654,866 (633,968).
- M. L. Gayford and W. D. Cragg, Negative Feedback in Magnetic Recording, 2,649,506 (583,120).
- L. Goldstein, High-Energy-Radiation Counter, 2,657,315.
- T. F. S. Hargreaves and W. F. Gould, Automatic Signal Attenuator, 2,651,684.
- A. S. Harris, Frequency-Oscillation Modulator, 2,654,071.
- G. C. Hartley, Electric Signalling System, 2,651,679.
- G. C. Hartley, F. H. Bray, and G. H. Hough, Alternating-Current Switching Device, 2,655,605 (622,954).
- R. A. Hill, Dry-Contact Rectifier, 2,657,346 (637,551).
- G. H. Hough and T. M. Jackson, Electric Discharge Tube, 2,654,044 (624,266).
- B. B. Jackson, C. T. Daly, D. L. Thomas, H. Wolfson, S. C. Shepard, and D. Green, Thermosensitive Resistance Elements, 2,651,699 (625,999).
- R. Kelly, Electrical Power-Supply System for Communication-System Repeaters, 2,657,279 (599,981).
- J. Kruithof, Flat Cross-Bar Mechanism, 2,651,682.
- J. J. B. Lair, Electrical Intercommunication System, 2,651,677 (612,925).
- J. J. B. Lair, Electron Switching Device, 2,651,740 (635,635).
- M. A. Lalande, Retardation-Line Subdivision into Sections, 2,651,760.
- A. V. Lapish, Changer Cycle-Control Mechanism, 2,657,060.
- S. H. Marrow, Dry-Rectifier Assembly, 2,651,745 (626,143).
- K. A. Matthews and C. deB. White, Electric Semiconductor, 2,653,374.
- L. S. Munck, Control of Teleprinter Driving Motors, 2,649,497.
- A. D. Odell, Electrical Circuit Employing Gaseous-Discharge Tube, 2,649,502.
- P. T. O'Neil, Rectifier Stack, 2,657,344.
- L. W. Parker, Electronic Color Television, 2,657,331.
- H. T. Prior, Carrier Telegraph System, 2,657,262 (620,360).

- D. H. Ransom, Electric Potential-Comparing Circuit, 2,649,557.
- D. H. Ransom, Pulse-Time-Position Switching System, 2,649,505 (569,982).
- A. H. Reeves, Electric Delay Device Employing Semiconductors, 2,655,607.
- W. Reinhard, Sawtooth-Wave Generator, 2,654,050.
- E. Richon, Blind-Landing Systems, 2,657,381 (620,362).
- R. D. Salmon, Printing-Telegraph Apparatus, 2,655,555 (613,742).
- N. H. Saunders, C. J. Hackett, and J. I. Bellamy, Multicontact Relays, 2,647,961.
- W. C. Schmitt, Jacket for Water-Cooled Tubes, 2,657,019 (635,638).
- W. K. Sindzinski, Receiver for Pneumatic Post System with Horizontal Capsule Ejection, 2,648,785.
- A. T. Starr and H. Grayson, Electric Pulse-Modulation System of Communication, 2,657,269 (569,983).
- L. Staschover and H. A. French, Automatic-Frequency-Control System, 2,654,032.
- W. G. Storey, Telephone Subset Wiring-Plan System, 2,651,683.
- M. C. Tournier, Integral Electrode with Lead-Wire Anchor for Piezoelectric Crystal, 2,648,785.
- F. B. Turner, Electric Coil-Winding Machine, 2,653,771 (575,000).
- A. S. Vanderhoof, Rectifier Stack, 2,652,522 (602,491).
- A. Von Hippel and M. C. Bloom, Electrodeposition of Selenium, 2,649,409 (516,750).
- A. J. Warner and S. G. Foord, Methods and Apparatus for Growing Crystals, 2,651,566.
- W. K. Weston, Coaxial Electric Cable with Corrugated Seam, 2,653,989 (593,886).
- E. P. G. Wright, Echo-Suppressor Insertion, 2,653,999 (573,834).
- E. P. G. Wright, Electric Telegraph System, 2,653,996 (622,812).
- E. P. G. Wright and D. G. Weir, Electrical Decoding Circuits, 2,648,725 (608,263).

Electric Delay Device Employing Semiconductors

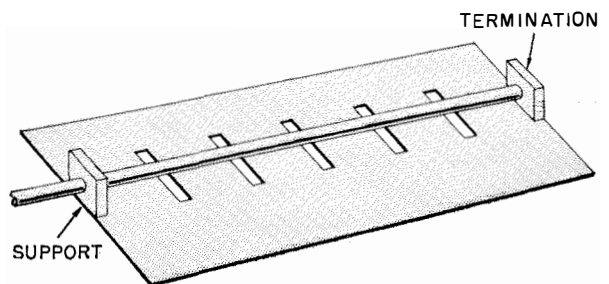
A. H. Reeves
2,655,607—October 13, 1953

An electric pulse delay circuit made of a semiconducting material having a base and two or more point-contact electrodes in contact with the semiconducting material, these point-contact electrodes forming parts of trigger circuits. The trigger circuits are interconnected so that on operation of one of the circuits, a pulse is transmitted that causes the gap between the following point and base electrodes to operate after a delay dependent on the separation of successive electrodes.

Radio-Frequency Antenna

H. F. Engelmann
2,654,842—October 6, 1953

A strip-line radio-frequency antenna, employing a ground plane that has slots transverse to the line conductor, these slots providing an antenna array coupled to the line.



Electric Semiconductor

K. A. Matthews and C. deB. White
2,653,374—September 29, 1953

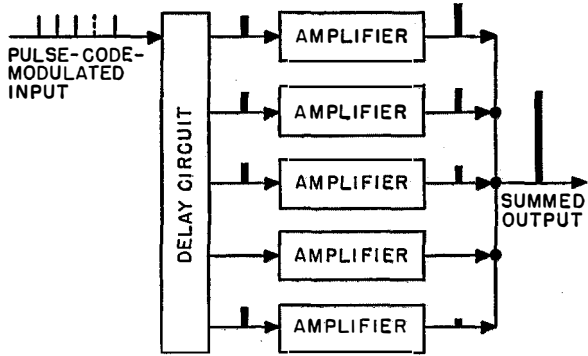
A circuit arrangement and process for electroforming a crystal triode that consists in passing a relatively small direct current between the emitter and collector electrodes of the triode with the base electrode left unconnected. The direct current is then momentarily increased to a relatively large value resulting in a unit having an emitter-collector current-voltage characteristic curve such that when the emitter is biased to make a low-resistance-rectifier contact with the semiconductor material, no portion of the characteristic curve has a negative slope.

Pulse-Code-Modulation Demodulator

H. Feissel
2,651,716—September 8, 1953

A pulse-code demodulator in which the successive pulses of a code combination are

applied through delay lines as gating pulses to several amplifiers of differing fixed gains. The combined output of the amplifiers produced by

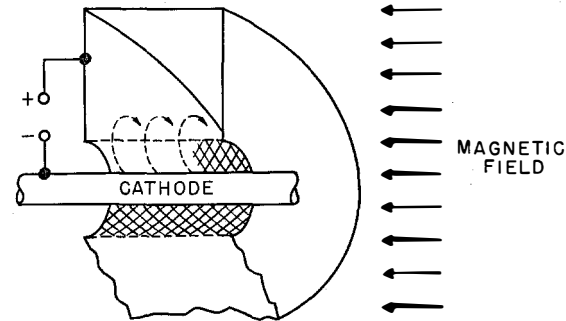
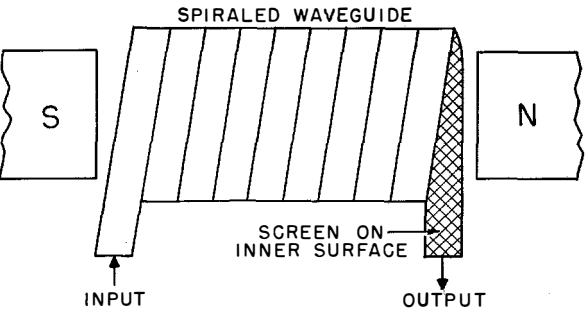


simultaneous opening of the code-selected gate circuits will produce a signal of an amplitude corresponding to the code combination.

Travelling-Wave Amplifier

A. G. Clavier and E. C. de Faymoreau
2,651,686—September 8, 1953

A travelling-wave amplifier in which the wave-transmitting line is a spiral waveguide wound about a cathode, the surface of the waveguide adjacent to the electron source being perforated to permit the electrons to enter the waveguide and interact with the wave.



Dry-Contact Rectifier

R. A. Hill
2,657,346—October 27, 1953

A dry-contact rectifier using a layer of titanium nitride in intimate contact with a metallic-oxide counterelectrode.

Coaxial Cable With Corrugated Seam

W. K. Weston
2,653,989—September 29, 1953

A coaxial communication cable in which the outer conductor is made of a metallic strip folded longitudinally to form a tube, the opposite longitudinal edges of this strip being corrugated and deformed from a symmetrical shape, the deformations being in opposite directions on the two edges so that the abutting edges of the tube are prevented from overriding one another.

Electronic Color Television

L. W. Parker
2,657,331—October 27, 1953

An arrangement for controlling the sweep speed of the cathode-ray beam, particularly for color-television tubes, to assure proper registration. The invention comprises an electron-permeable conductive coating in the form of metallic combs insulated from one another and placed in the inner surface of the fluorescent coating. Depending on the speed at which the cathode-ray beam is swept across these combs, a pulsating output wave will be obtained, the frequency of which can be used to produce a regulating voltage.

Negative Feedback Applied to Magnetic Recording

M. L. Gayford and W. D. Cragg
2,649,506—August 18, 1953

A magnetic recording head for tape or wire recording provided with an auxiliary head that serves to pick up the recorded signals and feed them back in inverse phase to the input of the recorder, thus reducing distortion.

In Memoriam



HENRY CONRAD ROEMER

HENRY C. ROEMER was born in Baltimore, Maryland, on April 16, 1898. He became associated with the International Telephone and Telegraph Corporation in 1927 and was elected a director of the corporation in 1943, a vice-president in 1944, and comptroller in 1946.

In 1951, Mr. Roemer was elected president of Federal Telephone and Radio Corporation, now a division of the International Telephone and Telegraph Corporation. At his death, in addition to being a director, he held the recently created post of vice-president in charge of the administration of the five domestic divisions of the corporation.

During his long association with the International System, Mr. Roemer played an important role in the development of its domestic and foreign activities, holding numerous offices and directorships in associated companies.

Mr. Roemer was beloved, respected, and admired by his many friends and associates for his warm human qualities and superior abilities. With his passing, the International System has been deprived of a resourceful executive and able counselor, and his associates have lost a good and true friend.

Mr. Roemer died suddenly at his home in New York City on November 15, 1953 in his 55th year.

Contributors to This Issue



GEORGE H. BRODIE

ringing-current generator for telephone central offices.

He is a member of American Society for Metals, American Society for Testing Materials, Institute of Radio Engineers, Armed Forces Communications Association, and a Registered Professional Engineer in the State of Illinois. He holds a number of patents pertaining to wire communications and is the author of several published technical articles.

• • •

JOHN H. BRYANT was born in Baird, Texas, on April 15, 1920. He received the B.S. degree in electrical engineering from the A. and M. College of Texas in 1942 and the Ph.D. degree from the University of Illinois in 1949.

From 1942 to 1946, he served as an officer in the United States Army Signal Corps.

During the summer of 1947, he was temporarily employed by the vacuum-tube department of Federal Telecommunication Laboratories, and in 1949 joined the staff as a project engineer. Dr. Bryant is now a department head in the electron-tube laboratory. In this issue, he reports on some of the properties of helical conductors.

He is a member of Sigma Xi, American Physical Society, and the Institute of Radio Engineers.

• • •

GEORGES A. DESCHAMPS was born in Vendôme, France, on October 18, 1911. He was graduated from the Ecole Normale Supérieure of Paris in 1934, and received the following degrees from the Sorbonne: license in mathematics and physics, diplôme d'étude supérieure, and agrégation in mathematics. After two years of research in pure mathematics, one in Paris and one at Princeton University, he joined the Lycée Français de New York as a professor of mathematics and physics. At that time, he also did some work on relativity and the theory of elementary particles.

The outcome of some of Mr. Deschamps' work in mathematics is his new solutions for transmission-line problems, as reported in this issue.

Mr. Deschamps served in the French army during the war and in 1947 joined Federal Telecommunication Laboratories where he is presently in the aviation development laboratory. He is a member of the American Physical Society.

• • •

PAMELA A. HANDLEY was born in 1929 in Portsmouth, England. She received an Honours B.Sc. degree in



GEORGES A. DESCHAMPS

Mathematics (London) from Southampton University in 1951.

In that year, she joined the development staff of the Brimar valve engineering division of Standard Telephones and Cables, Limited, and has been engaged principally on work on reliable valves, a joint report on which is included in this issue.

• • •

ROBERT W. HUTTON was born on August 2, 1919 at Egeland, North Dakota.

After serving in the Army Air Force from March 1941, he joined the Kellogg Switchboard and Supply Company in 1946. Since 1949, he has been engaged in telephone central-office development. He describes the type-7 crossbar selector in this issue.

Mr. Hutton is a member of the American Institute of Electrical Engineers.



JOHN H. BRYANT



PAMELA A. HANDLEY



ROBERT W. HUTTON

GERARD J. LEHMANN was born in Paris in 1909. He graduated from Ecole Centrale des Arts et Manufactures in 1931.

On graduation, he joined Sadir Company in Paris and became its technical director. While working on aerial navigation and radar in 1937, he invented the folded-dipole antenna.

Mr. Lehmann came to Laboratoire Central de Télécommunications in 1940 and is now its director of research. He serves also as the general manager of Société des Servomécanismes Electroniques. He was assigned to Federal Telecommunication Laboratories in New York from 1943 to 1945.

He has had charge successively of courses in radio navigation, radar, servomechanisms, and, now, information theory at Ecole Supérieure d'Electricité in Paris. He has published over 60 scientific and technical papers. One of his latest papers, in this issue, describes a temperature-regulated furnace.



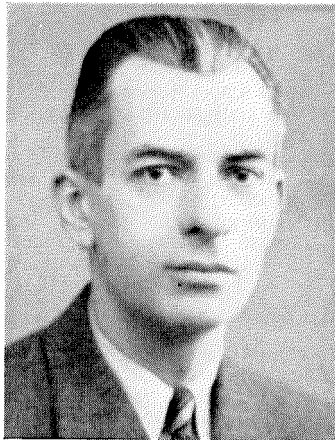
GERARD J. LEHMANN

Mr. Lehmann is chairman of the French national committee of the International Scientific Radio Union. He was made a Chevalier of the Legion of Honor in 1948 by the French Government.

• • •

CHARLES A. MEULEAU was born in Paris, France in 1908. He graduated from Ecole Supérieure de Physique et Chimie and also received the Licence ès Sciences degree from the Paris University.

In 1929, he joined the staffs of Les Laboratoires, Le Matériel Téléphonique. From 1931 to 1938, he worked in the chemical industry on plastics and varnishes. Returning to the International System, he was placed in charge of the production of piezoelectric crystals in the Paris laboratories. After the war, he was active in the



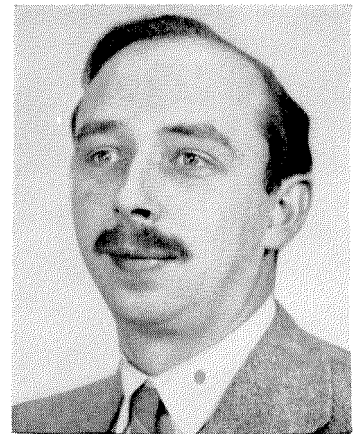
CHARLES A. MEULEAU

production of artificial piezoelectric crystals. Since 1950, Mr. Meuleau has been in charge of the development of semiconductor products at Laboratoire Central de Télécommunications. He reports in this issue on means for producing single crystals of germanium of high purity.

• • •

ALAN C. SIM was born in London, England on October 29, 1925. In 1942, he was apprenticed to the British Thomson-Houston Company, where he developed and designed high-power pulse generators and special magnetic devices. In 1945, he received the external B.Sc. (Eng.) degree from the University of London.

Early in 1950, he joined the staff of Standard Telecommunication Laboratories Limited, and is now primarily



ALAN C. SIM

engaged in mathematical researches into the properties of semi-conductors and associated products.

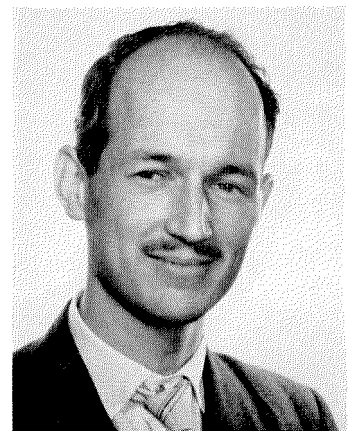
His interest in the skin-effect problems discussed in this issue was stimulated when excessive losses were encountered in high-power pulse transformers.

• • •

PETER WELCH was born in 1922 in Windsor, England. Since 1938 he has worked for Standard Telephones and Cables, Limited, in various aspects of thermionic-valve work.

In 1949, he joined the Brimar valve engineering division and for a year headed the development group on valve reliability. Since 1952, he has headed the product engineering group responsible for factory technical control of valves and cathode-ray tubes.

He is joint author of a paper on the design and fabrication of trustworthy valves.



PETER WELCH

INTERNATIONAL TELEPHONE AND TELEGRAPH CORPORATION

MANUFACTURE AND SALES

North America

UNITED STATES OF AMERICA —

Divisions of International Telephone and Telegraph Corporation

Capehart-Farnsworth Company; Fort Wayne, Indiana
Coolerator Company; Duluth, Minnesota

Federal Telephone and Radio Company; Clifton, New Jersey

Kellogg Switchboard and Supply Company; Chicago, Illinois

Federal Electric Corporation; Clifton, New Jersey

International Standard Electric Corporation; New York, New York

International Standard Trading Corporation; New York, New York

IT&T Distributing Corporation; New York, New York

Kellogg Credit Corporation; Chicago, Illinois

Thomasville Furniture Corporation; Thomasville, North Carolina

CANADA — (See *British Commonwealth of Nations*)

MEXICO — Standard Electrica de Mexico, S.A., Mexico City

British Commonwealth of Nations

ENGLAND —

Standard Telephones and Cables, Limited, London

Creed and Company, Limited, Croydon

International Marine Radio Company Limited, Croydon

Kolster-Brandes Limited, Sidecup

CANADA — Federal Electric Manufacturing Company, Ltd., Montreal

AUSTRALIA —

Standard Telephones and Cables Pty. Limited, Sydney

Silovac Electrical Products Pty. Limited, Sydney

Austral Standard Cables Pty. Limited, Melbourne

NEW ZEALAND — New Zealand Electric Totalisators Limited, Wellington

South America

ARGENTINA — Compañía Standard Electric Argentina, S.A.I.C., Buenos Aires

BRAZIL — Standard Electrica, S.A., Rio de Janeiro

CHILE — Compañía Standard Electric, S.A.C., Santiago

Europe

AUSTRIA — Vereinigte Telefon- und Telegraphenfabriks A. G., Czeija, Nissl & Co., Vienna

BELGIUM — Bell Telephone Manufacturing Company, Antwerp

DENMARK — Standard Electric Aktieselskab, Copenhagen

FRANCE —

Compagnie Générale de Constructions Téléphoniques, Paris

Le Matériel Téléphonique, Paris

Les Téléimprimeurs, Paris

GERMANY —

C. Lorenz, A.G., Stuttgart

Mix & Genest A. G., and Subsidiaries, Stuttgart

G. Schaub Apparatebau G.m.b.H., Pforzheim

Süddeutsche Apparatefabrik G.m.b.H., Nuremberg

ITALY — Fabbrica Apparecchiature per Comunicazioni Elettriche, Milan

NETHERLANDS — Nederlandsche Standard Electric Maatschappij N.V., The Hague

NORWAY — Standard Telefon og Kabelfabrik A/S, Oslo

PORTUGAL — Standard Eléctrica, S.A.R.L., Lisbon

SPAIN —

Compañía Radio Aérea Marítima Española, Madrid

Standard Eléctrica, S.A., Madrid

SWEDEN — Aktiebolaget Standard Radiofabrik, Stockholm

SWITZERLAND — Standard Telephone et Radio S.A., Zurich

TELEPHONE OPERATIONS

BRAZIL — Companhia Telefônica Nacional, Rio de Janeiro

CHILE — Compañía de Teléfonos de Chile, Santiago

CUBA — Cuban American Telephone and Telegraph Company, Havana

CUBA — Cuban Telephone Company, Havana

PERU — Compañía Peruana de Teléfonos Limitada, Lima

PUERTO RICO — Porto Rico Telephone Company, San Juan

CABLE AND RADIO OPERATIONS

UNITED STATES OF AMERICA —

American Cable & Radio Corporation; New York, New York

All America Cables and Radio, Inc.; New York, New York

The Commercial Cable Company; New York, New York

Mackay Radio and Telegraph Company; New York, New York

ARGENTINA —

Compañía Internacional de Radio, Buenos Aires

Sociedad Anónima Radio Argentina, Buenos Aires (*Subsidiary of American Cable and Radio Corporation*)

BOLIVIA — Compañía Internacional de Radio Boliviana, La Paz

BRAZIL — Companhia Radio Internacional do Brasil, Rio de Janeiro

CHILE — Compañía Internacional de Radio, S.A., Santiago

CUBA — Radio Corporation of Cuba, Havana

PUERTO RICO — Radio Corporation of Porto Rico, San Juan

RESEARCH

UNITED STATES OF AMERICA —

Federal Telecommunication Laboratories; Nutley, New Jersey; a division of *International Telephone and Telegraph Corporation*

International Telecommunication Laboratories, Inc.; New York, New York

ENGLAND — Standard Telecommunication Laboratories, Limited, London

FRANCE — Laboratoire Central de Télécommunications, Paris

ASSOCIATE LICENSEES FOR MANUFACTURE AND SALES IN JAPAN

Nippon Electric Company, Limited, Tokyo

Sumitomo Electric Industries, Limited, Osaka